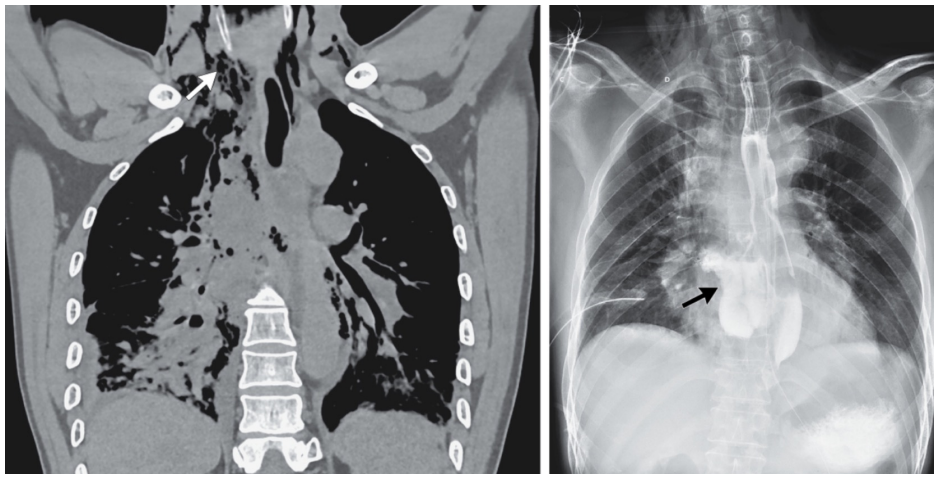
https://www.mdc-berlin.de/de/veroeffentlichungstypen/clinical-journal-club



Als gemeinsame Einrichtung von MDC und Charité fördert das Experimental and Clinical Research Center die Zusammenarbeit zwischen Grundlagenwissenschaftlern und klinischen Forschern. Hier werden neue Ansätze für Diagnose, Prävention und Therapie von Herz-Kreislauf- und Stoffwechselerkrankungen, Krebs sowie neurologischen Erkrankungen entwickelt und zeitnah am Patienten eingesetzt. Sie sind eingeladen, uns beizutreten. Bewerben Sie sich!



A previously healthy 59-year-old man presented to the emergency department with a 5-hour history of severe, pleuritic chest pain. Half an hour before the onset of symptoms, he vomited a large amount of gastric contents after eating street food. On physical examination, his breathing was found to be rapid and shallow. Palpable crepitus was noted in the neck, and breath sounds at the base of the right lung were diminished. Computed tomography of the chest is shown here. What is the most likely diagnosis?

Aortoesophageal fistula

Aspiration pneumonitis

Esophageal rupture

Perforated Peptic Ulcer

Tension Pneumothorax with subcutaneous emphysema

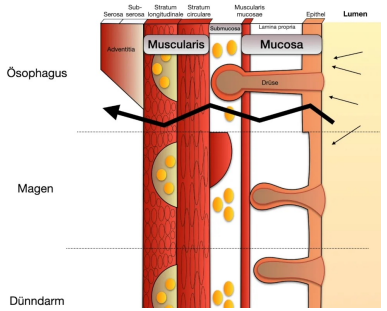
Computed tomography of the chest revealed air in the mediastinum extending up to the neck, a perforation of the esophagus, a pleural effusion on the right side, and atelectasis in the right lung. An esophagram that was obtained with the use of water-soluble contrast material confirmed a large laceration of the esophagus with extravasation of the contrast material into the mediastinum. A diagnosis of the Boerhaave syndrome — life-threatening, spontaneous rupture of the esophagus owing to severe vomiting or retching — was made.

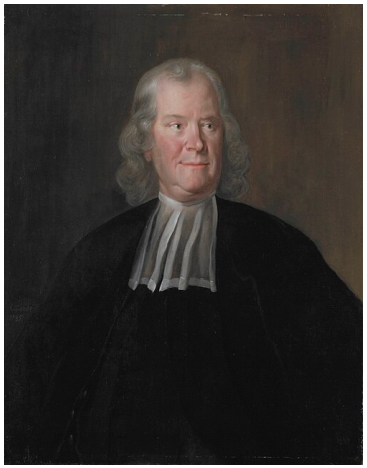
Das Boerhaave-Syndrom ist eine seltene, aber lebensbedrohliche Erkrankung, bei der es zu einem Riss (Ruptur) in der Speiseröhre (Ösophagus) kommt, meist ausgelöst durch starkes Erbrechen. Es ist eine Form der Ösophagusperforation und wird auch als spontane Ösophagusruptur bezeichnet.

Das Boerhaave-Syndrom, welches nach ihm benannt wurde, bezeichnet die Ruptur der Speiseröhre bei heftigem Würgen, Husten oder Erbrechen. Boerhaave soll selbst gern an ausschweifenden Essgelagen teilgenommen haben. Als dabei einmal einem Freund die Speiseröhre riss und dieser anschließend starb, wurde er kurz nach seinem Tod durch Boerhaave obduziert. Dieser erkannte die Todesursache und gab ihr seinen Namen.

Boerhaave-Syndrom

Ruptur aller Wandschichten des Ösophagus
>90% ist diese Ruptur im distalen Drittel des Ösophagus
retrosternale Sschmerzen nach massivem Erbrechen





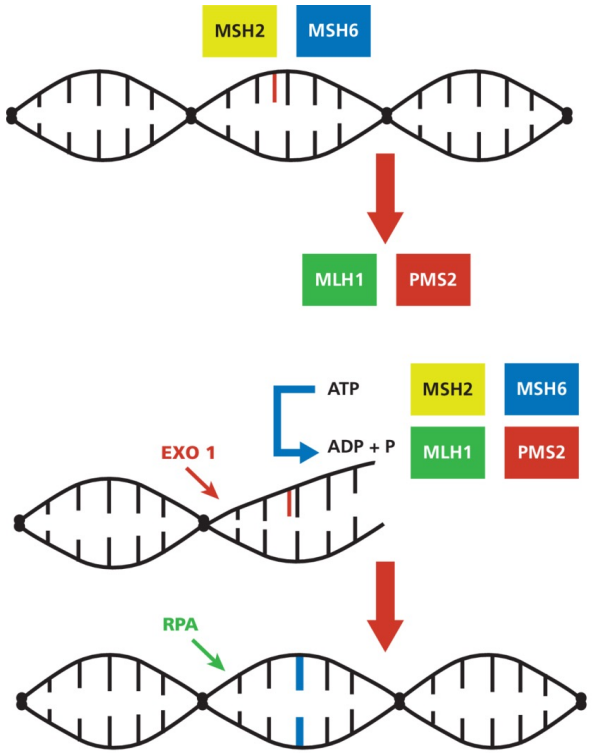
Herman Boerhaave 31. Dezember 1668 in Voorhout; † 23. September 1738 in Leiden) war ein niederländischer Mediziner, Chemiker und Botaniker. Er war Hochschullehrer (Professor) in Leiden. Sein botanisches Autorenkürzel lautet „Boerh.“.

Eine DNA-Mismatch-Reparatur (MMR) ist ein zellulärer Mechanismus, der DNA-Basenfehlpaarungen (Mismatches) und kleine Insertionen/Deletionen, die während der DNA-Replikation oder durch andere Schäden entstehen, korrigiert. Dieser Prozess trägt zur Aufrechterhaltung der genetischen Stabilität bei, indem er Fehler in der DNA-Sequenz beseitigt.

Was ist eine DNA-Fehlpaarung?
Eine DNA-Fehlpaarung (Mismatch) liegt vor, wenn zwei Basen, die nicht komplementär zueinander sind, in der Doppelhelix des DNA-Moleküls nebeneinander liegen. Dies kann beispielsweise passieren, wenn während der Replikation eine falsche Base in den neu synthetisierten DNA-Strang eingebaut wird.

Erkennung:
Proteine, wie z.B. MutS-Homologe (MSH2, MSH3, MSH6 in Eukaryoten) binden an die Fehlpaarung und leiten den Reparaturprozess ein.

Entfernung:
Ein oder mehrere DNA-Abschnitte, die die Fehlpaarung enthalten, werden von Enzymen (Exonukleasen) entfernt.



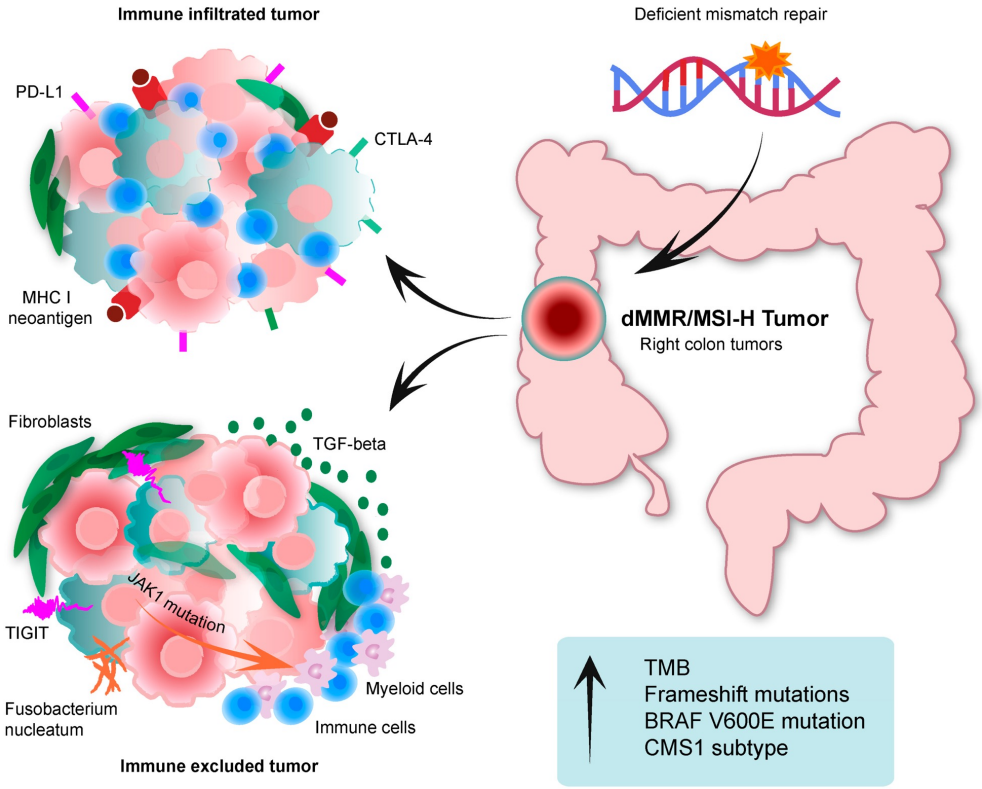
Mismatch repair mechanism. The MMR pathway consists of several steps: MSH2-MSH6 detects mismatch and recruits MLH1-PMS2, hence the complex activates EXO1, exonuclease 1, which proceeds to the excision at the strand break. The resulting DNA gap is filled by RPA, replication protein A and DNA polymerase.

dMMR steht für "defiziente Mismatch-Reparatur" (deficient mismatch repair). Es handelt sich um eine genetische Veränderung, bei der die Fähigkeit des Körpers, Fehler bei der DNA-Replikation zu reparieren, beeinträchtigt ist. Diese Fehlpaarungsreparatur (MMR) ist wichtig, um Mutationen und somit auch Krebs zu verhindern. Ein dMMR-Tumor hat eine erhöhte Wahrscheinlichkeit, Mutationen anzusammeln, was zu Krebs führen kann, insbesondere bei Darmkrebs, Endometriumkrebs und anderen gastrointestinalen Tumoren.

dMMR ist ein Mechanismus, der Fehler bei der DNA-Replikation korrigiert. Ein defektes MMR-System führt zu einer Anhäufung von Mutationen.

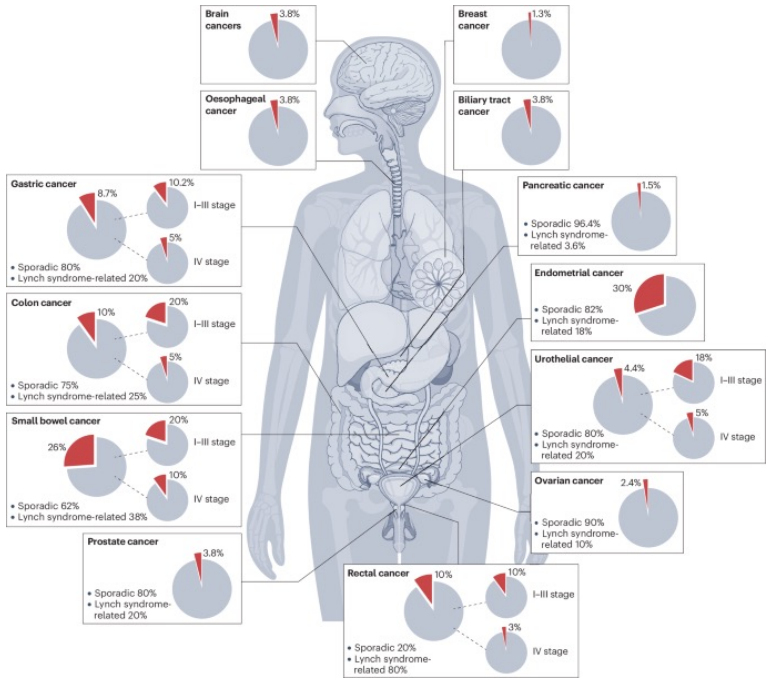
Wie wird dMMR festgestellt?

DMMR kann durch Tests auf Mikrosatelliteninstabilität (MSI) oder durch den Nachweis fehlender MMR-Proteine festgestellt werden



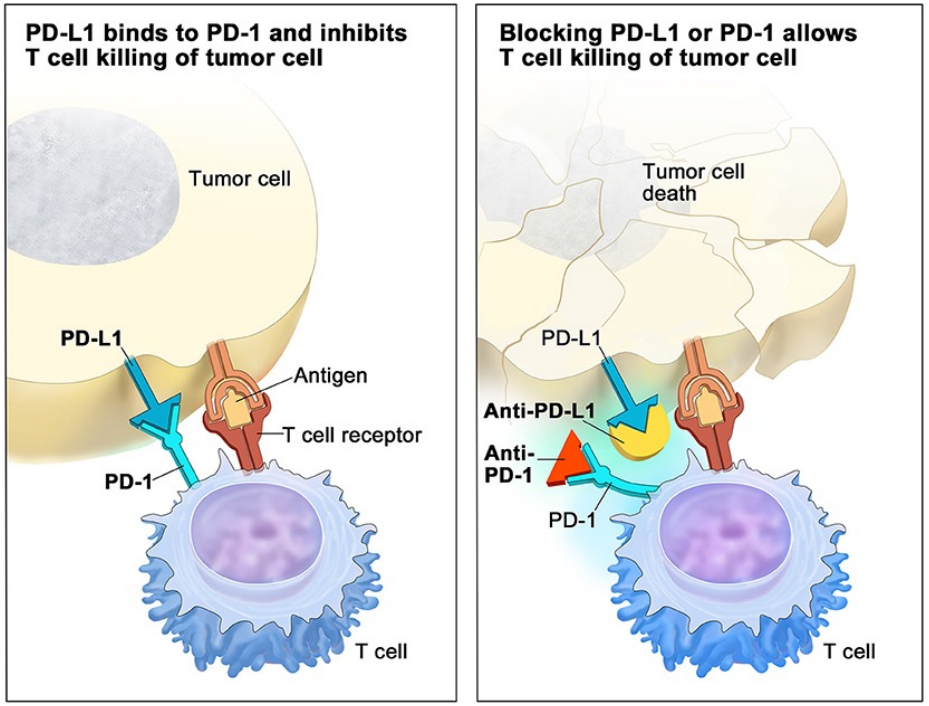
Epidemiology, pathogenesis, biology and evolving management of MSI-H/dMMR cancers

Deficiency in DNA mismatch repair (dMMR) is a common pathway of carcinogenesis across different tumour types and confers a characteristic microsatellite instability-high (MSI-H) molecular phenotype. The prevalence of the MSI-H/dMMR phenotype is highest in endometrial and colorectal cancers, and this phenotype is associated with a distinct tumour biology, prognosis and responsiveness to various anticancer treatments. Interest in this tumour molecular subtype has increased following the discovery of the high sensitivity of metastatic MSI-H/dMMR cancers to immune-checkpoint inhibitors (ICIs) in a histology-agnostic manner, which reflects the genomic hypermutation resulting from dMMR that renders these tumours highly immunogenic and immune infiltrated. This vulnerability is now also being exploited in early stage disease settings. Despite this common biological foundation, different MSI-H/dMMR cancers have histotype-specific features that correspond to their particular cell or tissue of origin, which might be associated with differences in prognosis and sensitivity to ICIs. In this Review, we provide an overview of the epidemiology, biology, pathogenesis, clinical diagnosis and treatment of MSI-H/dMMR tumours as a histology-agnostic cancer phenomenon. We also highlight peculiarities associated with specific pathogenetic alterations and histologies of MSI-H/dMMR tumours.



dMMR (mismatch repair deficient) tumors are highly immunogenic due to a high tumor mutational burden (TMB) and the resulting generation of numerous neoantigens. These neoantigens, which are essentially mutated protein fragments, are recognized as foreign by the immune system, triggering an immune response, particularly by T cells. This increased immunogenicity makes dMMR tumors highly responsive to immunotherapies like checkpoint inhibitors.

Neoantigen Production:
These mutations lead to the production of novel, mutated proteins (neoantigens) that are not normally present in the body.
Immune Recognition:
The immune system recognizes these neoantigens as foreign and mounts a T cell response against the tumor cells.
Immunotherapy Response:
This robust immune response makes dMMR tumors highly susceptible to immunotherapies that block immune checkpoints, such as PD-1 and CTLA-4, allowing the T cells to effectively target and kill the cancer cells.



Nonoperative Management of Mismatch Repair–Deficient Tumors

Background

Among patients with mismatch repair–deficient (dMMR), locally advanced rectal cancer, neoadjuvant checkpoint blockade eliminated the need for surgery in a high proportion of patients. Whether this approach can be extended to all early-stage dMMR solid tumors, regardless of tumor site, is unknown.

Methods

We conducted a phase 2 study in which patients with stage I, II, or III dMMR solid tumors that were amenable to curative-intent surgery were treated with neoadjuvant dostarlimab, a programmed cell death 1 (PD-1) blocking agent, for 6 months. The response to treatment was assessed in two cohorts: patients in cohort 1 had dMMR, locally advanced rectal cancer, and patients in cohort 2 had dMMR nonrectal solid tumors. Patients with a clinical complete response could elect to proceed with nonoperative management; those with residual disease were to undergo resection. In this analysis, the primary end point, assessed in cohort 1, was a sustained clinical complete response at 12 months. Recurrence-free survival and safety were evaluated.

Conclusions

Among patients with early-stage dMMR solid tumors that were amenable to curative-intent surgery, neoadjuvant PD-1 blockade led to organ preservation in a high proportion of patients.

Mismatch repair–deficient (dMMR) tumors are highly sensitive to immune checkpoint blockade, and in the context of metastatic disease, a substantial clinical benefit has been seen with this treatment across tumor types. This finding resulted in the first tumor-agnostic approval by the Food and Drug Administration, with immune checkpoint blockade indicated for all metastatic dMMR cancers, regardless of tumor site. As neoadjuvant therapy, immune checkpoint blockade has resulted in elimination of the primary tumor in patients with colorectal cancers, and for rectal cancer specifically, data from our earlier study suggested that surgery can be averted when a clinical complete response is attained.

The complete elimination of dMMR primary tumors with the use of programmed cell death 1 (PD-1) blockade alone in patients with rectal cancer has led to the question of whether this approach could be extended beyond rectal cancer to all early-stage dMMR solid tumors, regardless of tumor site — mirroring the benefit of immune checkpoint blockade across metastatic dMMR cancers. The potential effect is substantial, given that 2 to 3% of all early-stage solid tumors have an dMMR phenotype.

Despite data supporting the efficacy of this treatment for metastatic disease, a concern with neoadjuvant therapy is that the “window of opportunity” for curative resection may lapse if the tumor progresses and becomes unresectable during the course of treatment with an immune checkpoint inhibitor.

To test the premise of nonoperative management of early-stage dMMR solid tumors, patients were treated with neoadjuvant dostarlimab, a PD-1 blocking agent, for 6 months and were monitored for response, progression, or recurrence.

Methods

Patients

Patients underwent screening at Memorial Sloan Kettering Cancer Center, Hartford HealthCare, and Baptist Health Miami Cancer Institute. Patients were referred for enrollment in the study if they had a newly diagnosed stage I, II, or III solid tumor that was amenable to curative-intent surgery and was dMMR, with loss of expression of MLH1, MSH2, MSH6, or PMS2 on immunohistochemical staining.

Study Design

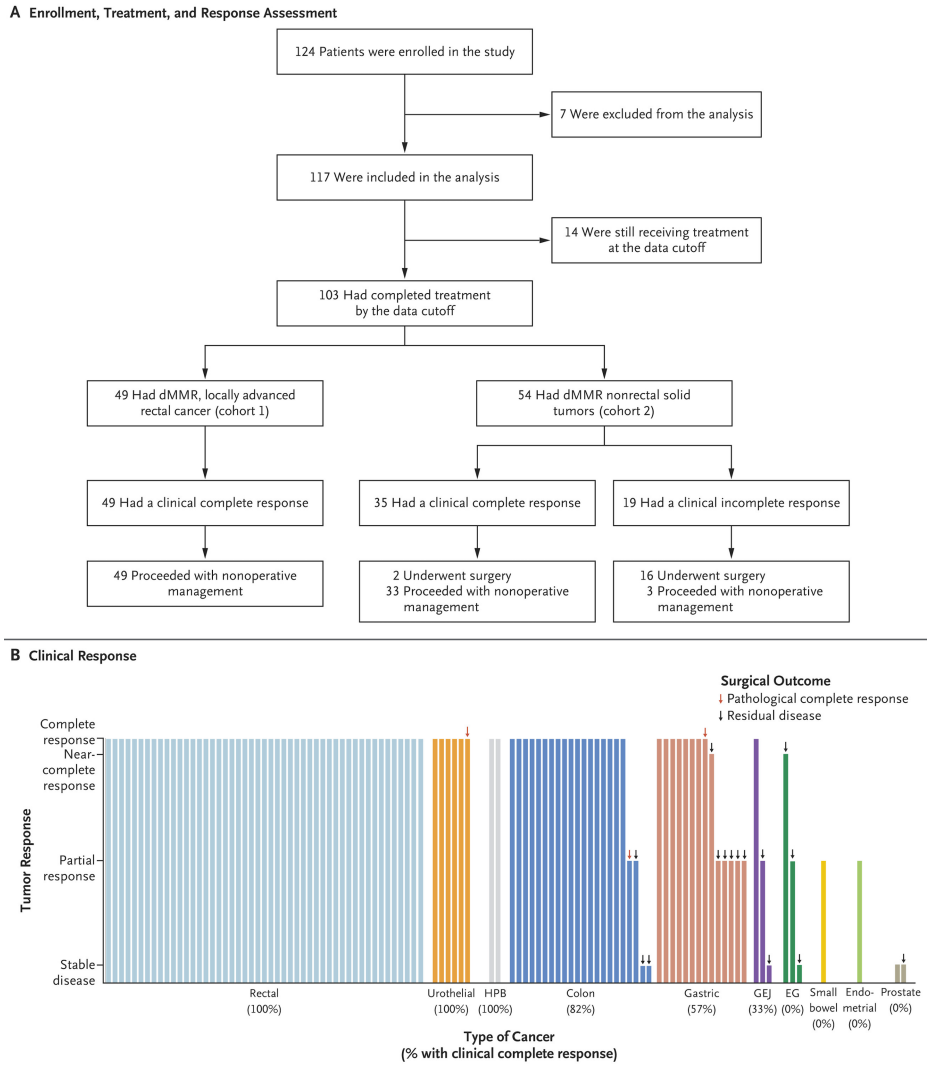
This phase 2 study was designed to evaluate the response to neoadjuvant dostarlimab, which was administered intravenously at a dose of 500 mg every 3 weeks for 6 months (nine cycles), in two cohorts: patients in cohort 1 had dMMR, locally advanced rectal cancer, and patients in cohort 2 had dMMR nonrectal solid tumors.

End Points

The first primary end point was overall response. The second primary end point was a sustained clinical complete response at 12 months after completion of dostarlimab therapy, with or without chemoradiotherapy, in patients who had not undergone surgery or had proceeded to surgery and had a pathological complete response.

Tumor Genomic Analyses

Genomic sequencing was performed on DNA from tumor tissue and matched normal blood samples for the detection of somatic and germline genomic alterations.



Enrollment, Treatment, and Response Assessment.

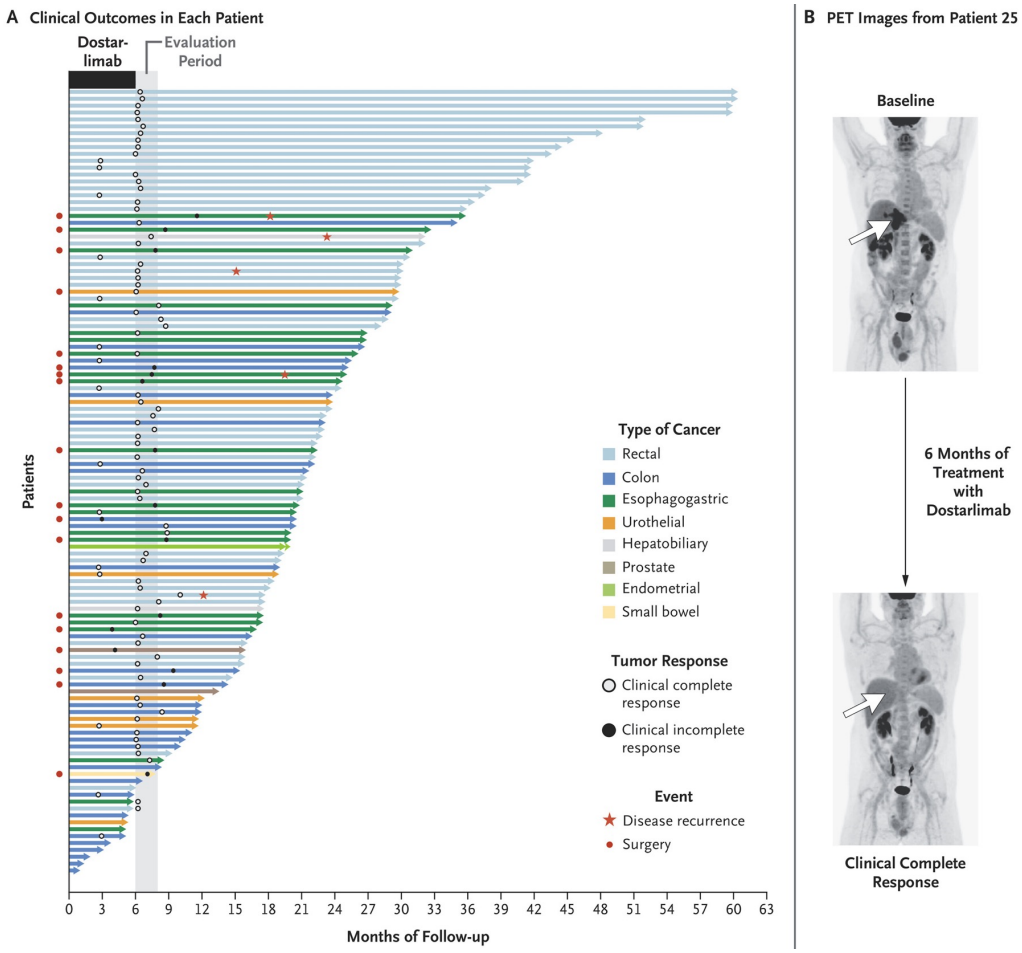
Panel A shows the distribution of patients after enrollment, treatment, and response assessment. Panel B shows the clinical response for each patient according to tumor type. Hepatobiliary (HPB) cancers consist of periampullary cancer and cholangiocarcinoma. EG denotes esophageal and GEJ gastroesophageal junction.

Characteristics of the Patients and the Tumors at Baseline.

Characteristic	Cohorts 1 and 2 (N=117)	Cohort 1 (N=50)	Cohort 2 (N=67)
Sex — no. (%)			
Female	57 (49)	28 (56)	29 (43)
Male	60 (51)	22 (44)	38 (57)
Median age (range) — yr	57.0 (26–87)	51.0 (26–78)	67.0 (28–87)
ECOG performance-status score — no. (%)†			
0	88 (75)	40 (80)	48 (72)
1	29 (25)	10 (20)	19 (28)
Tumor type — no. (%)			
Rectal cancer	50 (43)	50 (100)	0
Colon cancer	33 (28)	0	33 (49)
Esophageal cancer	3 (3)	0	3 (4)
Gastroesophageal junction cancer	3 (3)	0	3 (4)
Gastric cancer	15 (13)	0	15 (22)
Urothelial cancer	7 (6)	0	7 (10)
Prostate cancer	2 (2)	0	2 (3)
Periampullary cancer	1 (1)	0	1 (1)
Cholangiocarcinoma	1 (1)	0	1 (1)
Small-bowel cancer	1 (1)	0	1 (1)
Endometrial cancer	1 (1)	0	1 (1)
Clinical tumor stage — no. (%)			
T0	1 (1)	1 (2)	0
T1–2	27 (23)	10 (20)	17 (25)
T3	65 (56)	23 (46)	42 (63)
T4	24 (21)	16 (32)	8 (12)
Clinical nodal stage — no. (%)			
Node-positive	75 (64)	42 (84)	33 (49)
Node-negative	42 (36)	8 (16)	34 (51)
Mismatch-repair gene with pathogenic Lynch syndrome–associated germline variants — no. (%)			
MLH1	16 (14)	7 (14)	9 (13)
MSH2	23 (20)	9 (18)	14 (21)
MSH6	12 (10)	8 (16)	4 (6)
None	60 (51)	23 (46)	37 (55)
Unknown	6 (5)	3 (6)	3 (4)
Deficient mismatch-repair proteins on immunohistochemical staining — no. (%)			
MLH1 and PMS2	61 (52)	21 (42)	40 (60)
MSH2 and MSH6	37 (32)	16 (32)	21 (31)
MLH1 and MSH6	1 (1)	0	1 (1)
MSH2 alone	3 (3)	3 (6)	0
MSH6 alone	9 (8)	5 (10)	4 (6)
PMS2 alone	6 (5)	5 (10)	1 (1)
Median microsatellite instability sensor score (range)‡	18.8 (0.2–39.4)	19.3 (2.2–37.6)	18.7 (0.2–39.4)
Median tumor mutational burden (range) — mutations per megabase§	53.2 (4.9–145.0)	62.3 (27.2–106.3)	50.3 (4.9–145.0)

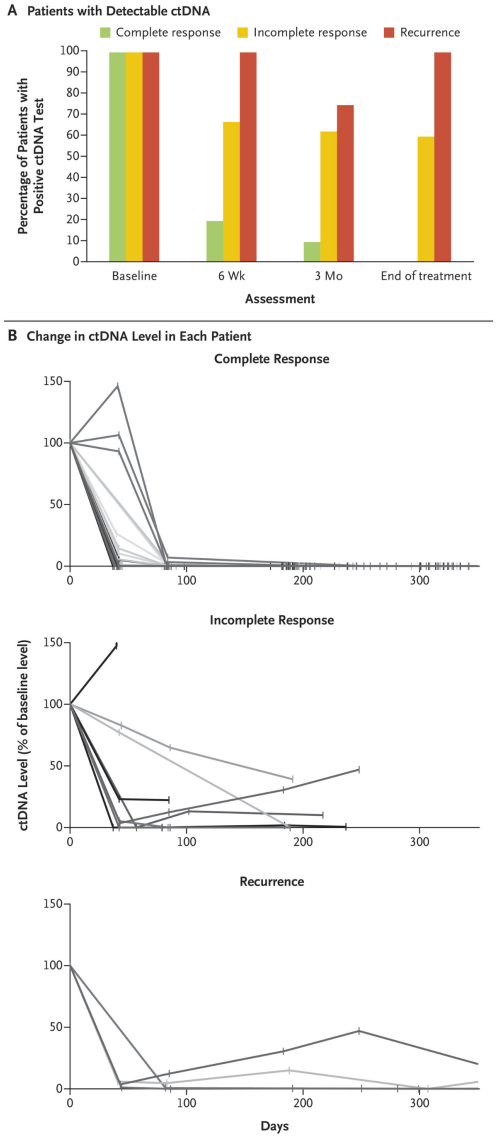
Adverse Events.

Event	Cohorts 1 and 2 (N=124)	
	Grade 1 or 2†	Grade 3 or 4
	number of patients (percent)	
Dermatologic		
Rash or dermatitis	26 (21)	0
Flushing	2 (2)	0
Pruritus	24 (19)	0
Dry skin	5 (4)	0
Gastrointestinal		
Colitis	2 (2)	0
Constipation	4 (3)	0
Diarrhea	11 (9)	0
Nausea	8 (6)	0
Dry mouth	8 (6)	0
Constitutional		
Fatigue	28 (23)	0
Chills	4 (3)	0
Fever	3 (2)	0
Myalgia	3 (2)	0
Hot flashes	2 (2)	0
Arthralgia	9 (7)	0
Arthritis	2 (2)	0
Neurologic		
Headache	4 (3)	0
Encephalitis	0	1 (1)
Endocrine		
Diabetes	0	1 (1)
Hyperthyroidism	4 (3)	0
Hypothyroidism	16 (13)	1 (1)
Respiratory		
Cough	2 (2)	0
Lung infection	0	1 (1)
Renal, hydration, or nutrition		
Increased creatinine level	2 (2)	0
Ophthalmologic		
Dry eye	3 (2)	0
Other		
Decreased neutrophil count	0	1 (1)
Febrile neutropenia	0	1 (1)
Infusion-related reaction	3 (2)	0



Clinical Outcomes.

Panel A shows a swimmer plot of clinical outcomes for each patient according to tumor type. Esophagogastric cancers consist of esophageal, gastroesophageal junction, and gastric cancers; hepatobiliary cancers consist of periampullary cancer and cholangiocarcinoma. Panel B shows axial positron-emission tomographic (PET) images from Patient 25, who had mismatch repair–deficient, localized intrahepatic cholangiocarcinoma. The top image shows the tumor at baseline, and the bottom image shows a clinical complete response after the administration of dostarlimab therapy for 6 months.



Clearance of Circulating Tumor DNA According to Clinical Response.

Panel A shows the percentage of patients who had detectable circulating tumor DNA (ctDNA) over time according to clinical response. Panel B shows the change in the ctDNA level in each patient over time according to clinical response.

Discussion

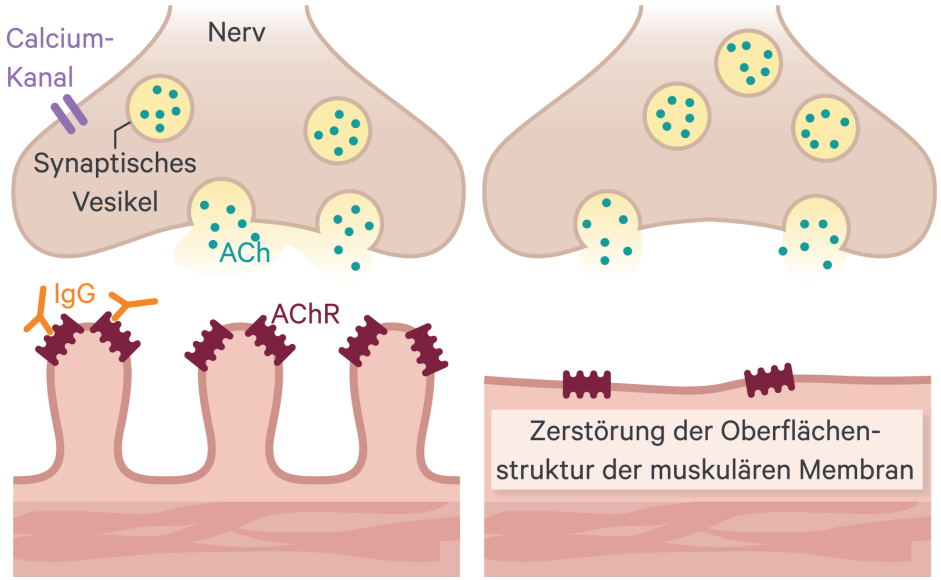
The data from this study, which were obtained from a small group of patients with stage I, II, or III dMMR solid tumors, showed that neoadjuvant PD-1 blockade enabled a nonoperative management strategy in a high proportion of patients. As seen in the context of metastatic disease, the efficacy of immune checkpoint blockade appeared to be relatively tumor-agnostic, driven primarily by the dMMR phenotype rather than the tumor site of origin.

Among patients with dMMR solid tumors that were amenable to curative-intent surgery, the use of neoadjuvant PD-1 blockade for 6 months was associated with few adverse events. The option for curative resection was not compromised in any of the patients, although the course of treatment was longer than that in other studies of neoadjuvant therapy. A major concern with neoadjuvant therapy is that the “window of opportunity” for resection may lapse if the tumor grows and spreads to the point of no longer being amenable to curative-intent surgery. Therefore, the duration of treatment is often limited to a few cycles. To maximize the clinical response, we administered immune checkpoint blockade for 6 months — a duration of treatment that in previous studies appeared to result in a higher clinical complete response rate than shorter durations. Organs were preserved without additional therapy. Three patients who had rectal cancer were subsequently able to conceive and deliver healthy children, which would not have been possible with standard treatment for rectal cancer.

Among patients who did not have a clinical complete response, the most common tumor types were prostate and gastroesophageal tumors. Beyond these cases, the reason that different sites of primary disease were associated with different results for clinical complete response is unclear. The microbiome and other cellular components of the tumor microenvironment, such as myeloid cells, and the underlying tumor heterogeneity probably contributed to these outcomes. It is possible that a longer duration of treatment or the administration of combination immune checkpoint blockade would have led to a complete response in these patients.

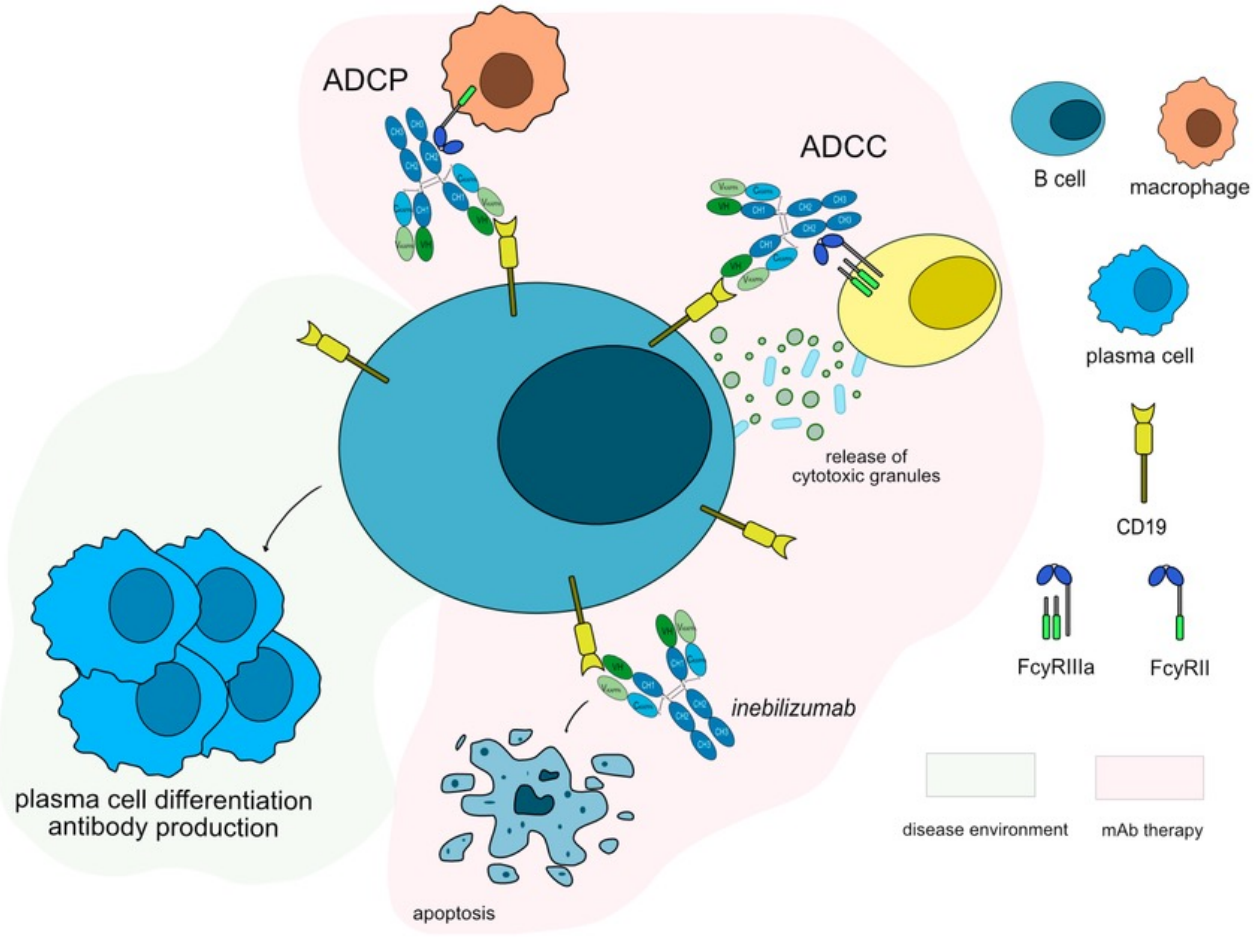
This study provides a foundation for altering the traditional therapeutic paradigm for early-stage dMMR solid tumors and eliminating the need for surgery and other therapies in most patients.

Myasthenie, auch bekannt als Myasthenia gravis, ist eine seltene autoimmune Erkrankung. Krankhafte Antikörper verwechseln das eigene Gewebe mit Fremdkörpern und bekämpfen es. Die Kommunikation zwischen den Nerven und Muskeln wird nachhaltig gestört. Typischerweise macht sich das zunächst an den Augen bemerkbar.



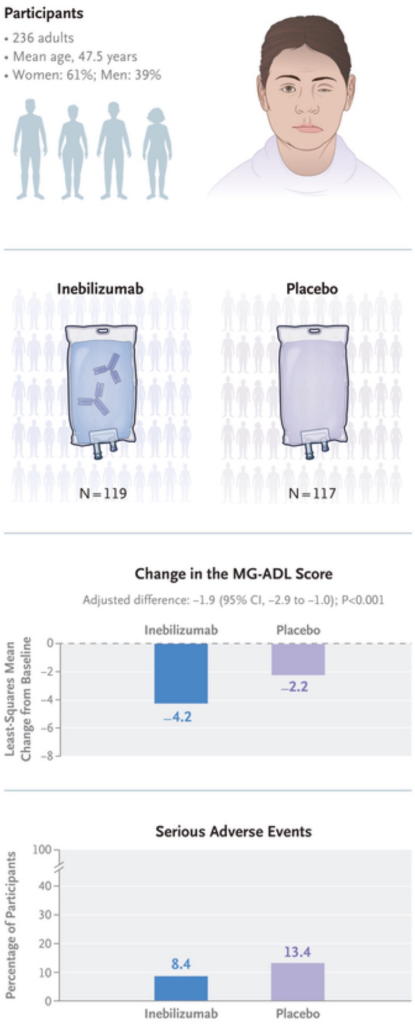


Inebilizumab



A Phase 3 Trial of Inebilizumab in Generalized Myasthenia Gravis

Autoimmune generalized myasthenia gravis is a disease that manifests with fluctuating muscle weakness. Inebilizumab is a monoclonal antibody that depletes CD19+ B cells, which are central to disease pathogenesis. In this phase 3, double-blind, randomized, placebo-controlled trial, we enrolled participants with myasthenia gravis who had anti–acetylcholine receptor antibodies or anti–muscle-specific kinase antibodies. Participants were randomly assigned, in a 1:1 ratio, to receive intravenous inebilizumab (300 mg administered on days 1 and 15 for all, and additionally on day 183 for participants who were acetylcholine receptor antibody–positive) or matching placebo for 52 weeks (in participants who were acetylcholine receptor antibody–positive) or 26 weeks (in those who were muscle-specific kinase antibody–positive). Glucocorticoid therapy was tapered, starting at week 4, to a target of 5 mg per day by week 24. The primary end point was the change from baseline in the score on the Myasthenia Gravis Activities of Daily Living scale (MG-ADL; scores range from 0 to 24, with higher scores indicating greater disease activity) at week 26 in the combined acetylcholine receptor antibody–positive and muscle-specific kinase antibody–positive trial populations. A key secondary end point was the change from baseline in the score on the Quantitative Myasthenia Gravis scale (QMG; scores range from 0 to 39, with higher scores indicating greater disease activity) at week 26 in the combined population. Safety was assessed.



Autoimmune myasthenia gravis is a disorder in which autoreactive B cells (including antibody-secreting plasmablasts and plasma cells) produce autoantibodies that affect postsynaptic neuromuscular transmission by targeting acetylcholine receptors or related molecules, causing fluctuating muscle weakness. Most patients have generalized myasthenia gravis, and approximately 80% have detectable antibodies against acetylcholine receptors; however, a smaller percentage (7 to 10%) have detectable antibodies against muscle-specific kinase. Although patients with different antibody subtypes may present with similar symptoms, the underlying immunopathologic features are distinct. Long-lived plasma cells (CD19+ and, more commonly, CD20−) are believed to be the primary source of acetylcholine receptor autoantibodies, whereas short-lived plasmablasts (CD19+ and CD20+) may be the main source of muscle-specific kinase autoantibodies.

Participants

Participants were positive for anti–acetylcholine receptor antibodies or anti–muscle-specific kinase antibodies, were at least 18 years of age, and had received a diagnosis of generalized myasthenia gravis.

End Points

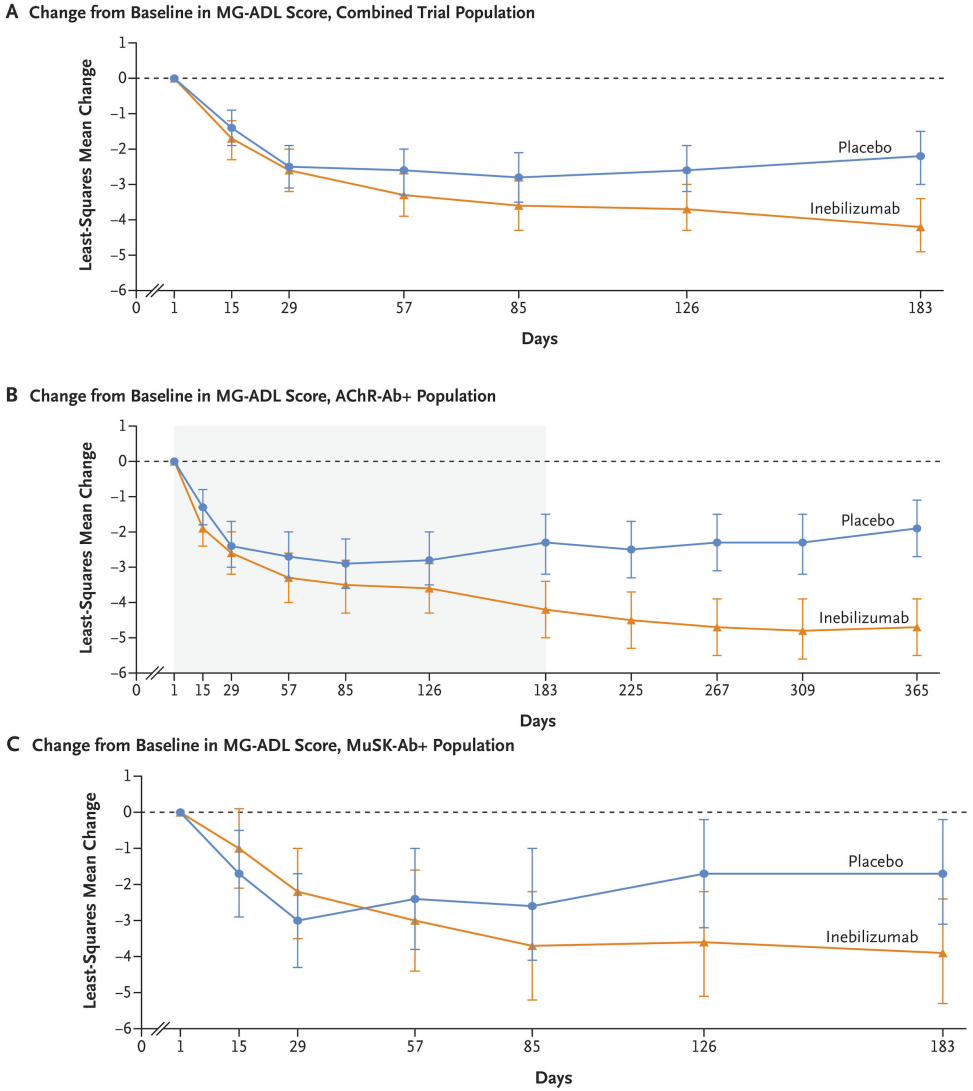
The primary end point was the change from baseline in the MG-ADL score at week 26 in the combined population, a revision from the original primary end point that separated the two subpopulations at different time points.

Demographic and Clinical Characteristics of the Participants

Characteristic	Full Analysis Population			Acetylcholine Receptor Antibody–Positive Participants		Muscle-Specific Kinase Antibody–Positive Participants	
	Placebo (N=117)	Inebilizumab (N=119)	Overall (N=236)	Placebo (N=93)	Inebilizumab (N=95)	Placebo (N=24)	Inebilizumab (N=24)
Mean age — yr	47.9±15.0	47.1±15.7	47.5±15.3	48.9±15.4	46.9±16.3	43.9±12.8	47.5±13.3
Female sex — no. (%)	65 (56)	79 (66)	144 (61)	48 (52)	60 (63)	17 (71)	19 (79)
Mean body-mass index†	27.8±8.8	27.1±6.2	27.4±7.6	28.3±9.0	27.6±6.5	25.7±7.9	25.1±4.7
Race or ethnic group — no. (%)‡							
Hispanic or Latino	8 (7)	9 (8)	17 (7)	5 (5)	8 (8)	3 (12)	1 (4)
American Indian or Alaska Native	1 (1)	—	1 (<1)	1 (1)	—	—	—
Asian	54 (46)	46 (39)	100 (42)	39 (42)	31 (33)	15 (62)	15 (62)
Black or African American	3 (3)	2 (2)	5 (2)	2 (2)	2 (2)	1 (4)	—
White	56 (48)	69 (58)	125 (53)	48 (52)	60 (63)	8 (33)	9 (38)
MG-ADL score	9.1±2.8	9.0±2.8	9.1±2.8	9.3±2.8	9.1±2.7	8.3±2.5	8.8±3.1
QMG score§	17.3±4.2	16.7±4.2	17.0±4.2	17.3±4.3	16.9±4.1	17.2±3.9	16.1±4.8
MGFA class — no. (%)¶							
II	48 (41)	56 (47)	104 (44)	36 (39)	43 (45)	12 (50)	13 (54)
III	61 (52)	58 (49)	119 (50)	49 (53)	49 (52)	12 (50)	9 (38)
IV	7 (6)	4 (3)	11 (5)	7 (8)	3 (3)	—	1 (4)
Thymoma — no. (%)	14 (12)	18 (15)	32 (14)	12 (13)	16 (17)	2 (8)	2 (8)
Thymectomy — no. (%)	32 (27)	29 (24)	61 (26)	28 (30)	26 (27)	4 (17)	3 (12)
Mean daily dose of glucocorticoids at baseline — mg	18.8±13.0	17.0±12.5	17.5±12.0	17.8±12.1	18.2±12.9	22.4±15.7	12.6±9.8
Glucocorticoid or immunosuppressive therapy — no. (%)							
Glucocorticoid only	68 (58)	82 (69)	150 (64)	56 (60)	69 (73)	12 (50)	13 (54)
Nonsteroidal immunosuppressive therapy only	9 (8)	8 (7)	17 (7)	8 (9)	5 (5)	1 (4)	3 (12)
Glucocorticoid plus one nonsteroidal immunosuppressive therapy	39 (33)	29 (24)	68 (29)	28 (30)	21 (22)	11 (46)	8 (33)
Type of nonsteroidal immunosuppressive therapy — no. (%)							
Azathioprine	29 (25)	28 (24)	57 (24)	22 (24)	20 (21)	7 (29)	8 (33)
Mycophenolate mofetil	16 (14)	7 (6)	23 (10)	13 (14)	5 (5)	3 (12)	2 (8)
Mycophenolic acid	—	1 (1)	1 (<1)	—	1 (1)	—	—
Tacrolimus‖	3 (3)	1 (1)	4 (2)	1 (1)	—	2 (8)	1 (4)

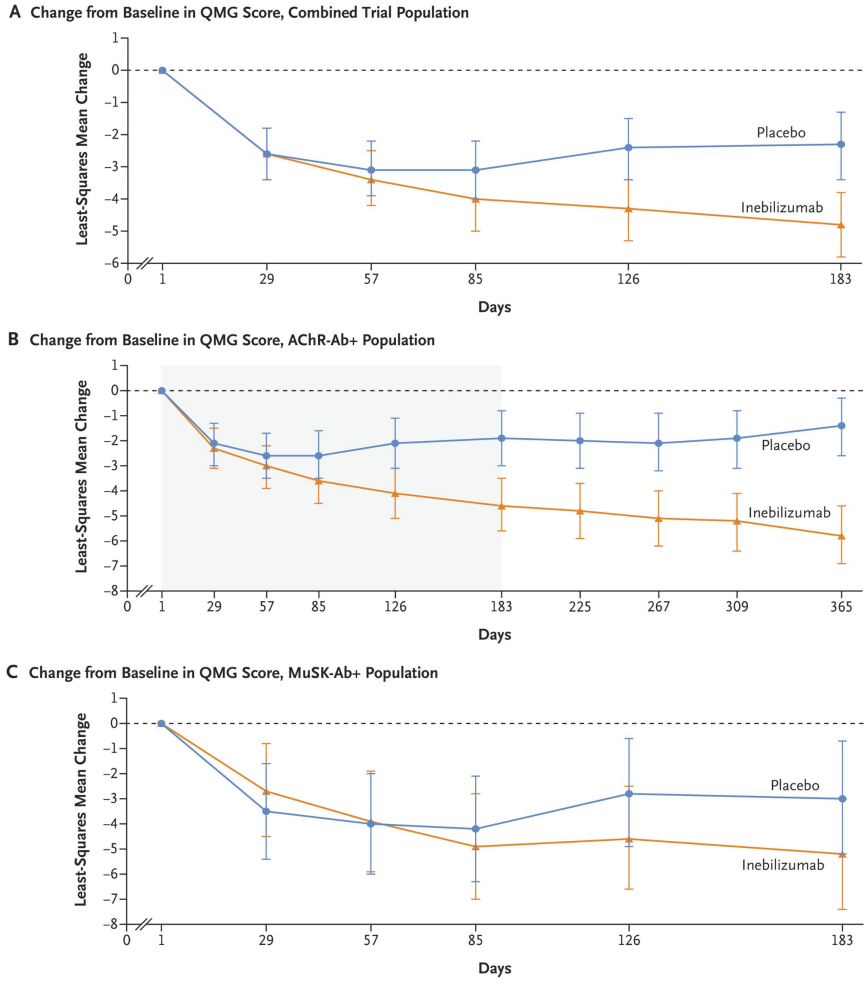
Primary and Key Secondary End Points (Full Analysis Population).

End Point	Placebo (N=117)	Inebilizumab (N=119)	P Value
Primary end point: change from baseline in MG-ADL score at wk 26 in the combined trial population†			
Least-squares mean (95% CI)	−2.2 (−3.0 to −1.5)	−4.2 (−4.9 to −3.4)	
Difference (95% CI)		−1.9 (−2.9 to −1.0)	<0.001
Key secondary end points			
Change from baseline in QMG score at wk 26 in the combined trial population			
Least-squares mean (95% CI)	−2.3 (−3.4 to −1.3)	−4.8 (−5.8 to −3.8)	
Difference (95% CI)		−2.5 (−3.8 to −1.2)	<0.001
Change from baseline in MG-ADL score at wk 26 in the acetylcholine receptor antibody–positive population			
No. of participants in primary analysis population	93	95	
Least-squares mean (95% CI)	−2.4 (−3.2 to −1.6)	−4.2 (−5.0 to −3.4)	
Difference (95% CI)		−1.8 (−2.9 to −0.7)	0.002
Change from baseline in QMG score at wk 26 in the acetylcholine receptor antibody–positive population			
No. of participants in primary analysis population	93	95	
Least-squares mean (95% CI)	−2.0 (−3.1 to −0.9)	−4.4 (−5.5 to −3.3)	
Difference (95% CI)		−2.5 (−3.9 to −1.0)	0.001
Change from baseline in MG-ADL score at wk 26 in the muscle-specific kinase antibody–positive population			
No. of participants in primary analysis population	24	24	
Least-squares mean (95% CI)	−1.7 (−3.1 to −0.2)	−3.9 (−5.3 to −2.4)	
Difference (95% CI)		−2.2 (−4.2 to −0.2)	0.03
Change from baseline in QMG score at wk 26 in the muscle-specific kinase antibody–positive population			
No. of participants in primary analysis population	24	24	
Least-squares mean (95% CI)	−3.0 (−5.2 to −0.7)	−5.2 (−7.4 to −3.0)	
Difference (95% CI)		−2.3 (−5.3 to 0.7)	0.13



Change from Baseline in MG-ADL Score (Full Analysis Population).

Panel A shows the least-squares mean change from baseline in the score on the Myasthenia Gravis Activities of Daily Living scale (MG-ADL; scores range from 0 [normal] to 24 [severe]) for the combined trial population (which included both the acetylcholine receptor antibody–positive [AChR-Ab+] and muscle-specific kinase antibody–positive [MuSK-Ab+] populations) by week 26 (the primary end point). Panel B shows the least-squares mean change in the MG-ADL score from baseline for participants in the AChR-Ab+ population during the 52-week randomized, controlled period; shading denotes the 26-week primary-analysis period. Panel C shows the least-squares mean change in the MG-ADL score from baseline for participants in the MuSK-Ab+ population during the 26-week randomized, controlled period. Widths of the confidence intervals have not been adjusted for multiplicity and should not be used in place of hypothesis testing. The full analysis population included all the participants who underwent randomization, received at least one dose of inebilizumab or placebo, and had a baseline MG-ADL score and at least one postbaseline MG-ADL score.



Change from Baseline in QMG Score (Full Analysis Population).

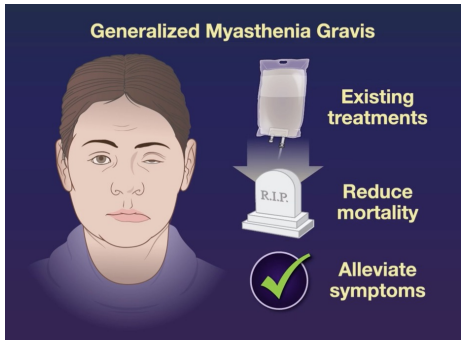
Panel A shows the least-squares mean change from baseline in the score on the Quantitative Myasthenia Gravis scale (QMG; a 13-item scale with cumulative scores ranging from 0 [normal] to 39 [severe]) in the combined trial population (which included both the AChR-Ab+ and MuSK-Ab+ populations) by week 26. Panel B shows the least-squares mean change from baseline in the QMG score during the 52-week randomized, controlled period in the AChR-Ab+ population; shading denotes the 26-week primary-analysis period. Panel C shows the least-squares mean change from baseline in the QMG score. Widths of the confidence intervals have not been adjusted for multiplicity and should not be used in place of hypothesis testing. The full analysis population included all the participants who underwent randomization, received at least one dose of inebilizumab or placebo, and had a baseline MG-ADL score and at least one postbaseline MG-ADL score.

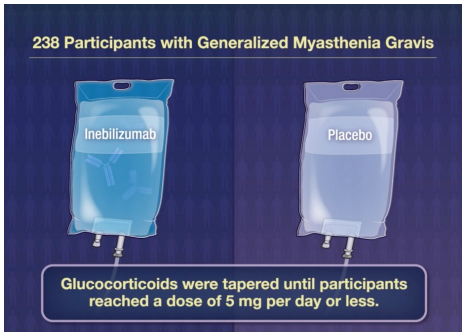
Summary of Adverse Events Occurring during the Randomized, Controlled Period (Safety Analysis Population).

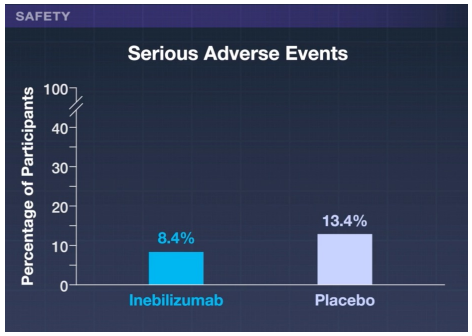
Adverse Event	Placebo (N=119)	Inebilizumab (N=119)
	number (percent)	
At least one adverse event	87 (73.1)	96 (80.7)
At least one adverse event related to inebilizumab or placebo	22 (18.5)	20 (16.8)
At least one serious adverse event	16 (13.4)	10 (8.4)
At least one adverse event leading to discontinuation of inebilizumab or placebo	1 (0.8)	3 (2.5)
At least one adverse event of special interest	19 (16.0)	12 (10.1)
Death†	2 (1.7)	1 (0.8)
Adverse events occurring in ≥5% of participants		
Arthralgia	8 (6.7)	5 (4.2)
Coronavirus disease 2019	12 (10.1)	13 (10.9)
Cough	4 (3.4)	8 (6.7)
Diarrhea	8 (6.7)	4 (3.4)
Headache	8 (6.7)	18 (15.1)
Hypertension	8 (6.7)	2 (1.7)
Infusion-related reaction	3 (2.5)	7 (5.9)
Nasopharyngitis	3 (2.5)	8 (6.7)
Upper respiratory tract infection	7 (5.9)	4 (3.4)
Urinary tract infection	3 (2.5)	8 (6.7)

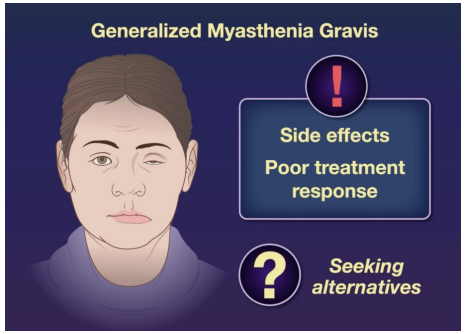
Discussion

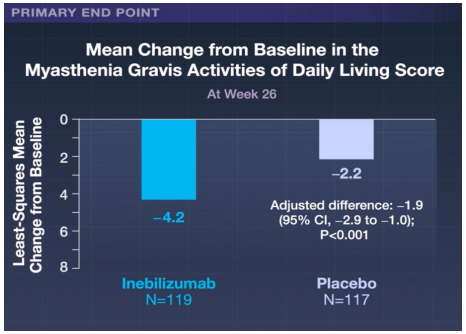
This phase 3 trial provided evidence for the efficacy and safety of inebilizumab in adults with generalized myasthenia gravis. Improvements in the inebilizumab group were apparent across outcome measures. A −1.9-point difference relative to placebo in the mean change from the baseline in the MG-ADL score and a −2.5-point difference in the mean change from the baseline in the QMG score at week 26 were observed in the combined trial population. In both the acetylcholine receptor antibody–positive and muscle-specific kinase antibody–positive subpopulations at week 26, improvements were seen in the mean MG-ADL score; however, the difference in the mean QMG score at week 26 for the muscle-specific kinase antibody–positive subpopulation was not significant. In addition, more participants treated with inebilizumab had an improvement of at least 3 points in the mean MG-ADL score.

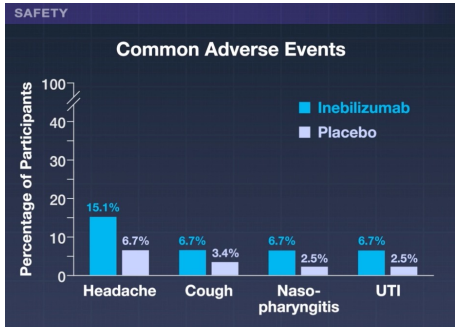

Generalized Myasthenia Gravis
Existing treatments
Reduce mortality
Alleviate symptoms
R.I.P.

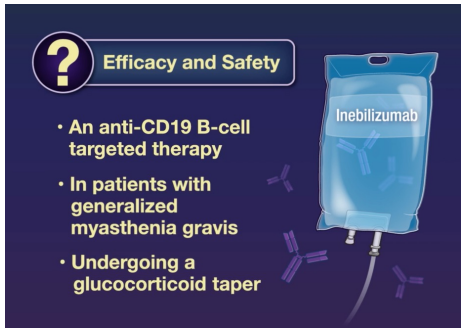

238 Participants with Generalized Myasthenia Gravis
Inebilizumab
Placebo
Glucocorticoids were tapered until participants reached a dose of 5 mg per day or less.

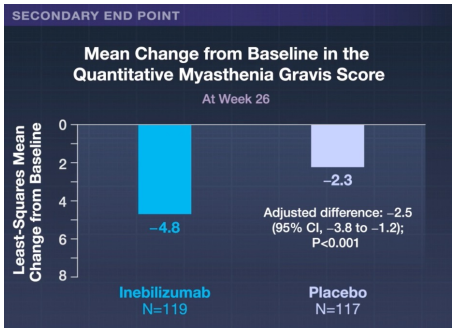

SAFETY
Serious Adverse Events
Percentage of Participants
100
40
30
20
10
0
8.4%
13.4%
Inebilizumab
Placebo


Generalized Myasthenia Gravis
Side effects
Poor treatment response
Seeking alternatives


PRIMARY END POINT
Mean Change from Baseline in the Myasthenia Gravis Activities of Daily Living Score
At Week 26
Least-Squares Mean Change from Baseline
0
2
4
6
8
−4.2
−2.2
Adjusted difference: −1.9 (95% CI, −2.9 to −1.0); P<0.001
Inebilizumab N=119
Placebo N=117

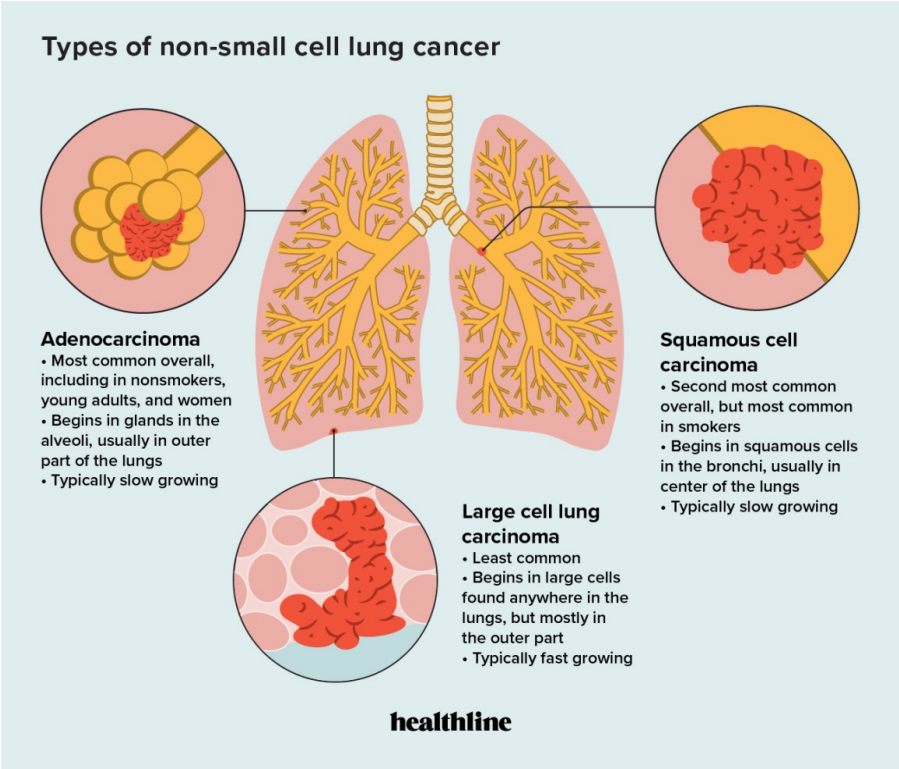

SAFETY
Common Adverse Events
Inebilizumab
Placebo
Percentage of Participants
100
40
30
20
10
0
15.1%
6.7%
6.7%
3.4%
6.7%
2.5%
6.7%
2.5%
Headache
Cough
Naso-pharyngitis
UTI

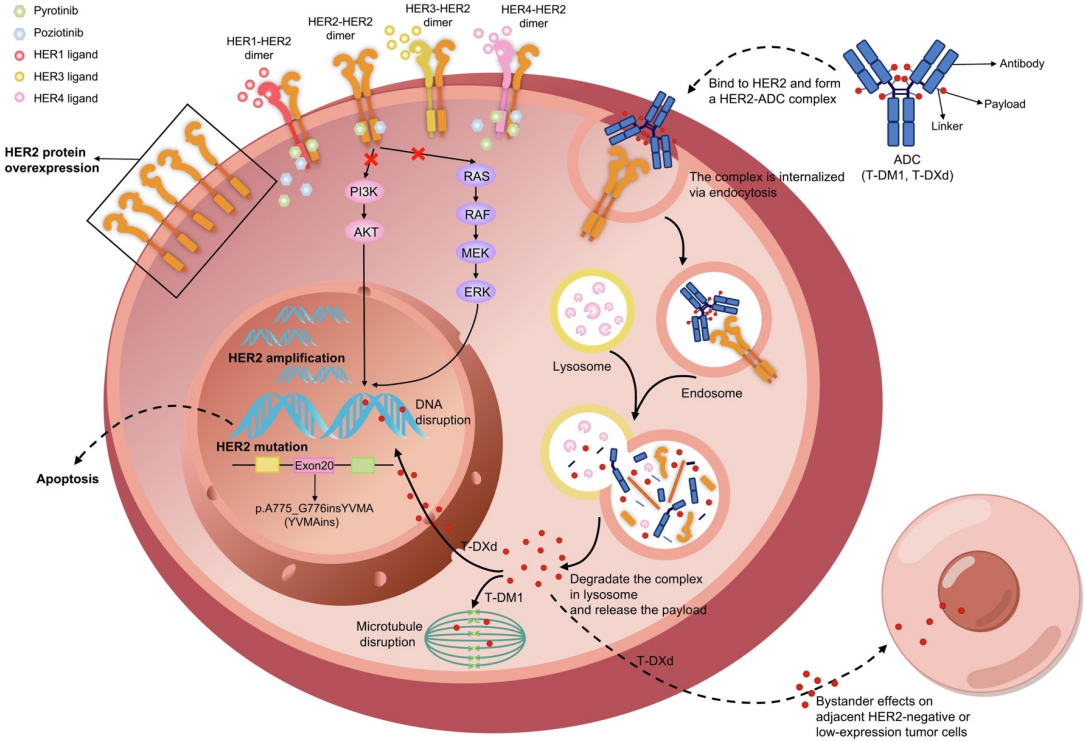

Efficacy and Safety
• An anti-CD19 B-cell targeted therapy
• In patients with generalized myasthenia gravis
• Undergoing a glucocorticoid taper
Inebilizumab


SECONDARY END POINT
Mean Change from Baseline in the Quantitative Myasthenia Gravis Score
At Week 26
Least-Squares Mean Change from Baseline
0
2
4
6
8
−4.8
−2.3
Adjusted difference: −2.5 (95% CI, −3.8 to −1.2); P<0.001
Inebilizumab N=119
Placebo N=117

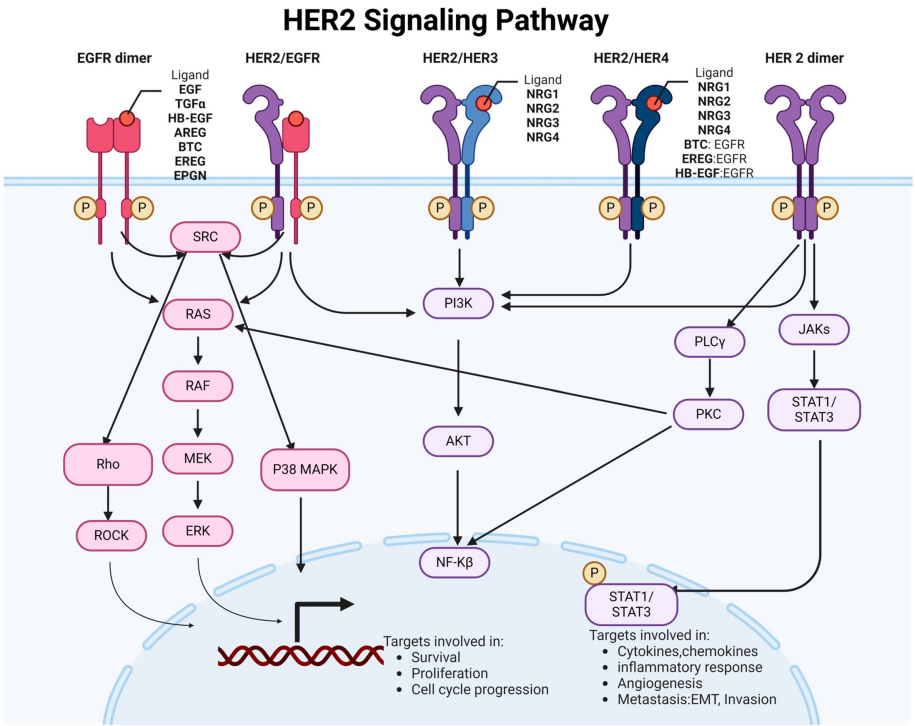

Inebilizumab
Improved function and disease activity at 26 weeks

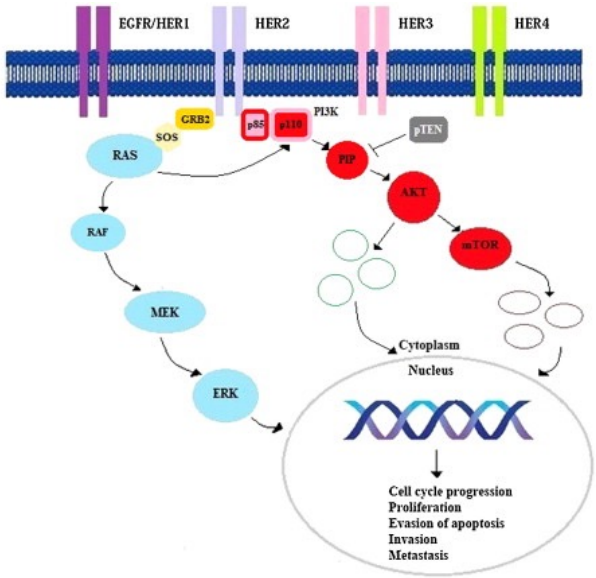
NSCLC with HER2 (4%)





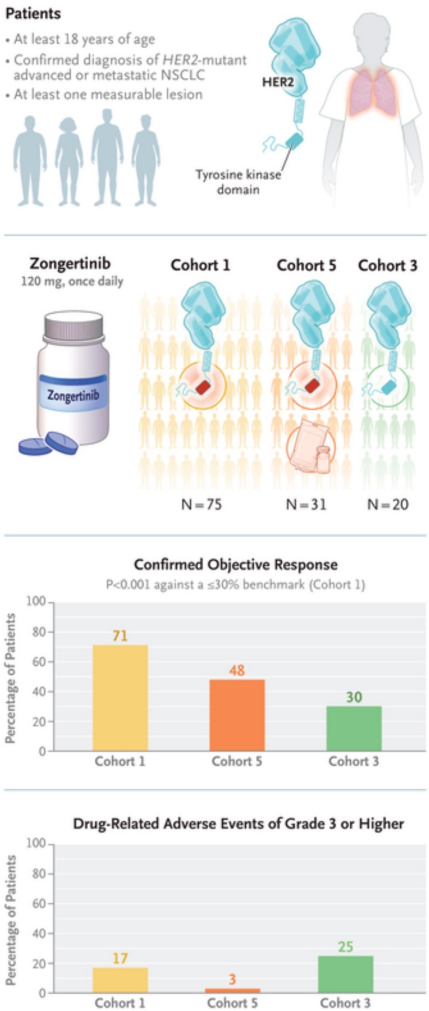
HER2 (human epidermal growth factor receptor 2) ist ein Protein, das das Wachstum von Zellen anregt. Bei Brustkrebs kann eine Überexpression von HER2 zu einem aggressiveren Tumorwachstum führen. Tumore, die viel HER2 produzieren, werden als HER2-positiv bezeichnet und sprechen oft gut auf zielgerichtete Therapien an, die auf das HER2-Protein abzielen.





Zongertinib in Previously Treated *HER2*-Mutant Non–Small-Cell Lung Cancer

Innovative oral targeted therapies are warranted for patients with human epidermal growth factor receptor 2 (*HER2*)–mutant non–small-cell lung cancer (NSCLC). Zongertinib is an oral, irreversible, HER2-selective tyrosine kinase inhibitor that has been shown to have efficacy in persons with advanced or metastatic solid tumors with HER2 alterations in a phase 1 study. We evaluated zongertinib in a multicohort, phase 1a–1b trial involving patients with advanced or metastatic *HER2*-mutant NSCLC. Here we report the primary analysis of zongertinib in previously treated patients: those with tumors harboring a mutation in the tyrosine kinase domain (cohort 1), those with tumors harboring a mutation in the tyrosine kinase domain previously treated with a HER2-directed antibody–drug conjugate (cohort 5), and those with tumors harboring a non–tyrosine kinase domain mutation (cohort 3). In cohort 1, patients were initially randomly assigned to receive zongertinib at a dose of 120 mg or 240 mg once daily. Patients in cohorts 5 and 3 initially received 240 mg daily. After an interim analysis of data from cohort 1, subsequently recruited patients across all cohorts received zongertinib at a dose of 120 mg. The primary end point was an objective response assessed by blinded independent central review (cohorts 1 and 5) or by investigator review (cohort 3). Secondary end points included the duration of response and progression-free survival.



According to recent real-world studies involving patient registries, mutations in human epidermal growth factor receptor 2 (*HER2*; also known as ErbB-2 receptor tyrosine kinase 2 [*ERBB2*]) are present in approximately 2 to 4% of non–small-cell lung cancers (NSCLCs). *HER2* mutations are most common within the active site of the tyrosine kinase domain (approximately 53% occur in exons 18 to 21), particularly exon 20, and are mostly insertion mutations. Other *HER2* mutations are highly heterogeneous and occur predominantly in the extracellular domain (approximately 25%) and the transmembrane domain (approximately 10%) of the receptor.

Study Design and Patients

Phase 1b of the trial assessed the efficacy and safety of zongertinib in patients with previously treated *HER2*-mutant advanced or metastatic NSCLC: those with nonsquamous NSCLC with a mutation in the tyrosine kinase domain (cohort 1), those with nonsquamous NSCLC with a mutation in the tyrosine kinase domain who had been previously treated with a HER2-directed antibody–drug conjugate (cohort 5), and those with nonsquamous NSCLC with a non–tyrosine kinase domain mutation or with squamous NSCLC with a mutation in the tyrosine kinase domain (exploratory cohort 3).

End Points

The primary end point was an objective response (a best overall complete or partial response) as assessed by blinded independent central review (cohorts 1 and 5) or investigator review (cohort 3) according to RECIST, version 1.1.

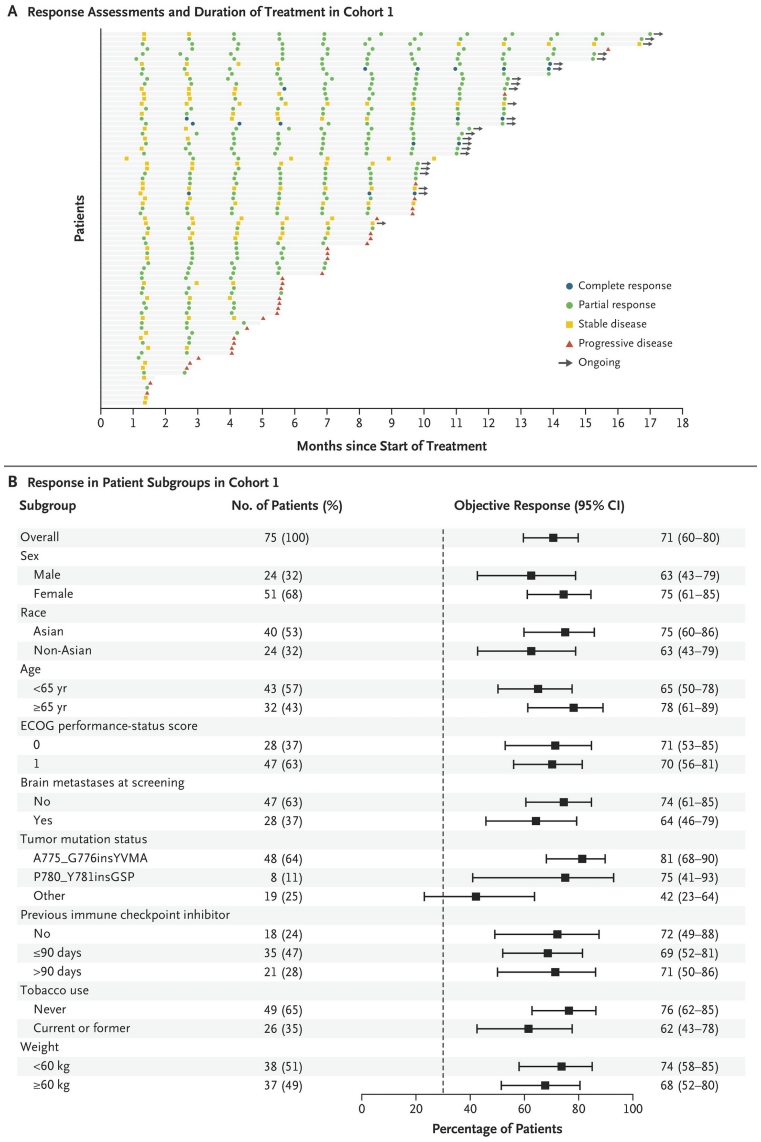
Characteristic	Cohort 1 (N=75)
Median age (range) — yr	62 (30–80)
Sex — no. (%)	
Female	51 (68)
Male	24 (32)
Race — no. (%)†	
Asian	40 (53)
White	24 (32)
Missing‡	11 (15)
ECOG performance-status score — no. (%)§	
0	28 (37)
1	47 (63)
Tobacco use — no. (%)	
Never	49 (65)
Current	2 (3)
Former	24 (32)
No. of previous lines of systemic anticancer treatment — no. (%)	
0	3 (4)¶
1	43 (57)
2	12 (16)
3 or 4	13 (17)
5 or 6	2 (3)
≥7	2 (3)
Previous systemic therapy — no. (%)	
Chemotherapy	71 (95)
Antibody therapy	18 (24)
Immunotherapy	52 (69)
Tyrosine kinase inhibitor therapy	2 (3)
Previous HER2-targeted therapy — no. (%)‖	7 (9)
Previous immune checkpoint inhibitor therapy — no. (%)	57 (76)
Previous brain radiotherapy — no. (%)	13 (17)
Site of metastases at screening — no. (%)	
Brain	28 (37)
Liver	17 (23)
Method used for *HER2* sequencing — no. (%)	
Next-generation sequencing	70 (93)
Polymerase chain reaction	3 (4)
Other	1 (1)
Missing	1 (1)
HER2 tyrosine kinase domain mutation — no. (%)	
A775_G776insYVMA	43 (57)
P780_Y781insGSP	8 (11)
A775_G776insYVMA, other	5 (7)
G776>VC	3 (4)
L755P	2 (3)
G776V	2 (3)
Other	12 (16)

Response to Zongertinib at a Dose of 120 mg in Cohort 1.

Response	Cohort 1 (N=75)
Objective response	
Total no. of patients	53
Percent (95% CI)	71 (60–80)
P value	<0.001
Complete response — no. (%)	5 (7)
Partial response — no. (%)	48 (64)
Disease control	
Total no. of patients	72
Percent (95% CI)	96 (89–99)
Stable disease — no. (%)	19 (25)
Progressive disease — no. (%)	3 (4)

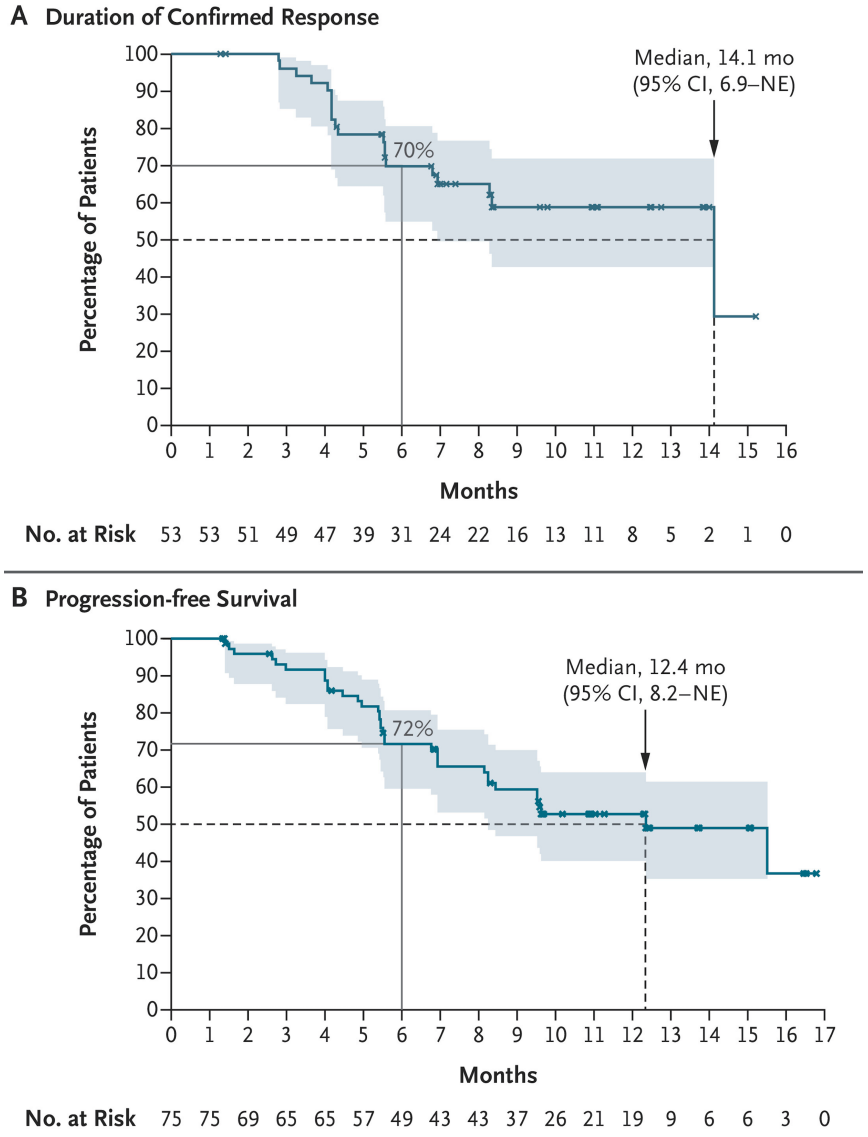
Safety Summary and the Most Common Drug-Related Adverse Events among the 75 Patients in Cohort 1 Treated with Zongertinib at a Dose of 120 mg.

Event	All	Grade 1	Grade 2	Grade 3	Grade 4	Grade 5
			number of patients (percent)			
Adverse events that occurred during the treatment period						
Any	75 (100)	11 (15)	29 (39)	26 (35)	2 (3)	7 (9)
Led to dose reduction*	5 (7)	1 (1)	0	3 (4)	1 (1)	0
Led to treatment discontinuation†	2 (3)	1 (1)	0	1 (1)	0	0
Serious drug-related adverse events‡	3 (4)	0	0	2 (3)	1 (1)	0
Any drug-related adverse event§	73 (97)	27 (36)	33 (44)	12 (16)	1 (1)	0
Diarrhea¶	42 (56)	36 (48)	5 (7)	1 (1)	0	0
Rash‖	25 (33)	18 (24)	7 (9)	0	0	0
Increased aspartate aminotransferase	18 (24)	11 (15)	3 (4)	4 (5)	0	0
Increased alanine aminotransferase	16 (21)	9 (12)	1 (1)	5 (7)	1 (1)	0
Nausea	11 (15)	10 (13)	1 (1)	0	0	0
Dry skin	11 (15)	11 (15)	0	0	0	0
Pruritus	10 (13)	9 (12)	1 (1)	0	0	0
Decreased white-cell count	10 (13)	5 (7)	5 (7)	0	0	0
Anemia	9 (12)	6 (8)	3 (4)	0	0	0
Decreased neutrophil count	9 (12)	3 (4)	5 (7)	1 (1)	0	0
Nail disorder	8 (11)	8 (11)	0	0	0	0



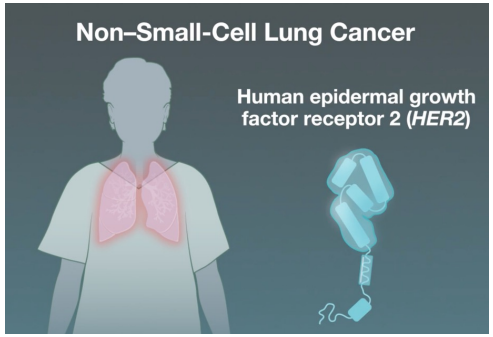
Tumor Response in Cohort 1.

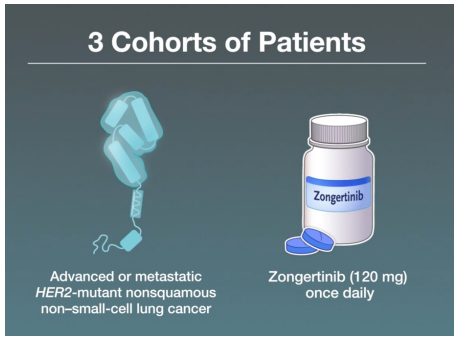
Panel A shows the tumor response among patients in cohort 1 with previously treated *HER2*-mutant NSCLC with mutations in the tyrosine kinase domain who received zongertinib at a dose of 120 mg. Panel B shows the tumor response among patients in cohort 1 with stratification according to subgroups. Eastern Cooperative Oncology Group (ECOG) performance-status scores range from 0 to 5, with higher scores indicating greater disability. Data on whether an immune checkpoint inhibitor had been received previously were not available for one patient. Response was assessed by blinded independent central review according to the Response Evaluation Criteria in Solid Tumors, version 1.1. The 95% confidence intervals were not adjusted for multiplicity, and no formal testing was defined. The date of data cutoff was November 29, 2024.

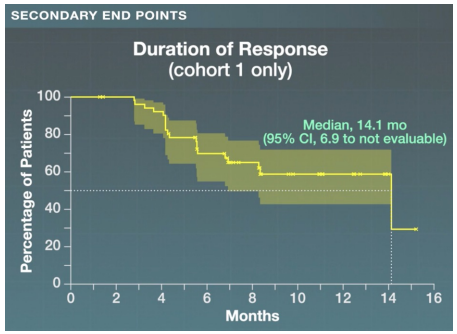


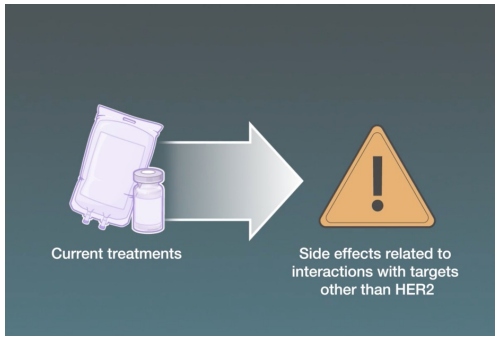
Durability of Response in Cohort 1.

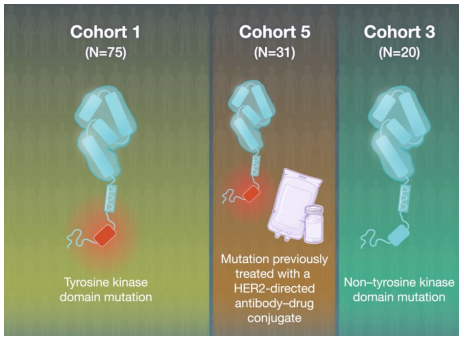
Panel A shows the duration of confirmed response and Panel B the progression-free survival among patients in cohort 1 treated with zongertinib at a dose of 120 mg. Response was assessed by blinded independent central review according to the Response Evaluation Criteria in Solid Tumors, version 1.1. Shaded areas denote 95% confidence intervals. The date of data cutoff was November 29, 2024. NE denotes not evaluable.

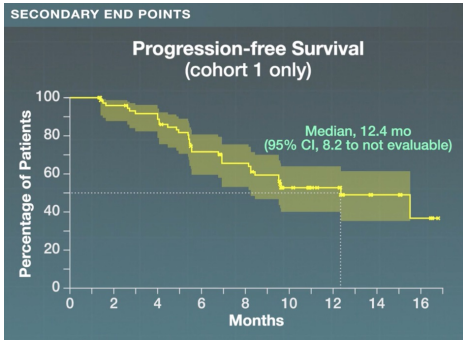

Non–Small-Cell Lung Cancer
Human epidermal growth factor receptor 2 (*HER2*)

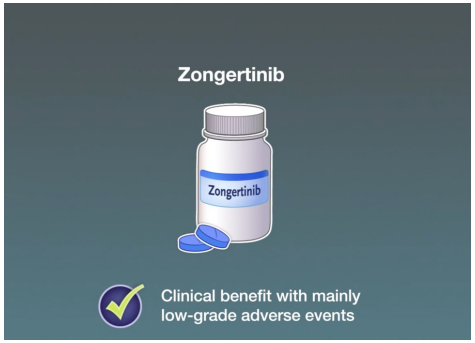

3 Cohorts of Patients
Zongertinib
Advanced or metastatic *HER2*-mutant nonsquamous non–small-cell lung cancer
Zongertinib (120 mg) once daily

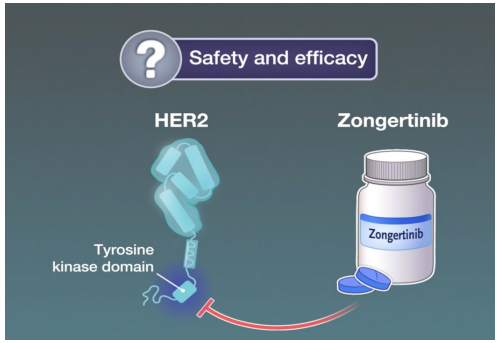

SECONDARY END POINTS
Duration of Response (cohort 1 only)
Median, 14.1 mo (95% CI, 6.9 to not evaluable)
Percentage of Patients
Months

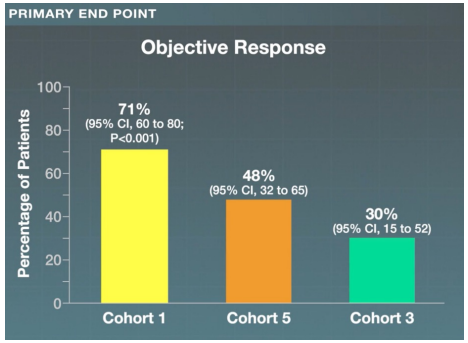

Current treatments
Side effects related to interactions with targets other than HER2

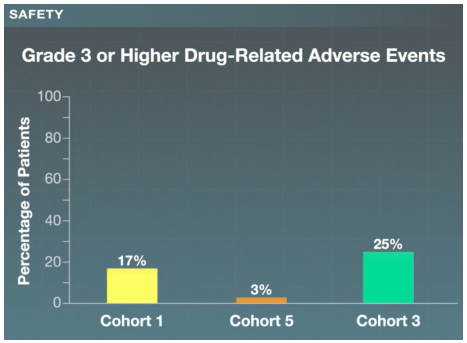

Cohort 1 (N=75)
Cohort 5 (N=31)
Cohort 3 (N=20)
Tyrosine kinase domain mutation
Mutation previously treated with a HER2-directed antibody–drug conjugate
Non–tyrosine kinase domain mutation


SECONDARY END POINTS
Progression-free Survival (cohort 1 only)
Median, 12.4 mo (95% CI, 8.2 to not evaluable)
Percentage of Patients
Months

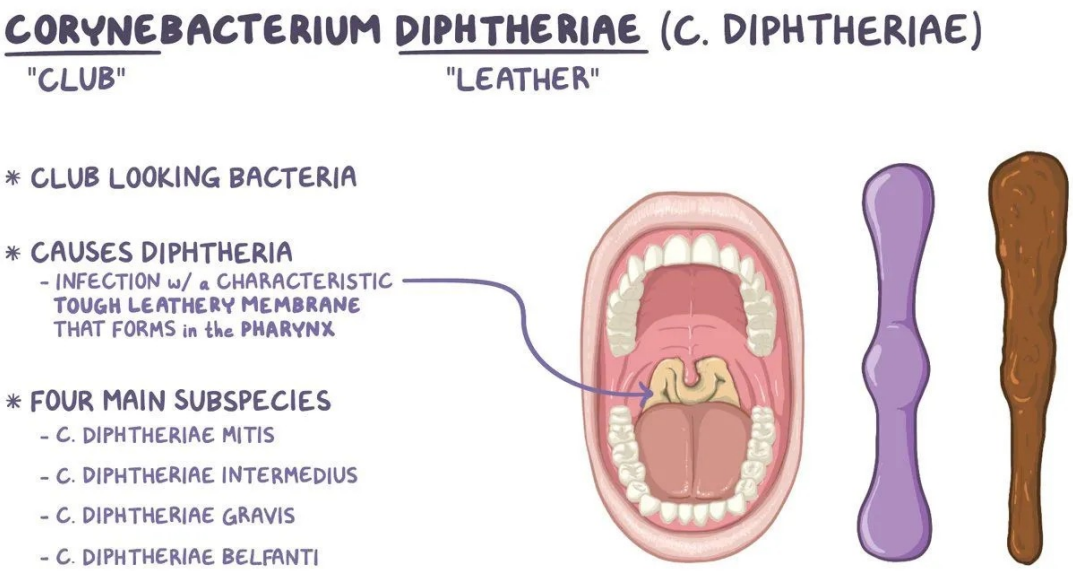

Zongertinib
Clinical benefit with mainly low-grade adverse events


Safety and efficacy
HER2
Zongertinib
Tyrosine kinase domain


PRIMARY END POINT
Objective Response
71% (95% CI, 60 to 80; P<0.001)
48% (95% CI, 32 to 65)
30% (95% CI, 15 to 52)
Percentage of Patients
Cohort 1
Cohort 5
Cohort 3


SAFETY
Grade 3 or Higher Drug-Related Adverse Events
17%
3%
25%
Percentage of Patients
Cohort 1
Cohort 5
Cohort 3

Jahrhunderts noch „Würgeengel der Kinder“ genannt, ist eine vor allem im Kindesalter auftretende, akute Infektionskrankheit, die durch eine Infektion der oberen Atemwege mit dem grampositiven Corynebacterium diphtheriae, dem „Diphtheriebazillus“, hervorgerufen wird (Rachendiphtherie).





Corynebacterium diphtheriae Outbreak in Migrant Populations in Europe

A surge of cases of *Corynebacterium diphtheriae* infection was observed in reception centers for migrants in Europe beginning in the summer of 2022. Most of the cases were cutaneous, although some respiratory cases as well as one death were reported. A pan-European consortium was created to assess the clinical, epidemiologic, and microbiologic features of this outbreak.

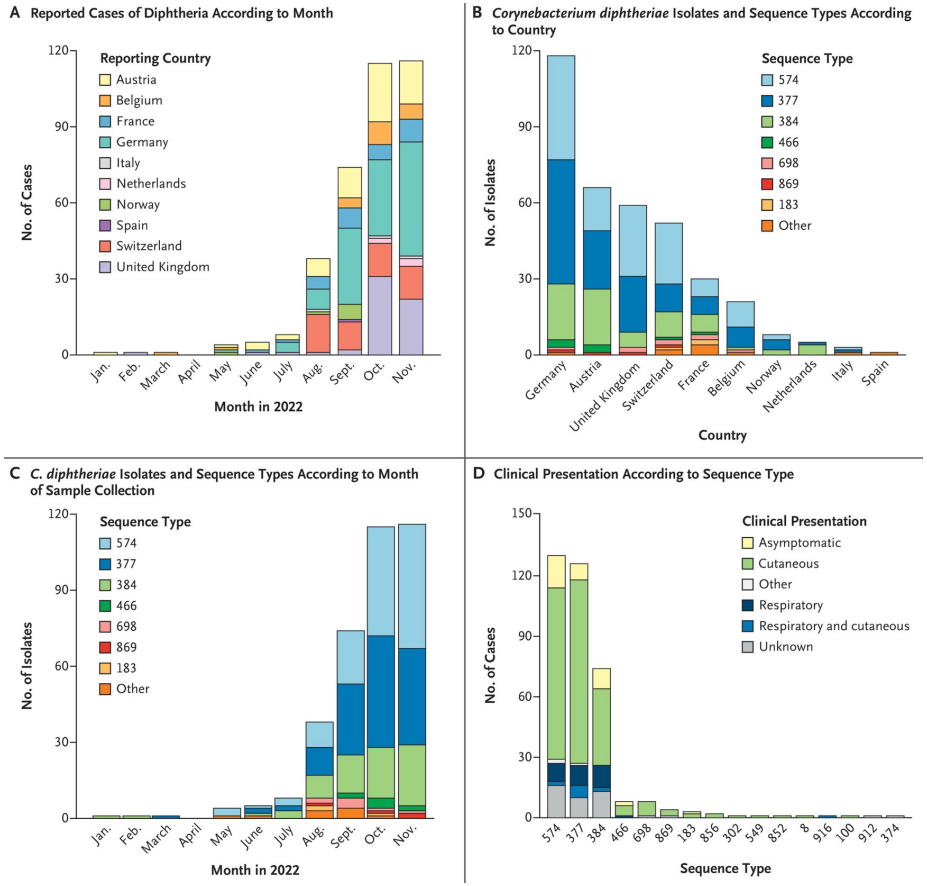
We assessed cases of toxigenic *C. diphtheriae* infection that were reported in 10 European countries from January through November 2022. Data regarding countries of origin and transit routes were obtained from interviews with the patients. Whole-genome sequencing and antimicrobial-susceptibility testing were performed on bacterial isolates that were obtained from the patients. The phylogenetic relationships of the isolates and their antimicrobial-resistance genes were evaluated.

Conclusions

The distribution of each genetic cluster of *C. diphtheriae* isolates across multiple countries in Europe showed repeated cross-border spread. The large number of *C. diphtheriae* infections among migrants is a cause for concern, particularly given that antimicrobial-resistance phenotypes threaten the efficacy of first-line treatments. (Funded by the Bavarian State Ministry of Health, Care, and Prevention and others.)

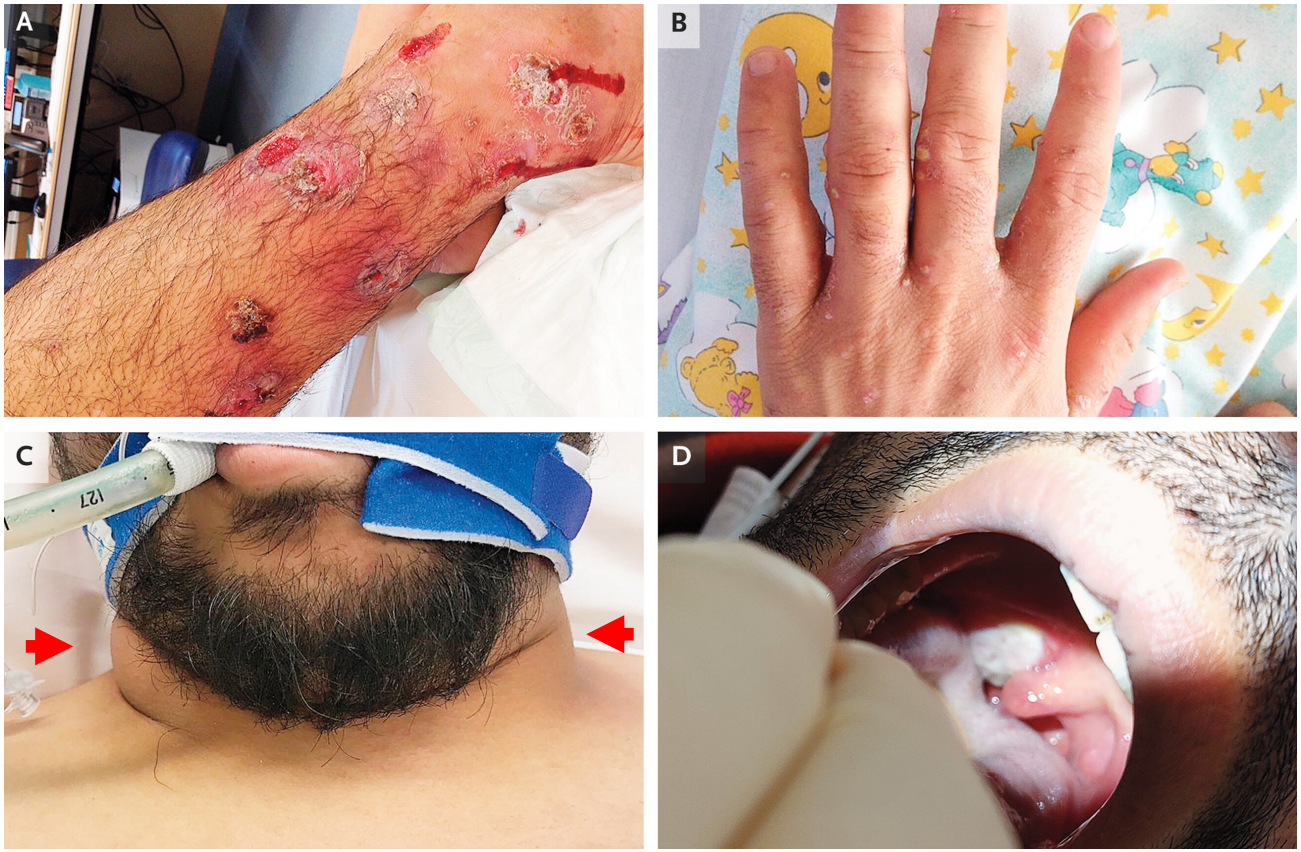
Diphtheria is a potentially life-threatening and highly transmissible disease that typically causes respiratory illness but can also cause cutaneous lesions. The main causative agents are toxigenic strains of the bacterium *Corynebacterium diphtheriae*, which express diphtheria toxin, a potent exotoxin that inhibits protein synthesis in eukaryotic cells. Respiratory diphtheria is historically the most frequently detected form; patients with respiratory diphtheria present with symptoms such as sore throat with pseudomembranes and low-grade fever. Cutaneous diphtheria, characterized by skin ulcers sometimes surrounded by a greyish membrane, typically does not lead to severe complications but can play an important role in transmission. The production of diphtheria toxin can result in complications such as myocarditis, polyneuropathy, and acute kidney disease. Unvaccinated children younger than 5 years of age are particularly susceptible to diphtheria. The estimated case fatality rate among unvaccinated persons with untreated respiratory diphtheria is 29%.

Between 2016 and 2021, an annual mean of 27 cases of *C. diphtheriae* infection in the European Union (EU) and the European Economic Area (EEA) were reported to the European Center for Disease Prevention and Control (ECDC). However, diphtheria remains endemic or can become epidemic in regions of the world where vaccine coverage is suboptimal. Diagnosed cases in the EU and EEA are often observed among travelers and migrants from such regions.



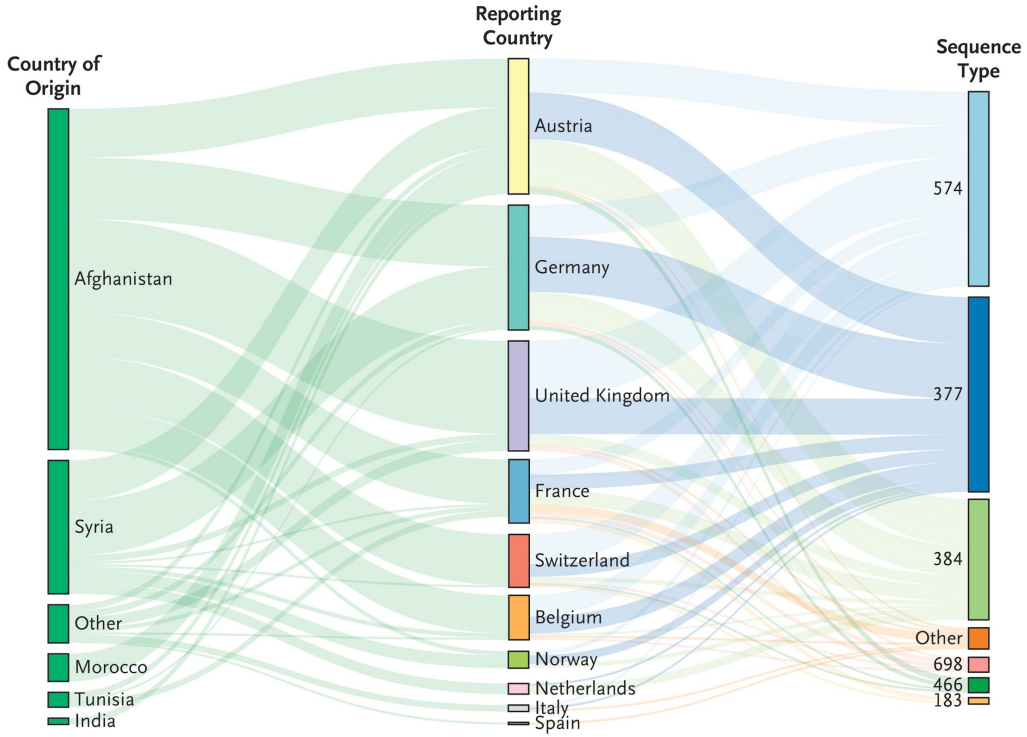
Diphtheria Cases, Isolates and Sequence Types, and Clinical Presentation.

The study included *Corynebacterium diphtheriae* isolates that were obtained from January through November 2022; 362 cases of diphtheria and 363 isolates were identified. Panel A shows the numbers of cases in each reporting country according to month. Panel B shows the number of isolates and their sequence types according to the reporting country. Panel C shows the number of isolates and sequence type according to month. Panel D shows the clinical presentation of the 325 cases for which clinical presentation was reported, according to sequence type.



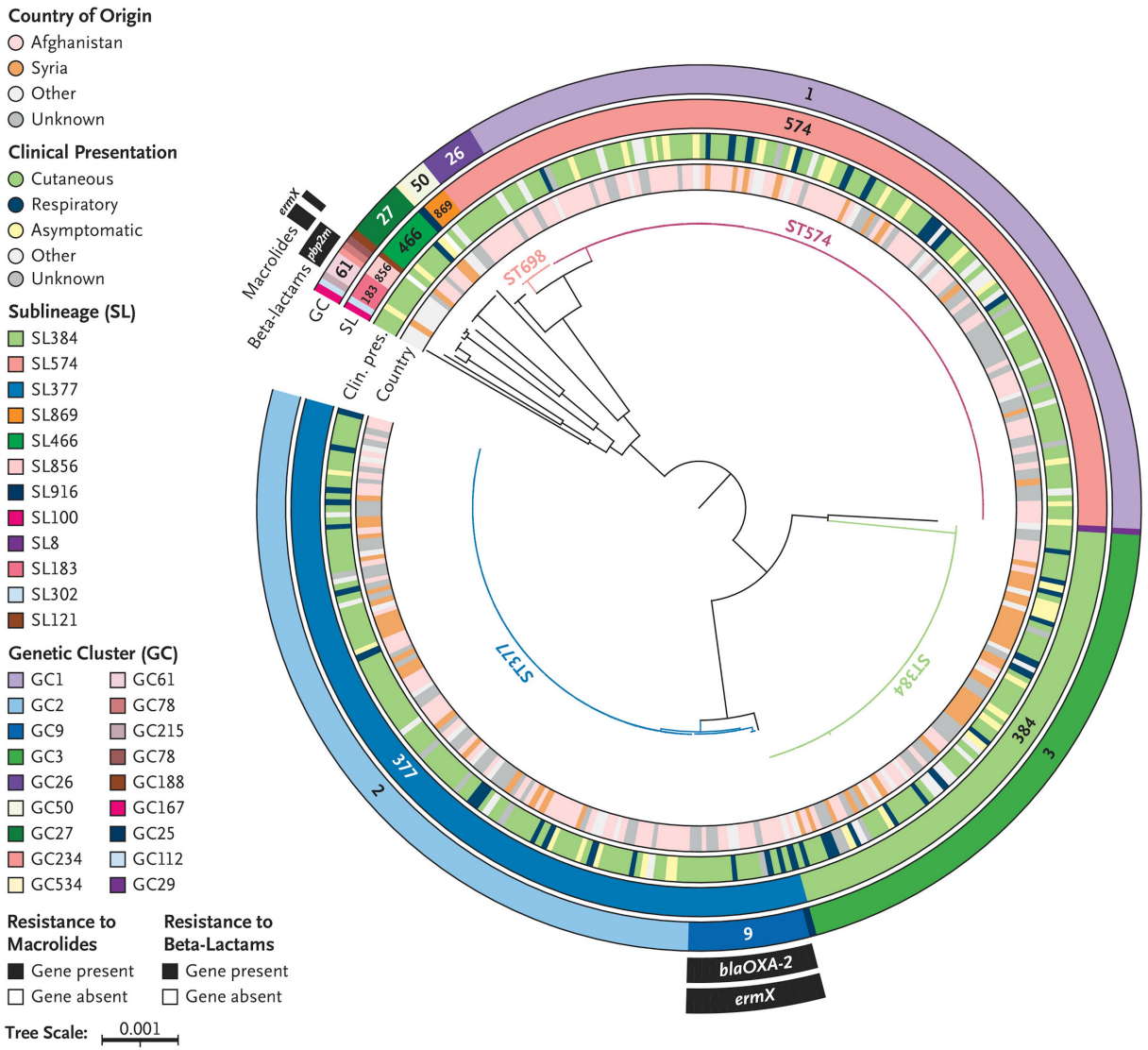
Clinical Presentations of Cutaneous and Respiratory Diphtheria.

Panel A shows a patient with cutaneous diphtheria with inflammatory plaques with pustules, erosions, and crusts with superinfection with *Streptococcus pyogenes* (photograph obtained at the Department of Dermatology, Klinikum Klagenfurt am Wörthersee). Panel B shows a patient with cutaneous diphtheria with multiple pustules on the feet and hands; the patient had superinfection with *S. pyogenes* and methicillin-resistant *Staphylococcus aureus* (photograph obtained at the Department of Dermatology, Klinikum Klagenfurt am Wörthersee). Panel C shows a patient with respiratory diphtheria with the characteristic bull's neck appearance due to massive lymphadenopathy and swelling (photograph obtained at the Department of Infectious Diseases, Klinik Favoriten). Panel D shows a patient with respiratory diphtheria with a peritonsillar abscess and pseudomembranes on the right tonsil (photograph obtained at the Department of Infectious Diseases, Klinik Favoriten). Ethical approval was obtained for the release of images obtained in Switzerland.



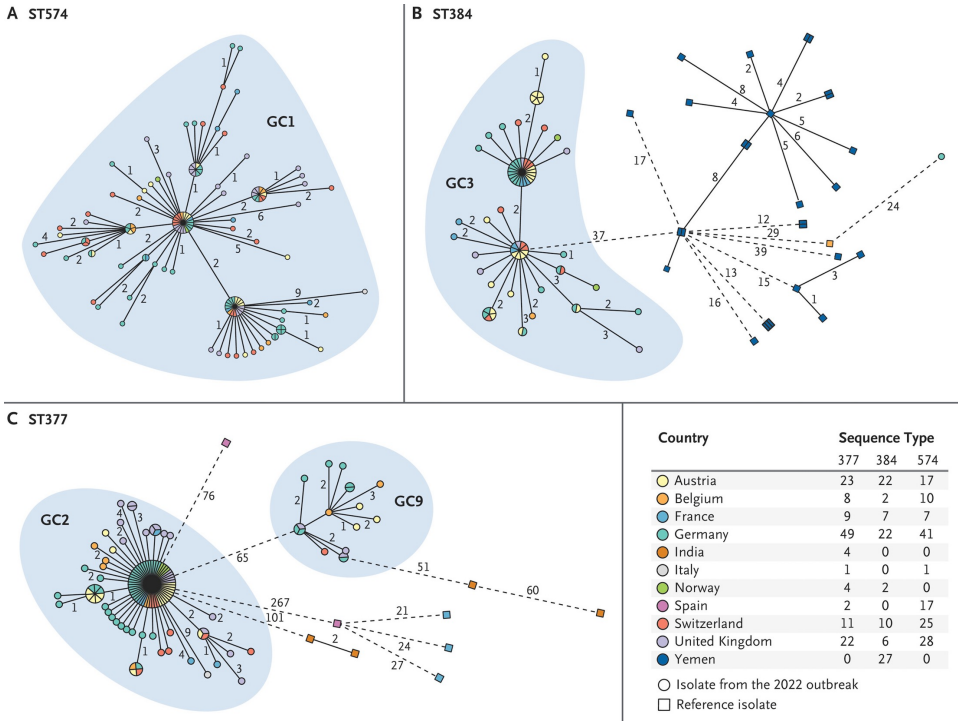
Association of Country of Origin, Reporting Country, and Sequence Type.

An alluvial diagram shows the frequency of migration from various countries of origin (left column) to the reporting countries (middle column) and which sequence types were identified (right column).



Phylogenetic Diversity of the 363 *C. diphtheriae* Isolates.

The phylogeny was obtained with the use of core gene sequences and is displayed radially. The branches corresponding to the four major sequence types (STs) are colored. The surrounding metadata circles show (from inside to outside) country of origin, clinical manifestation, sublineage (SL), genetic cluster (GC), and the presence of the following genes: *blaOXA-2* (which has no demonstrated phenotypic effect), *pbp2m* (which potentially confers resistance to penicillin and other beta-lactams), and *ermX* (which confers resistance to macrolides). The scale indicates the proportion of variable nucleotide sites.



The Genetic Diversity of the Four Main Genetic Clusters.

Shown are minimum spanning trees of *C. diphtheriae* isolates of ST574 (panel A), ST384 (panel B), and ST377 (panel C), on the basis of core-genome multilocus sequence typing.[19] Each tree includes the isolates of the outbreak described in this article (circles) as well as previous publicly available genome sequences retrieved from BIGSdb-Pasteur (squares). The blue shaded areas highlight the isolates included in this study that belong to four main genetic clusters.

Discussion

This outbreak represents the largest rise in diphtheria cases seen in western Europe in the past 70 years. It occurred primarily among displaced populations entering the region. No secondary infections were documented among the resident populations in 2022, and only seven such infections were detected in 2023.

The prevalence of cases among male migrants could potentially be explained by differences between women and men in health care–seeking behavior. However, countries that screen all incoming migrants did not identify higher proportions among women.

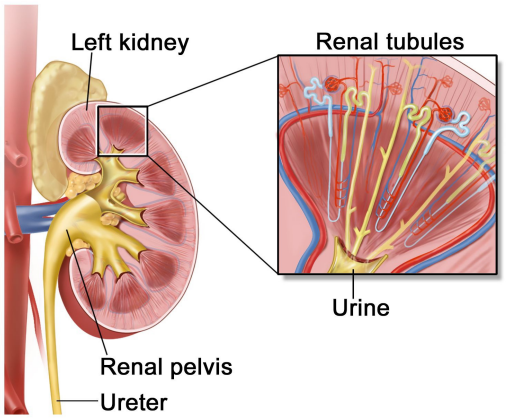
The macrolide resistance observed in GC9 poses a substantial threat to treatment outcomes, increases the likelihood of systemic complications warranting diphtheria antitoxin treatment, and may favor transmission. Although most cases were managed with antibiotics only, some patients with respiratory cases received diphtheria antitoxin treatment. In some countries (e.g., Switzerland), a booster vaccine was supplied in the refugee camps.

Increasing the global production of diphtheria antitoxin and maintaining a stable, communal stockpile that can be rapidly deployed in outbreak situations should also be an international public health priority.

Papillary Kidney Cancer

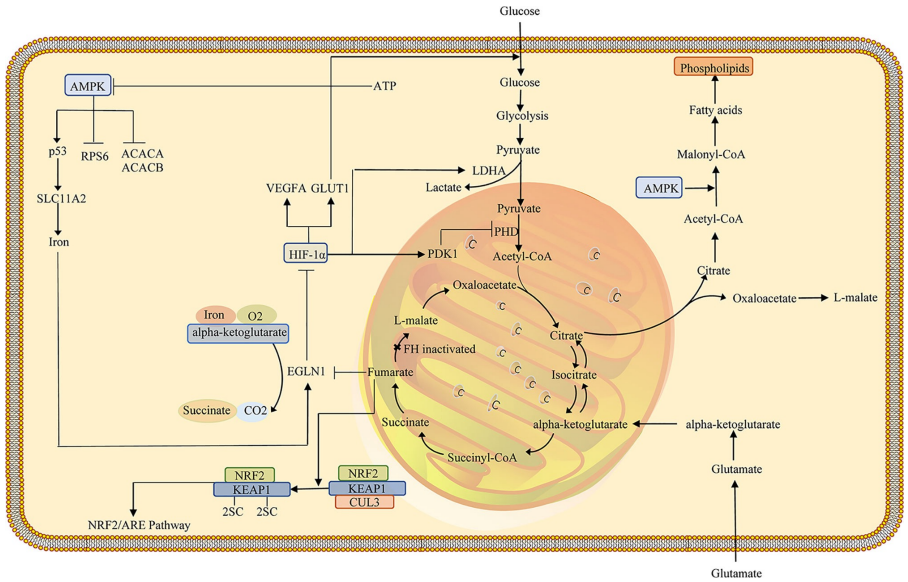
Hereditary papillary renal cell carcinoma (HPRC) is a rare, inherited disorder that significantly increases the risk of developing papillary renal cell carcinoma, a type of kidney cancer. It's characterized by the development of multiple, often bilateral (both kidneys) and multifocal (multiple tumors in one or both kidneys) tumors. HPRC is caused by mutations in the MET gene.

Papillary Renal Cancer

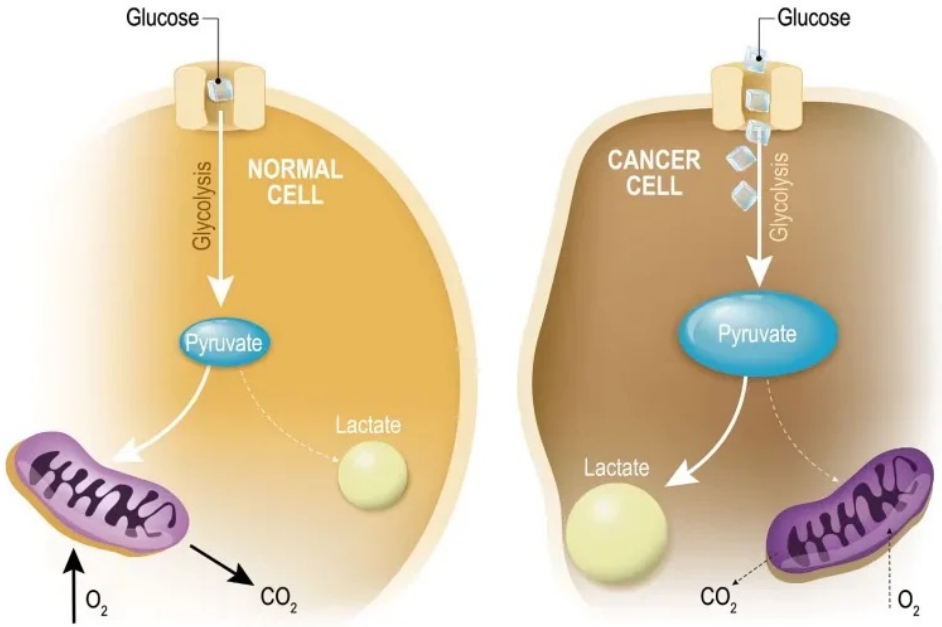


© 2018 Terese Winslow LLC
U.S. Govt. has certain rights

Hereditary leiomyomatosis and renal cell cancer (HLRCC) is a genetic disorder characterized by the development of benign smooth muscle tumors (leiomyomas) in the skin and uterus, and an increased risk of developing kidney cancer, specifically a type called papillary renal cell carcinoma. It is caused by mutations in the FH gene, which plays a role in a cellular process called the tricarboxylic acid cycle.

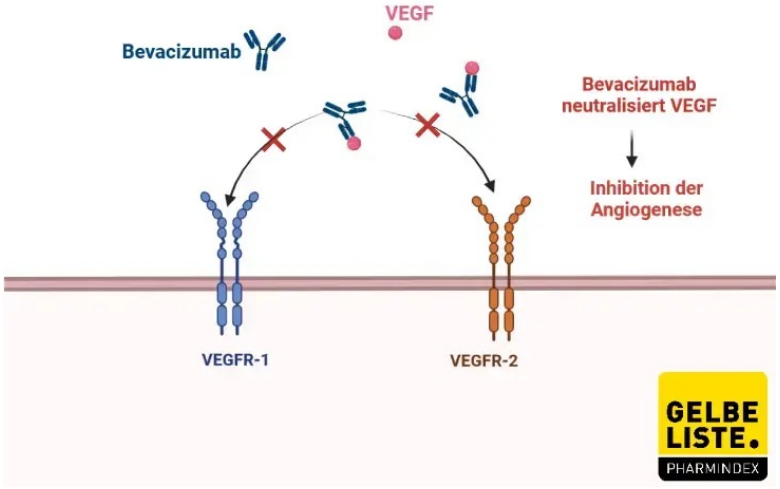


The Warburg effect, where cancer cells favor glycolysis even with oxygen present, is thought to benefit them by rapidly providing building blocks for cell growth and survival, as well as potentially aiding in evading cell death and promoting metastasis. While the exact reasons for this metabolic shift are still being researched, it's believed to be linked to the high demands of rapidly dividing cancer cells. “The Warburg effect drives cancer cells to metabolize glucose anaerobically, leading to lactate accumulation. This lactate drives a process that helps cancer cells repair DNA and resist chemotherapy. By reducing lactate, we can make cancer cells more sensitive to treatment.”

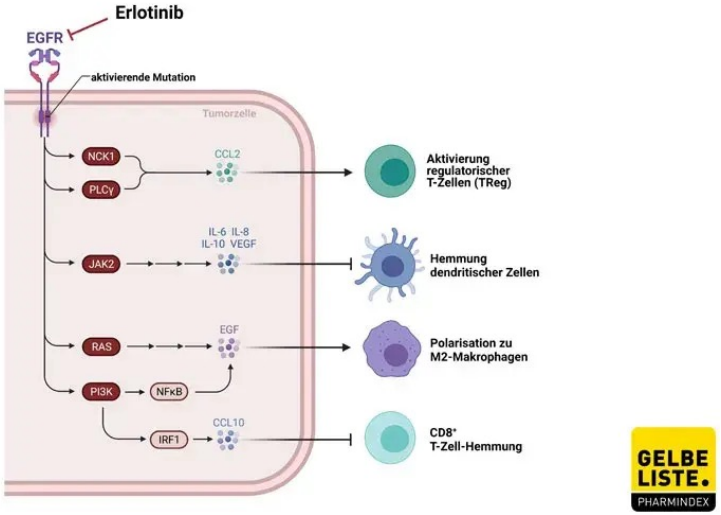


Warburg effect

Bevacizumab



Erlotinib



Bevacizumab and Erlotinib in Hereditary and Sporadic Papillary Kidney Cancer

Hereditary leiomyomatosis and renal-cell cancer (HLRCC) is an inherited disorder characterized by germline pathogenic variants in the gene encoding fumarate hydratase and an increased risk of papillary renal-cell carcinoma. No effective therapy is known for patients with advanced HLRCC-associated papillary renal-cell carcinoma, and most patients die from progressive disease.

In this open-label, phase 2 study, we evaluated the efficacy of bevacizumab (10 mg per kilogram of body weight every 2 weeks) and erlotinib (150 mg once daily) in patients with advanced HLRCC-associated or sporadic papillary renal-cell carcinoma. The primary end point was overall response; secondary end points included progression-free and overall survival.

Conclusions

The combination of bevacizumab and erlotinib showed antitumor activity in patients with HLRCC-associated or sporadic papillary renal-cell carcinoma. Toxic effects were those known to be associated with this combination.

Renal-cell carcinoma comprises several histologically defined subtypes with distinct genetic and clinical features; altogether, renal-cell carcinoma contributes to more than 179,000 deaths worldwide annually. Papillary renal-cell carcinoma is the second most common subtype and occurs in both sporadic and hereditary forms, but few effective treatments for advanced papillary renal-cell carcinoma exist. Hereditary leiomyomatosis and renal-cell cancer (HLRCC), an autosomal dominant inherited disorder characterized by inactivating germline variants in the gene encoding fumarate hydratase (*FH*), is associated with a predisposition to the development of an aggressive form of papillary renal-cell carcinoma.

Agents such as cabozantinib and immune checkpoint inhibitors have been shown to have activity in patients with advanced papillary renal-cell carcinoma, although their activity in patients with HLRCC has not been prospectively evaluated.

Loss of fumarate hydratase activity has been shown to lead to accumulation of its substrate, fumarate. Fumarate is an oncometabolite that can alter the transcriptional activity of various genes through dioxygenase inhibition and post-translational covalent modification of cysteine residues (succination) in specific proteins. Fumarate hydratase–deficient renal tumors are characterized by impaired oxidative phosphorylation and dependence on aerobic glycolysis for cellular bioenergetic requirements, thus providing a canonical example of the Warburg effect in human cancer.

Patients

Eligible patients had a diagnosis of either advanced HLRCC-associated papillary renal-cell carcinoma or sporadic papillary renal-cell carcinoma with measurable disease as outlined in the Response Evaluation Criteria in Solid Tumors (RECIST), version 1.1.

Study Design and Oversight

This open-label, single-group, phase 2 study of bevacizumab and erlotinib was conducted at the National Institutes of Health Clinical Center. Bevacizumab was administered at a dose of 10 mg per kilogram of body weight intravenously every 2 weeks, and erlotinib was administered at a dose of 150 mg orally once daily during each 28-day cycle.

End Points and Assessments

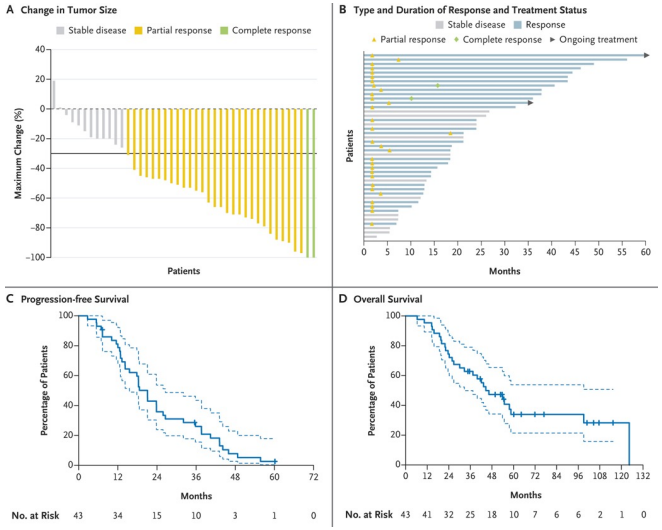
The primary end point was investigator-assessed overall response as measured according to RECIST, version 1.1. Key secondary end points included progression-free survival, overall survival, and response duration.

Characteristic	HLRCC-Associated Papillary RCC (N=43)	Sporadic Papillary RCC (N=40)
Median age (range) — yr	43 (19–74)	55.5 (24–74)
Sex — no. (%)		
Male	30 (70)	26 (65)
Female	13 (30)	14 (35)
Race or ethnic group — no. (%)†		
White, non-Hispanic	33 (77)	35 (88)
Black	5 (12)	3 (8)
Asian	3 (7)	1 (2)
Hispanic	2 (5)	1 (2)
ECOG performance-status score — no. (%)‡		
0	29 (67)	14 (35)
1	13 (30)	26 (65)
2	1 (2)	0
Previous radiation therapy — no. (%)		
Yes	6 (14)	6 (15)
No	37 (86)	34 (85)
IMDC risk stratification — no. (%)		
Favorable	11 (26)	3 (8)
Intermediate	24 (56)	29 (72)
Poor	8 (19)	8 (20)
Sites of metastasis — no. (%)		
Liver	20 (47)	15 (38)
Lung	11 (26)	17 (42)
Lymph nodes, regional	13 (30)	8 (20)
Lymph nodes, nonregional	11 (26)	15 (38)
Nonvisceral retroperitoneal and intrabdominal lesions§	28 (65)	23 (58)
Bone	16 (37)	9 (22)
Previous nephrectomy — no. (%)		
Yes	36 (84)	27 (68)
No	7 (16)	13 (32)
Previous lines of therapy — no. (%)		
0	34 (79)	22 (55)
1	5 (12)	8 (20)
≥2	4 (9)	10 (25)
Any previous therapy	9 (21)	18 (45)
Previous use of VEGFR-targeted TKI — no. (%)	8 (19)	14 (35)

Best Response in Papillary Renal-Cell Carcinoma.

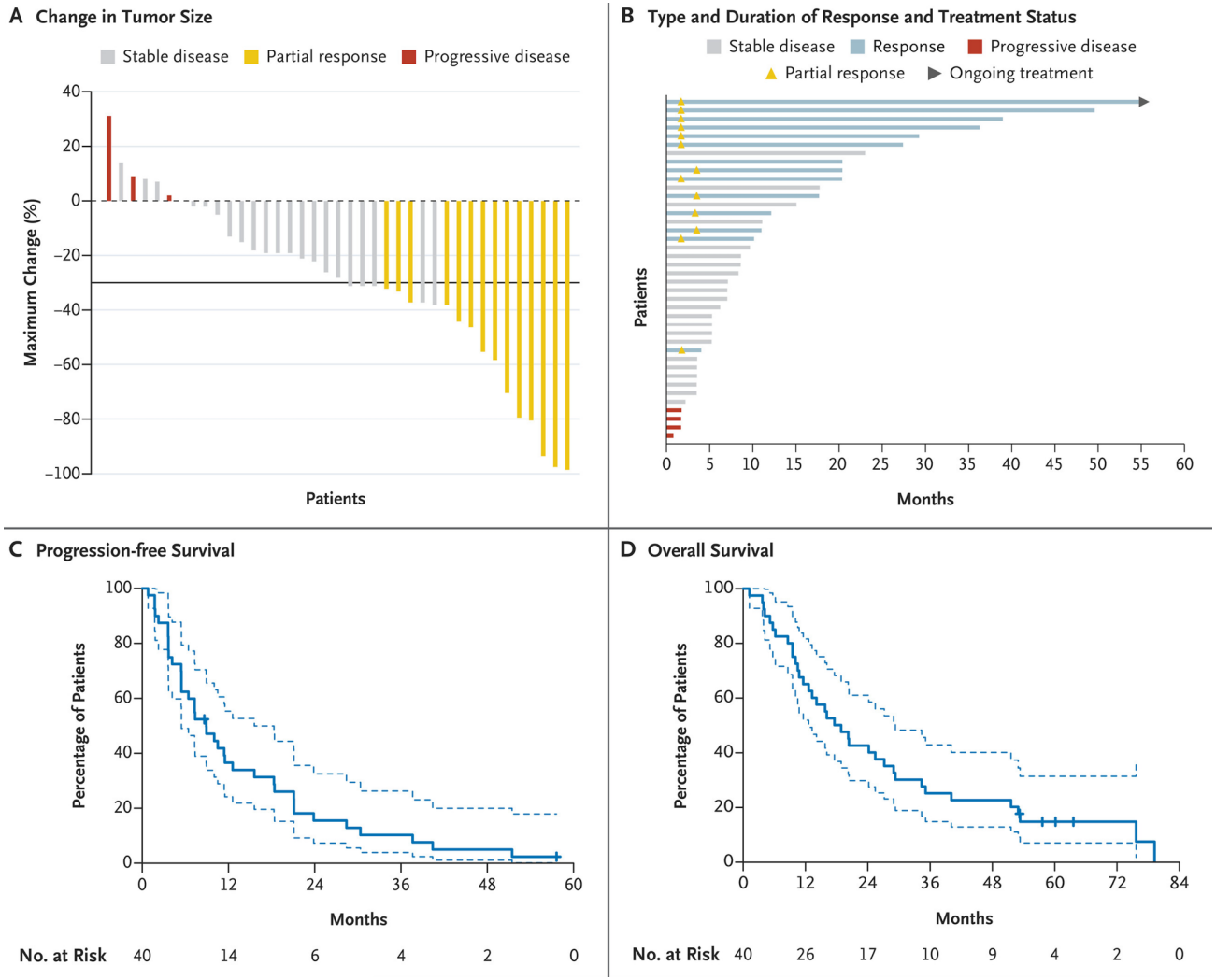
Variable	HLRCC-Associated Papillary RCC (N=43)	Sporadic Papillary RCC (N=40)
Objective response†		
No. with response	31	14
Percent (95% CI)	72 (57–83)	35 (22–51)
Best response — no. (%)		
Complete response	2 (5)	0
Partial response	29 (67)	14 (35)
Stable disease	12 (28)	21 (52)
Unconfirmed partial response‡	0	1 (2)
Progressive disease	0	4 (10)
Median time to response (range) — mo	1.8 (1.7–18.3)	1.8 (1.7–7.3)
Median duration of response (95% CI) — mo	19.3 (12.9–35.9)	18.4 (13.8–49.7)

Event	Grade <3	Grade ≥3
	number of patients (percent)	
Acneiform rash	77 (93)	4 (5)
Diarrhea	74 (89)	4 (5)
Proteinuria	65 (78)	14 (17)
Dry skin	53 (64)	0
Creatinine increased	48 (58)	0
Fatigue	46 (55)	0
Hemoglobinuria	45 (54)	0
Hypoalbuminemia	44 (53)	0
Hematuria	44 (53)	0
Hypertension	43 (52)	28 (34)
Epistaxis	40 (48)	0
Nausea	38 (46)	0
Aspartate aminotransferase increased	37 (45)	1 (1)
Alanine aminotransferase increased	30 (36)	3 (4)
Skin and subcutaneous tissue disorders, other	29 (35)	1 (1)
Dysgeusia	29 (35)	0
Alopecia	27 (33)	0
Paronychia	27 (33)	0
Gastroesophageal reflux disease	26 (31)	0
Hyperglycemia	24 (29)	0
Weight loss	22 (27)	1 (1)
Anorexia	22 (27)	0
Alkaline phosphatase increased	21 (25)	0
Hypomagnesemia	21 (25)	0
Hyponatremia	20 (24)	1 (1)
Hypothyroidism	19 (23)	0
Vomiting	19 (23)	0
Anemia	18 (22)	1 (1)
Pruritus	18 (22)	0
Platelet count decreased	15 (18)	1 (1)
Cough	14 (17)	0
Hypercalcemia	14 (17)	0
Dizziness	13 (16)	0
Hypoglycemia	13 (16)	0
Lymphocyte count decreased	13 (16)	0
Hyperkalemia	12 (14)	0
Hyperparathyroidism	12 (14)	0
Urine discoloration	10 (12)	0
Dry mouth	10 (12)	0
Palmar–plantar erythrodysesthesia syndrome	10 (12)	0
Abdominal pain	9 (11)	2 (2)
Oral mucositis	9 (11)	0
Hoarseness	9 (11)	0
Blood bilirubin increased	9 (11)	0
Constipation	9 (11)	0
Dry eye	9 (11)	0
Thromboembolic event	2 (2)	2 (2)
Neutrophil count decreased	2 (2)	1 (1)
Cardiac arrest	1 (1)	1 (1)
Hypotension	1 (1)	1 (1)
Multiorgan failure	1 (1)	1 (1)
Upper gastrointestinal hemorrhage	1 (1)	1 (1)
Myocardial infarction	1 (1)	1 (1)
Acute coronary syndrome	1 (1)	1 (1)



Patients with HLRCC-Associated Papillary Renal-Cell Carcinoma.

Panel A shows the greatest percent change from baseline in the sum of the longest dimension of all targeted lesions. Panel B shows the type and duration of response and the duration of treatment for all the patients with hereditary leiomyomatosis and renal-cell cancer (HLRCC)–associated renal-cell carcinoma. Panel C shows Kaplan–Meier analysis of progression-free survival, and Panel D shows Kaplan–Meier analysis of overall survival. The median progression-free survival was 21.1 months (95% confidence interval [CI], 15.6 to 26.6), and the median overall survival was 44.6 months (95% CI, 32.7 to could not be estimated). Data on patients who had not had an event were censored on February 7, 2022; censored data are denoted by a vertical tick mark. Dashed lines indicate 95% confidence intervals.



Patients with Sporadic Papillary Renal-Cell Carcinoma.

Panel A shows the greatest percent change from baseline in the sum of the longest dimension of all targeted lesions. Panel B shows the type and duration of response and the duration of treatment for all the patients with sporadic papillary renal-cell carcinoma. Panel C shows Kaplan–Meier analysis of progression-free survival, and Panel D shows Kaplan–Meier analysis of overall survival. The median progression-free survival was 8.9 months (95% CI, 5.5 to 18.3), and the median overall survival was 18.2 months (95% CI, 12.6 to 29.3). Data for patients who had not had an event were censored on February 7, 2022; censored data are denoted by a vertical tick mark. Dashed lines indicate 95% confidence intervals.

Discussion

Notable advances have been made over the past 15 years in the management of advanced clear-cell renal-cell carcinoma, with a combination of antiangiogenic agents and immune checkpoint inhibitors now the standard of care. Few effective options exist for other variants of renal-cell carcinoma, which is exemplified by HLRCC-associated papillary renal-cell carcinoma. This variant is typically associated with an aggressive clinical course; most patients die from progressive disease, with a median overall survival of 16 to 21 months in most retrospective series. This study showed that the combination of bevacizumab and erlotinib was effective in these patients, and durable responses were seen in a subset of patients with sporadic papillary renal-cell carcinoma. Standard VEGFR TKIs provide a low-level benefit for advanced HLRCC-associated papillary renal-cell carcinoma and are currently being evaluated in combination with immune checkpoint inhibitors. For patients with sporadic papillary renal-cell carcinoma, several phase 2 studies have shown the activity of immune checkpoint inhibitors and multi–tyrosine kinase inhibitors in previously untreated patients, but identifying additional treatments is critical.

CLINICAL PRACTICE

Unruptured Intracranial Aneurysms

A 55-year-old woman with well-controlled hypertension and a 20-pack-year smoking history presents to her primary care physician with occasional throbbing headaches on the left side and a recent episode of blurred vision. Her mother died of a subarachnoid hemorrhage at 62 years of age, and her uncle was treated for an unruptured brain aneurysm. On examination, her blood pressure is 135/85 mm Hg, with no focal neurologic deficits. Magnetic resonance angiography (MRA), performed as part of her headache evaluation, reveals a 6-mm saccular aneurysm in the posterior communicating artery, arising from the proximal aspect of the artery; the finding was confirmed by digital subtraction angiography. The patient is currently asymptomatic and concerned about the risk of aneurysm rupture and the risks associated with potential interventions. How should her care be managed?

Imaging in a Patient with a Posterior Communicating Aneurysm.

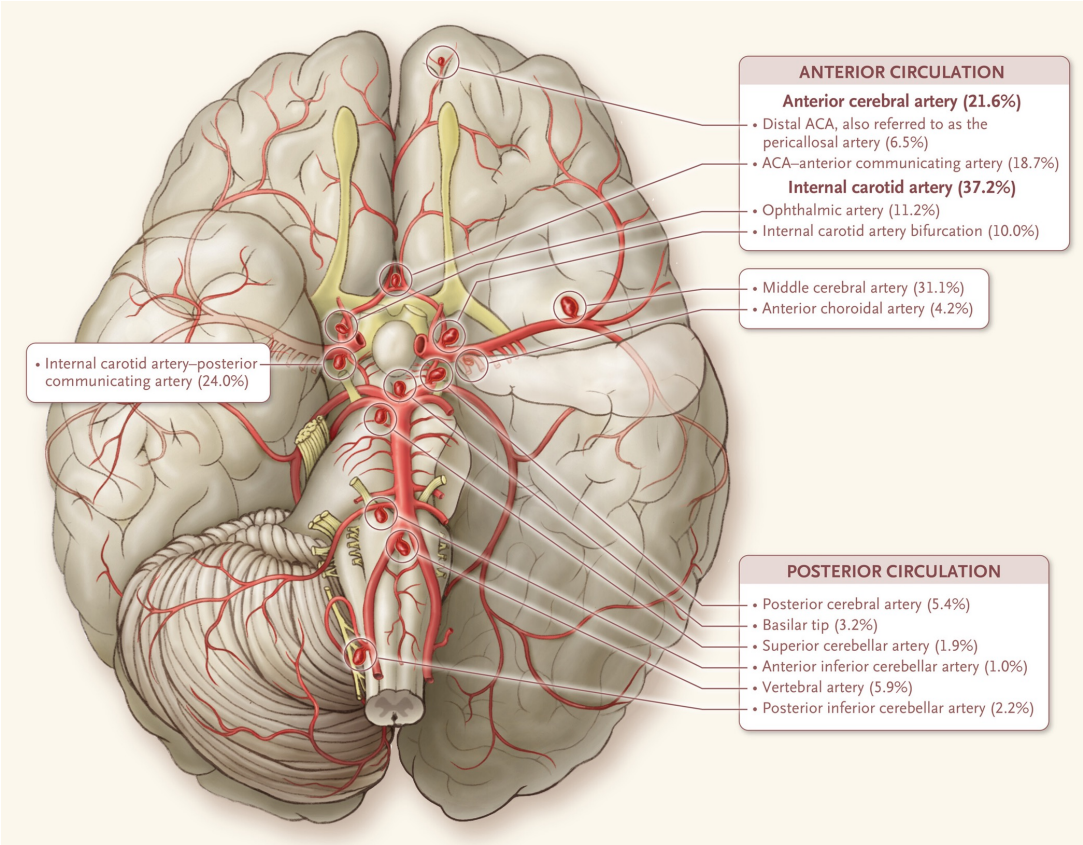
In Panel A, digital subtraction angiography shows a 6-mm posterior communicating aneurysm (arrow) in a woman 55 years of age. A three-dimensional reconstruction of the aneurysm is shown in Panel B.





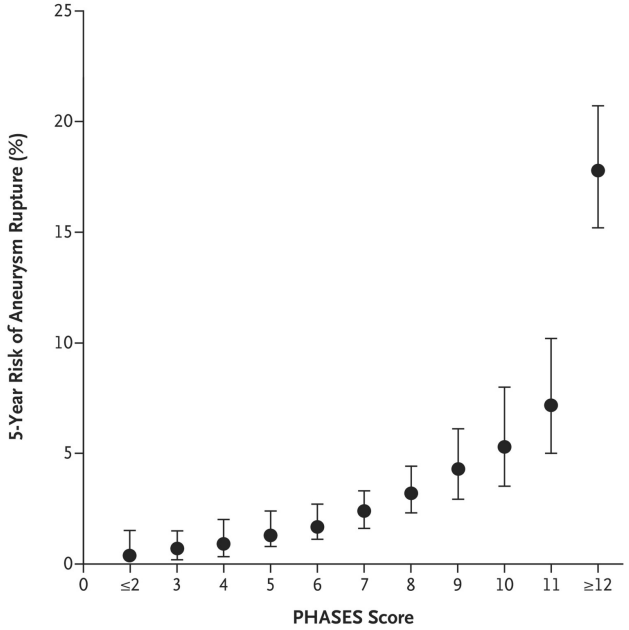
Unruptured Intracranial Aneurysms

- The risk of intracranial aneurysm rupture is influenced by aneurysm size, location, morphologic features, and patient-specific factors such as hypertension, smoking, and family history.
- Magnetic resonance angiography and computed tomographic angiography are preferred for the detection of intracranial aneurysms, with digital subtraction angiography reserved for complex cases or treatment planning.
- Conservative management focuses on smoking cessation, blood-pressure control, and routine imaging follow-up, whereas intervention (endovascular or surgical) is reserved for higher-risk aneurysms (i.e., ≥7 mm in diameter and located in the anterior circulation).
- Endovascular techniques, including coiling and flow diversion, are associated with lower perioperative risks but higher risks of recurrence, whereas surgical clipping provides durable results but with greater procedural risks.
- Living with an intracranial aneurysm can cause considerable anxiety. Patient education, psychological support, and shared decision making are essential in addressing patient concerns and ensuring adherence to the management plan.



Distribution of Unruptured Intracranial Aneurysms According to Arterial Location.

Data were synthesized from the most recent global prevalence systematic review by Vlak et al. (see the Supplementary Appendix).[4] ACA denotes anterior cerebral artery.



PHASES Score	Hazard Ratio for Rupture over 5 Yr (95% CI)
≤2	0.4 (0.1–1.5)
3	0.7 (0.2–1.5)
4	0.9 (0.3–2.0)
5	1.3 (0.8–2.4)
6	1.7 (1.1–2.7)
7	2.4 (1.6–3.3)
8	3.2 (2.3–4.4)
9	4.3 (2.9–6.1)
10	5.3 (3.5–8.0)
11	7.2 (5.0–10.2)
≥12	17.8 (15.2–20.7)

Five-Year Risk of Intracranial Aneurysm Rupture According to PHASES Score.

The PHASES score is based on population, hypertension, age, size of aneurysm, earlier subarachnoid hemorrhage, and site of aneurysm. Scores range from 0 to 22, with higher scores indicating a higher risk of rupture.

Incidence of Aneurysm Rupture According to the UCAS (1-Year Incidence) and the ISUIA (Overall Incidence).

Location	1-Yr Incidence of Rupture According to Size of Aneurysm					Overall Incidence of Rupture According to Size of Aneurysm: No Previous SAH		Overall Incidence of Rupture According to Size of Aneurysm: Previous SAH	
	3–4 mm	5–6 mm	7–9 mm	10–24 mm	≥25 mm†	<10 mm	≥10 mm	<10 mm	≥10 mm
					percent				
UCAS Japan[25]									
ACA	0.9	0.8	2.0	5.2	39.8	—	—	—	—
Basilar tip or SCA	0.2	0.5	1.0	6.9	117.8	—	—	—	—
ICA	0.1	0	1.2	1.1	10.6	—	—	—	—
ICA–PComA	0.4	1.0	3.2	6.1	127.0	—	—	—	—
MCA	0.2	0.3	1.6	4.1	16.9	—	—	—	—
VA–proximal BA	0	0	0	3.5	0	—	—	—	—
ISUIA[26]	—	—	—	—	—	0.05	1.0	0.5	1.0

Scoring Systems That Form the Basis of the Clinical Rationale for Monitoring Aneurysm Growth and Rupture.

Aneurysm Growth

ELAPSS Scoring System[32]

- Earlier SAH
  - Yes — 0
  - No — 1
- Location of aneurysm
  - ICA, ACA, or AComA — 0
  - MCA — 3
  - PComA or posterior circulation — 5
- Age
  - ≤60 yr — 0
  - >60 yr — 1 (per 5-yr interval after 60 yr)
- Population
  - North America, China, Europe (other than Finland) — 0
  - Japan — 1
  - Finland — 7
- Size of aneurysm, mm
  - 1.0 to 2.9 — 0
  - 3.0 to 4.9 — 4
  - 5.0 to 6.9 — 10
  - 7.0 to 9.9 — 13
  - ≥10.0 — 22
- Shape of the aneurysm
  - Regular — 0
  - Irregular — 4

Score and Growth Risk

- Score <5
  - 3-yr risk: 5.0%
  - 5-yr risk: 8.4%
- Score of 5–9
  - 3-yr risk: 7.8%
  - 5-yr risk: 13.0%
- Score of 10–14
  - 3-yr risk: 11.7%
  - 5-yr risk: 19.3%
- Score of 15–19
  - 3-yr risk: 17.5%
  - 5-yr risk: 28.1%
- Score of 20–24
  - 3-yr risk: 25.8%
  - 5-yr risk: 39.9%
- Score ≥25
  - 3-yr risk: 42.7%
  - 5-yr risk: 60.8%

Aneurysm Rupture

PHASES Scoring System[30]

- Population
  - North American, European (not Finnish) — 0
  - Japanese — 3
  - Finnish — 5
- Hypertension
  - No — 0
  - Yes — 1
- Age
  - <60 yr — 0
  - ≥70 yr (per 5 yr) — 1
- Size
  - <7.0 mm — 0
  - 7.0 to 9.9 mm — 3
  - 10.0 to 19.9 mm — 6
  - ≥20.0 mm — 10
- Earlier SAH from another aneurysm
  - No — 0
  - Yes — 1
- Site of aneurysm
  - ICA — 0
  - MCA — 2
  - ACA, PComA, or posterior circulation — 4

Finnish Scoring System[33]

- Age at diagnosis
  - <40 yr — 2
- Smoking status at baseline
  - Current smoker — 2
- Maximum diameter of UIA
  - ≥7 mm — 3
- Aneurysm location
  - ACA — 5
  - ICA — 4
  - PComA — 2

UCAS Scoring System[34]

- Age
  - <70 yr — 0
  - ≥70 — 1
- Sex
  - Male — 0
  - Female — 1
- Hypertension
  - No — 0
  - Yes — 1
- Location
  - ICA — 0
  - ACA or VA — 1
  - MCA or BA — 2
  - AComA or ICA–PComA — 3
- Daughter sac
  - No — 0
  - Yes — 1

Score and Rupture Risk

- Score ≤2
  - 5-yr risk: 0.4%
- Score of 3
  - 5-yr risk: 0.7%
- Score of 4
  - 5-yr risk: 0.9%
- Score of 5
  - 5-yr risk: 1.3%
- Score of 6
  - 5-yr risk: 1.7%
- Score of 7
  - 5-yr risk: 2.4%
- Score of 8
  - 5-yr risk: 3.2%
- Score of 9
  - 5-yr risk: 4.3%
- Score of 10
  - 5-yr risk: 5.3%
- Score of 11
  - 5-yr risk: 7.2%
- Score ≥12
  - 5-yr risk: 17.8%

- Score of 0
  - Annual risk: 0%
  - 10-yr risk: 0%
  - 30-yr risk: 0%
- Score of 1–4
  - Annual risk: 0.6%
  - 10-yr risk: 3%
  - 30-yr risk: 18%
- Score of 5–8
  - Annual risk: 2.2%
  - 10-yr risk: 16%
  - 30-yr risk: 49%
- Score of 9–12
  - Annual risk: 6.8%
  - 10-yr risk: 60%
  - 30-yr risk: 80%

- Score of 0
  - 3-yr risk: 0.2%
- Score of 1
  - 3-yr risk: 0.4%
- Score of 2
  - 3-yr risk: 0.6%
- Score of 3
  - 3-yr risk: 0.9%
- Score of 4
  - 3-yr risk: 1.4%
- Score of 5
  - 3-yr risk: 2.3%
- Score of 6
  - 3-yr risk: 3.7%
- Score of 7
  - 3-yr risk: 5.8%
- Score of 8
  - 3-yr risk: 7.6%
- Score of 9
  - 3-yr risk: 17%

Conclusion

The patient in the vignette has a small (6 mm), asymptomatic saccular aneurysm emanating from the posterior communicating artery, her medical history includes hypertension and smoking, and she has a family history of subarachnoid hemorrhage. According to size alone, the risk of rupture is low; however, given the patient's moderate risk of rupture (a PHASES score of 5 [on a range of 0 to 22, with higher scores indicating a higher risk of rupture]) based on her relatively young age, the irregular aneurysm shape, a positive family history, the presence of hypertension, and her smoking history, I would favor an invasive treatment strategy. Discussions with the patient will involve weighing the two treatment approaches, with surgical clipping offering a more definitive yet more invasive option, whereas endovascular techniques are less invasive, safer, and have similar long-term efficacy. The treatment for this patient will follow a shared decision-making process that involves weighing the risks, benefits, and the patient's lifestyle preferences. While waiting for treatment, or if the patient prefers surveillance monitoring, I would counsel the patient on signs of aneurysm rupture and recommend seeking immediate medical attention if symptoms arise, including a sudden severe headache that feels like the worst headache she has ever had, neck stiffness, and changes in vision.

Generalized Pustular Psoriasis



A 54-year-old woman with invasive ductal carcinoma of the breast and well-controlled chronic plaque psoriasis presented to the emergency department with a 2-day history of painful rash and fever. Five days before the onset of the rash, the patient had completed a 2-week course of systemic glucocorticoids to treat side effects of chemotherapy. The body temperature was 38.2°C, and heart rate 137 beats per minute. On physical examination, widespread erythematous patches with overlying, coalescing pustules were seen on the torso (Panel A), arms (Panel B), legs, face, and scalp, with sparing of mucosal surfaces. Laboratory testing was notable for neutrophilic leukocytosis and an elevated C-reactive protein level. Biopsy of the rash in the periumbilical region revealed neutrophil-rich pustules in the epidermis on histopathological testing. A diagnosis of generalized pustular psoriasis — a rare, autoinflammatory skin disease that manifests as widespread sterile pustules and systemic symptoms — was made. Generalized pustular psoriasis often occurs in patients with plaque psoriasis. It may be spontaneous or triggered by physiological stressors, such as medication withdrawal — as was thought to be the case here with withdrawal of glucocorticoids. Two doses of guselkumab were given. The pustules resolved in 1 week, and only sparse scaly patches remained at the 3-month follow-up visit.

Tongue Atrophy and Fasciculations in Advanced Motor Neuron Disease



A 32-year-old woman was brought to the hospital with a 3-year history of progressive weakness of the arms, legs, and trunk that had limited her ability to walk during the preceding 9 months. Because she resided in a remote rural community, she had been unable to consult with a neurologist. On physical examination, weakness and wasting were noted in the muscles of the arms and legs. She could not hold up her head or sit up without assistance, and her voice was strained. There was atrophy of the hand muscles. Her reflexes were brisk, and sensory testing was normal. Owing to oropharyngeal dysphagia, a nasogastric tube was inserted. Marked atrophy of the tongue with scalloping and fasciculations — findings suggestive of bulbar lower motor neuron disease — was present (see video; the patient's lips appear blue in the image and the video because of the lighting). On the basis of the upper and lower motor neuron signs, results on electromyography, and normal findings on magnetic resonance imaging of the brain and spine, a diagnosis of advanced motor neuron disease (probably amyotrophic lateral sclerosis) was made. Treatment with riluzole was started. Genetic testing was unavailable. The patient declined placement of a percutaneous gastrostomy tube and opted to follow up in a primary care clinic closer to her home.

VIDEO



Tongue Scalloping and Fasciculations 0m 10s

Case 17-2025: A 61-Year-Old Man with Respiratory Failure and Shock after Kidney Transplantation

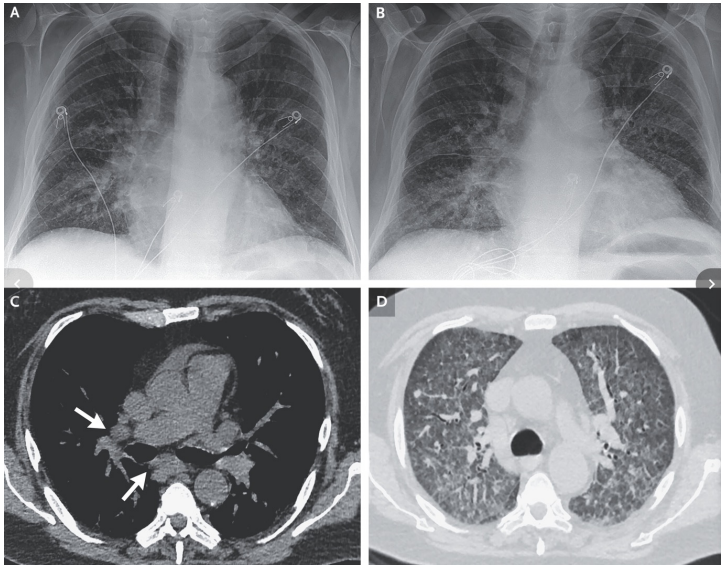
A 61-year-old man was transferred to this hospital because of acute hypoxemic respiratory failure and shock. Ten weeks earlier, the patient had undergone deceased-donor kidney transplantation at this hospital for hypertensive nephrosclerosis-related end-stage kidney disease. After transplantation, the patient's hospitalization was notable for the administration of antithymocyte globulin induction therapy; delayed graft function with hyperkalemia, for which he underwent two sessions of hemodialysis; and urinary retention. On postoperative day 4, he was discharged home with instructions to take oral prednisone, tacrolimus, mycophenolate sodium, trimethoprim–sulfamethoxazole, and valganciclovir.

Six weeks after transplantation (4 weeks before the current admission), during a follow-up visit in the transplantation clinic, the creatinine level was 1.60 mg per deciliter (141 µmol per liter; reference range, 0.60 to 1.50 mg per deciliter [53 to 133 µmol per liter]); however, hyperglycemia was noted, with a glycated hemoglobin level of 7.7% (reference value, <5.7). Treatment with a once-weekly injection of semaglutide was started.

One week later, the patient was evaluated at the emergency department of another hospital for erythema and swelling of the left ankle after being scratched by a domestic cat. A radiograph of the ankle reportedly showed soft-tissue swelling. A course of amoxicillin–clavulanate was prescribed.

Variable	Reference Range, Adults, Other Hospital	On Admission, Other Hospital	Fourth Day, Other Hospital	On Intensive Care Unit Transfer, Other Hospital	Reference Range, Adults, This Hospital†	On Admission, This Hospital
Hemoglobin (g/dl)	13.0–17.0	12.5	9.9	9.0	13.5–17.5	7.9
Hematocrit (%)	40.0–51.0	36.7	30.5	26.9	41.0–53.0	24.3
White-cell count (per μl)	3900–11,000	2500	3790	18,300	4500–11,000	24,600
Differential count (per μl)						
Neutrophils	1800–7700	1310	—	—	1800–7700	20,420
Lymphocytes	1000–4800	150	—	—	1000–4800	740
Monocytes	200–1200	200	—	—	0–1200	250
Eosinophils	0–900	550	—	—	0–900	980
Bands	—	—	—	—	—	3940
Metamyelocytes	<1	225	—	—	—	980
Myelocytes	<1	25	—	—	—	490
Promyelocytes	—	—	—	—	—	740
Platelet count (per μl)	130,000–400,000	215,000	209,000	397,000	150,000–400,000	409,000
Sodium (mmol/liter)	136–145	125	128	127	135–145	124
Potassium (mmol/liter)	3.4–5.1	4.0	4.0	4.6	3.4–5.0	4.6
Chloride (mmol/liter)	98–107	83	94	88	98–108	86
Carbon dioxide (mmol/liter)	20–31	30	25	25	23–32	23
Urea nitrogen (mg/dl)	8–23	29	22	51	8–25	56
Creatinine (mg/dl)	0.60–1.30	1.80	1.48	2.20	0.60–1.50	2.35
Glucose (mg/dl)	70–100	639	297	252	70–110	369
β-hydroxybutyrate (mmol/liter)	0.0–1.0	0.6	—	—	—	—
Albumin (g/dl)	3.3–5.0	4.2	3.0	3.1	3.3–5.0	3.0
Alanine aminotransferase (U/liter)	10–55	23	18	52	10–55	52
Aspartate aminotransferase (U/liter)	10–40	17	22	63	10–40	55
Total bilirubin (mg/dl)	0.0–1.0	0.6	0.4	1.3	0.0–1.0	1.0
Lipase (U/liter)	13–60	81	—	—	—	—
Lactate (mmol/liter)	0.5–2.0	—	—	1.7	0.5–2.2	1.3
N-terminal pro–B-type natriuretic peptide (pg/ml)	<900	—	3155	5817	—	—
Tacrolimus (ng/ml)	5.0–10.0	6.1	6.8	—	—	7.3
C-reactive protein (mg/liter)	0.0–5.0	—	—	>70.0	—	—
Procalcitonin (ng/ml)	0.00–0.50	—	—	1.53	—	—
1,3-β-D-glucan (pg/ml)	—	—	—	—	<59	87
Arterial blood gas						
Fraction of inspired oxygen	—	0.7	—	—	—	0.5
pH	7.35–7.45	7.34	—	—	7.35–7.45	7.41
Partial pressure of carbon dioxide (mm Hg)	35–42	54	—	—	35–42	36
Partial pressure of oxygen (mm Hg)	80–100	137	—	—	80–100	78

Under Steroids



Initial Imaging Studies of the Chest Obtained at the Other Hospital.
A posteroanterior chest radiograph obtained on the 9th day of hospitalization at the other hospital (Panel A) shows fullness in the hila, indistinctness of the pulmonary vasculature, thickening of the minor fissure, and peripheral interlobular septal thickening. A posteroanterior chest radiograph obtained on the 10th day of hospitalization at the other hospital (Panel B) shows mildly increased pulmonary edema. On the same day, axial projection CT images, obtained without the administration of contrast material, in soft-tissue and lung windows show mediastinal and hilar lymphadenopathy (Panel C, arrows) and diffuse ground-glass opacities and interlobular thickening (Panel D).

The patient's medical history included hypertension, type 2 diabetes mellitus, hyperlipidemia, coronary calcifications, ectasia of the aorta, hyperparathyroidism for which he had undergone parathyroidectomy, obstructive sleep apnea, kyphoplasty at the level of the first lumbar vertebra, and repair and internal fixation of a left ankle fracture. The patient had been undergoing hemodialysis for 6 years while awaiting kidney transplantation. Outpatient medications included oral prednisone, tacrolimus, mycophenolate sodium, trimethoprim–sulfamethoxazole, valganciclovir, furosemide, labetalol, famotidine, and tamsulosin, as well as subcutaneous semaglutide. (11 preparations) Atenolol had caused constipation, and amitriptyline had caused dry mouth.

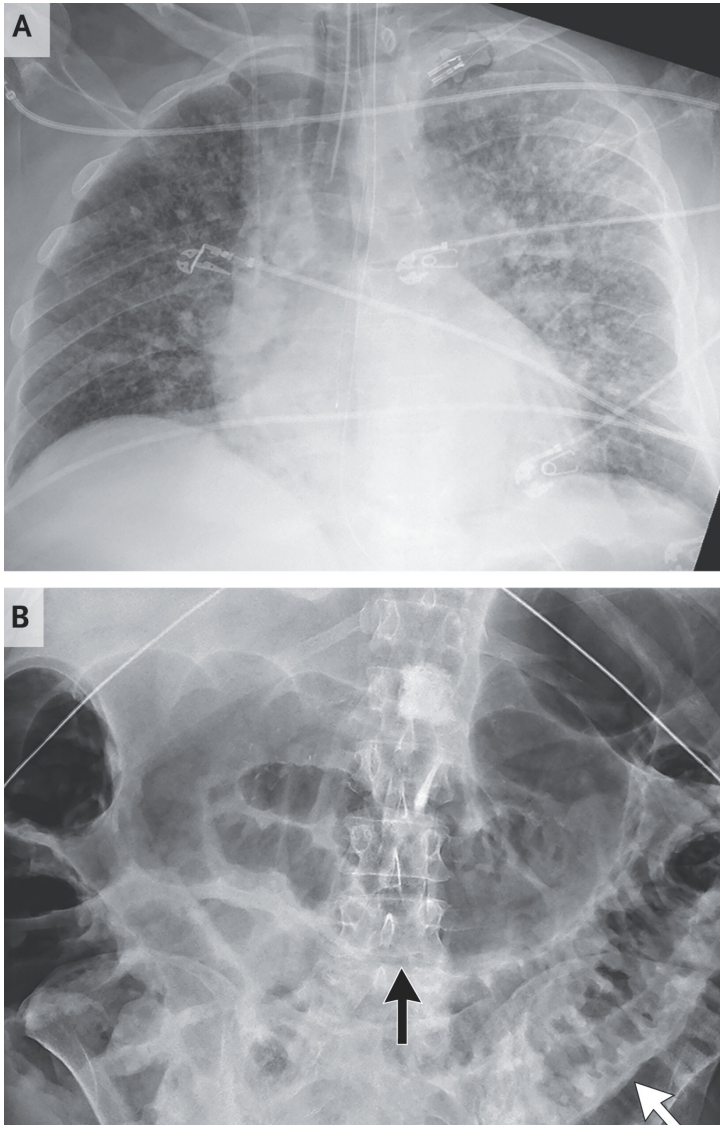
The patient's family history was notable for diabetes in multiple maternal relatives, renal insufficiency in his mother, and prostate cancer in his father. The patient had smoked cigarettes for 20 years but had quit 25 years before the current admission. He did not drink alcohol or use other substances. He had lived in New England his entire life, except for 18 months during his teenage years, when he resided in the southern United States; he had not otherwise traveled. He had been previously employed in food service and education and had not had any known occupational exposures. He enjoyed gardening and had healthy domestic cats and a dog at home.

On examination, the esophageal temperature was 38.1°C, the heart rate 123 beats per minute, and the blood pressure 114/58 mm Hg while the patient was receiving infusions of norepinephrine at a rate of 36 µg per minute and vasopressin. The weight was 109.0 kg. The oxygen saturation was 97% while he was receiving oxygen through a mechanical ventilator in volume-control mode (tidal volume, 500 ml at a rate of 20 breaths per minute; positive end-expiratory pressure, 8 cm of water; fraction of inspired oxygen, 0.50). No oral mucosal lesions were present. Auscultation of the chest revealed diffuse crackles in the lungs. The heart was tachycardic. The abdomen was distended and tense, with few bowel sounds. The kidney allograft site in the right lower quadrant was nonerythematous; no bruit was detected. A purpuric rash was present on the abdomen. An arteriovenous fistula in the left upper arm was associated with a weak thrill and bruit. Symmetric leg edema was present.



Photograph of Abdominal Rash.

A photograph obtained on admission to the intensive care unit at this hospital shows a purpuric rash on the abdomen.



Radiographs of the Chest and Abdomen Obtained at This Hospital.

An anteroposterior chest radiograph obtained while the trachea was intubated (Panel A) is notable for increased pulmonary edema, and an abdominal radiograph obtained on the same day (Panel B) shows diffuse gaseous distention of the small bowel (white arrow) and large bowel (black arrow).

A chest radiograph (Figure 3A) showed diffuse bilateral interstitial and airspace opacities that were more extensive in the left lung than in the right lung. The endotracheal tube, central venous catheter in the right internal jugular vein, and nasogastric tube were all in appropriate positions. An abdominal radiograph obtained on the same day (Figure 3B) showed diffuse gaseous distention of the small and large bowel.

Intravenous vancomycin and meropenem therapy was continued, and methylene blue therapy was started. Diagnostic tests were performed.

Differential Diagnosis

I participated in the care of this patient, and I am aware of the final diagnosis in this case.

Approximately 10 weeks after uneventful kidney transplantation, this 61-year-old man was transferred to this hospital with acute hypoxemic respiratory failure and shock. Features of his combined hospital course included progressively worsening acute kidney injury, leukocytosis, eosinophilia, volume overload, emesis, ileus, and abdominal pain. Chest imaging was notable for extensive interstitial and ground-glass opacities and mediastinal and hilar lymphadenopathy. Despite the administration of broad-spectrum antimicrobial therapy, the patient's condition progressively worsened.

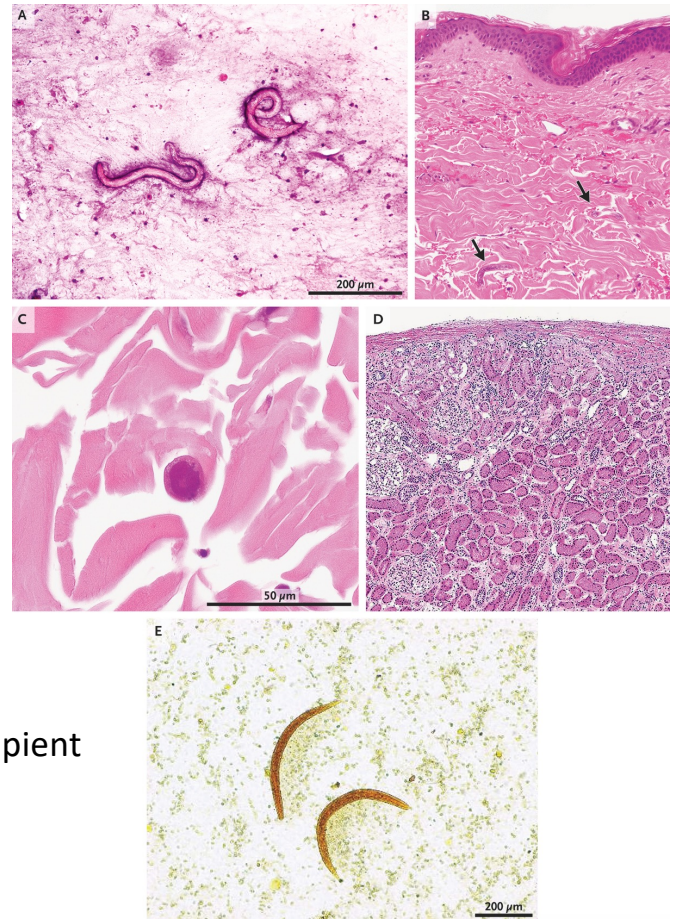
Looking back at the patient's history, I had seen him during routine telemedicine evaluations 2 years before transplantation. At that time, he had minimal exposure to sources of infection and few risk factors. On evaluation, we learned that he had four cats and a dog and volunteered at a cat rescue center, and he had lived in the southern United States for 18 months as a teenager. The absolute eosinophil count was normal at the time of transplantation (160 per microliter) and remained normal until 67 days after transplantation, when it increased to 550 per microliter and remained elevated until admission to this hospital (absolute eosinophil count on admission, 980 per microliter). We also learned that the patient had been scratched by a cat 3 weeks earlier; the cat scratch was unrelated to his current presentation, although disseminated bartonella infection would be in the differential diagnosis (especially given the presence of eosinophilia).

I was especially intrigued by the patient's eosinophilia, which is a very unusual feature in a patient who is taking prednisone. The cause of this patient's elevated eosinophil count could be a parasitic infection, a drug reaction, or allograft rejection, among others. Given that the patient's presentation is not consistent with a drug reaction or rejection of the kidney allograft, I think that the most likely explanation for his critical illness is a disseminated parasitic infection. The extent of eosinophilia in this patient is greater than that usually seen in patients with *T. gondii* or *P. jirovecii* infection, and these infections would also have been prevented with the prophylactic administration of trimethoprim–sulfamethoxazole. Other parasitic infections such as toxocariasis do not typically manifest with critical illness.

Although the patient did not have risk factors for previous exposure to strongyloides, donor-derived strongyloidiasis has been reported. Whenever I am caring for a recent transplant recipient with a clinical syndrome consistent with infection, I immediately contact New England Donor Services (a regional organ-procurement organization here in New England) to check the clinical status of other recipients who received an organ donation from the same donor. When I initially evaluated this patient, I thought that the most likely diagnosis was donor-derived disseminated strongyloidiasis, given his overall clinical presentation.

Diagnosis

Donor-derived disseminated strongyloidiasis.



Second recipient

Strongyloides stercoralis, the parasitic worm that causes strongyloidiasis, is considered endemic in certain areas of the United States, particularly in the southeastern U.S. and Appalachia.

Tracheal Aspirate and Biopsy Specimens and a Stool Specimen.

Tracheal aspirate and biopsy specimens were obtained on admission to this hospital. Gram's staining of the tracheal aspirate (Panel A) shows two larval forms with rounded heads and tapered tails, measuring approximately 250 to 300 microns in length and 18 to 25 microns in width, in a background of numerous eosinophils. Hematoxylin and eosin staining of a 4-mm punch-biopsy specimen of skin from the abdominal rash (Panels B and C) shows larvae (Panel B, arrows) infiltrating the dermal collagen with minimal inflammation. At higher magnification (Panel C), the larvae are seen in cross section, surrounded by dermal collagen. Hematoxylin and eosin staining of a frozen section of the wedge-biopsy specimen that had been obtained from the donated kidney at the time of transplantation (Panel D) shows cortical renal parenchyma with no specific pathological abnormality. A stool specimen was obtained from the second kidney-transplant recipient, who had received the deceased donor's other kidney. An iodine preparation of the stool specimen (Panel E) confirms the diagnosis of strongyloidiasis in the second kidney-transplant recipient.

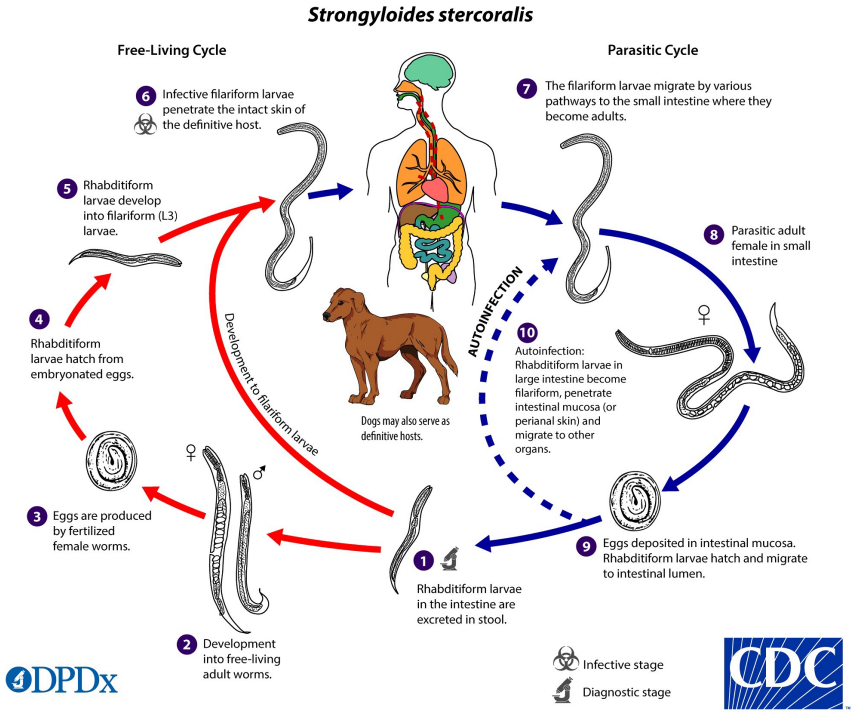
Donor-Derived Infection and Management

As soon as the patient was transferred to this hospital, I contacted New England Donor Services regarding my concern about a possible donor-derived infection. The organization verified that the donor had resided in the Caribbean and had not undergone testing for strongyloides. Subsequent post-transplantation testing of the donor's blood revealed seropositivity for strongyloides. Pretransplantation testing of the recipient's blood had been negative for strongyloides. These findings confirm a donor-derived infection. Other medical centers that had transplanted organs from the same deceased donor were notified.

Second Kidney-Transplant Recipient

The transplantation team received a call that day from the regional organ-procurement organization that the recipient of the donor's other kidney was critically ill with disseminated strongyloidiasis. A prompt infectious-disease consultation was requested. Testing of a stool specimen for microscopic ova and parasites was positive for rhabditiform larvae. Treatment with ivermectin at a dose of 200 µg per kilogram of body weight per day and empirical treatment with piperacillin–tazobactam were initiated. During the next 3 days, the patient's kidney function and volume overload worsened, which led to two hemodialysis sessions. A kidney biopsy revealed evidence of nephrotoxicity that was presumed to be associated with calcineurin inhibitor therapy.

After discussions between the infectious-disease specialists who were caring for these respective patients and an expert parasitologist, therapy was intensified; the daily dose of oral ivermectin was doubled, and oral albendazole at a dose of 400 mg twice per day was added. Within 10 days after initiation of the dual antiparasitic therapy, the kidney function returned to baseline, the white-cell count normalized, and two consecutive parasitic examinations of stool were negative. After 2 weeks, albendazole was discontinued, and the dose of ivermectin was reduced to the standard dose for 1 additional month. Two post-treatment stool studies were negative for strongyloides, and the patient has been thriving.



Autoinfection

Discussion of Management after Kidney Transplantion

Four weeks after kidney transplantation, the first patient's kidney graft had shown excellent function, with a nadir in the creatinine level of 1.46 mg per deciliter (129 µmol per liter). However, approximately 6 weeks after transplantation, BK virus viremia had developed, which led to a 50% dose reduction in mycophenolate sodium.

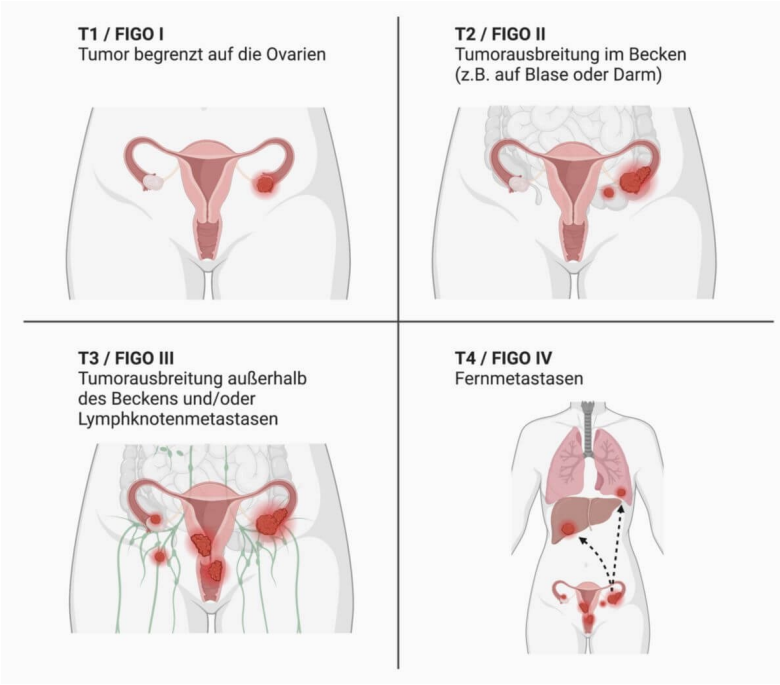
When the patient became critically ill with shock and respiratory failure due to disseminated strongyloidiasis, mycophenolate sodium and tacrolimus were discontinued, and stress-dose glucocorticoid therapy was started. The total IgG level was evaluated; the results ruled out hypogammaglobulinemia and thus obviated the need for intravenous immune globulin therapy. Tacrolimus therapy was reintroduced once the patient's condition became more hemodynamically stable. Mycophenolate sodium therapy was resumed 6 weeks after the patient was hospitalized, once control of strongyloidiasis had been established and a clinically significant decrease in BK virus viremia had occurred. Throughout the patient's critical illness, the allograft maintained adequate function despite fluctuating creatinine levels, which were notably low (<0.8 mg per deciliter [<71 µmol per liter]) and possibly reflected a reduction in muscle mass due to critical-illness myopathy, which occurred during hospitalization. Eleven months after the current admission, the patient's kidney function remains stable, with creatinine levels between 1.8 and 2.2 mg per deciliter (159 and 194 µmol per liter).

Final Diagnosis

Disseminated strongyloidiasis.

Das Ovarialkarzinom ist ein maligner Tumor des Ovars (Eierstocks), an dem jährlich etwa 9.000 Frauen in Deutschland erkranken. Es ist der zweithäufigste bösartige Genitaltumor der Frau, der mit einer hohen Mortalität verbunden ist.

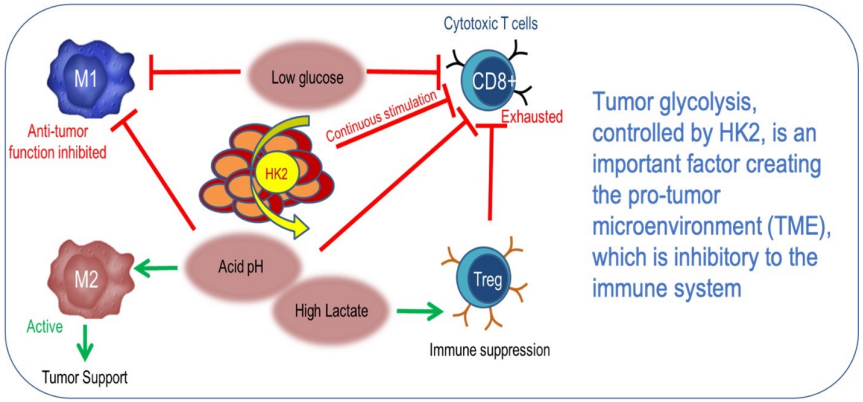
- Epitheliale Tumoren (60-70 %)
  - Low-grade seröses Karzinom (LGSC, LGOSC)
  - High-grade seröses Karzinom (HGSC, HGOSC)
  - Muzinöses Ovarialkarzinom (MOC)
  - Endometrioides Ovarialkarzinom (EnOC)
  - Klarzelliges Ovarialkarzinom (CCOC)
  - Maligner Brennertumor
  - Karzinosarkom (Müller-Mischtumor)
  - Nicht klassifizierbare Tumoren
- Keimzelltumoren (ca. 15-20 %)
  - Dysgerminom
  - Unreifes Teratom
  - Dottersacktumor
  - Nicht-gestationales Chorionkarzinom (NGOC)
- Keimstrang-Stroma-Tumoren (ca. 5-10 %)
  - Fibrosarkom
  - Gynandroblastom
- Ovarialmetastasen (ca. 5 %)
  - Endometriumkarzinom
  - Mammakarzinom
  - Gastrointestinale Karzinome
- Kleinzelliges Ovarialkarzinom vom hyperkalzämischen Typ (SCCOHT)

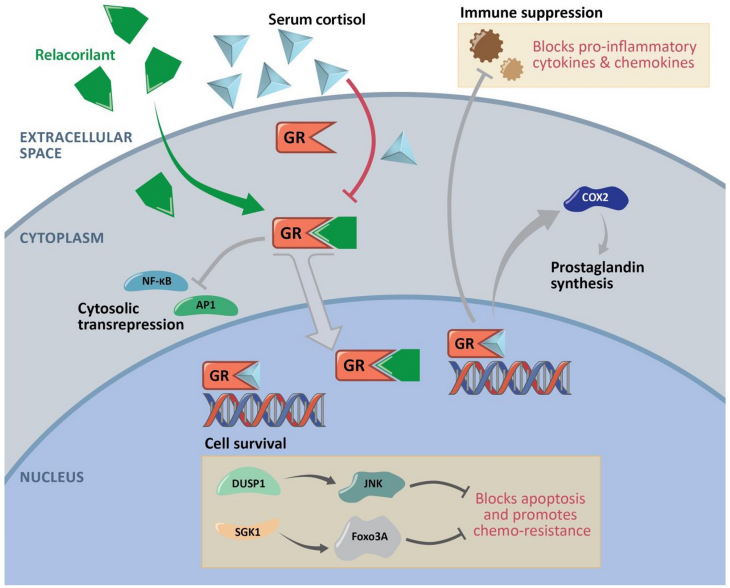


Relacorilant ist ein oraler, selektiver Glukokortikoidrezeptor-Modulator (SGRM), der von Corcept Therapeutics zur Behandlung von verschiedenen Erkrankungen, einschließlich des Cushing-Syndroms und verschiedener Tumorarten, untersucht wird. Es ist ein oraler, selektiver Glukokortikoidrezeptor-Antagonist, der die Cortisolaktivität durch Bindung an den Glukokortikoidrezeptor moduliert, ohne andere Hormonrezeptoren im Körper zu beeinflussen.

Anwendungsgebiete:
Neben dem Cushing-Syndrom wird Relacorilant auch zur Behandlung von verschiedenen Tumorarten, einschließlich Eierstockkrebs und Prostatakrebs, sowie zur Behandlung von Alkoholismus untersucht.

Potenzielle Anwendungen:
Relacorilant könnte auch eine Rolle bei der Überwindung von Chemoresistenz in bestimmten Krebsarten spielen, da es die Aktivierung des Glukokortikoidrezeptors blockiert, ein wichtiger Weg bei der Entstehung von Chemoresistenz.





Relacorilant and nab-paclitaxel in patients with platinum-resistant ovarian cancer (ROSELLA): an open-label, randomised, controlled, phase 3 trial

Summary

Background Relacorilant, a first-in-class selective glucocorticoid receptor antagonist, increases a tumour's sensitivity to chemotherapy by reducing cortisol signalling. This study aimed to show whether the addition of relacorilant to nab-paclitaxel improves progression-free and overall survival in females with platinum-resistant ovarian cancer.

Methods This randomised, controlled, open-label phase 3 trial (ROSELLA [GOG-3073/ENGOT-ov72]) was done at 117 hospitals and community oncology treatment centres in 14 countries across Australia, Europe, Latin America, North America, and South Korea. Patients had to be aged 18 years or older and had to have a confirmed diagnosis of platinum-resistant, epithelial (ie, high-grade serous, endometrioid, or carcinosarcoma with a ≥30% epithelial component) ovarian, primary peritoneal, or fallopian tube cancer; up to three previous lines of anticancer therapy and previous bevacizumab and disease progression or intolerance to the most recent therapy; measurable disease according to the Response Evaluation Criteria in Solid Tumours (RECIST; version 1.1); an Eastern Cooperative Oncology Group performance status of 0 or 1; and adequate organ function. Patients were assigned (1:1) to relacorilant (150 mg orally the day before, of, and after nab-paclitaxel infusion) plus nab-paclitaxel (80 mg/m² intravenously on days 1, 8, and 15 of each 28-day cycle) or nab-paclitaxel monotherapy (100 mg/m² intravenously on the aforementioned schedule). The dual primary endpoints were progression-free survival assessed by blinded independent central review per Response Evaluation Criteria in Solid Tumours (version 1.1) and overall survival, and were assessed in all randomly assigned patients by intention to treat. The safety population included all randomly assigned patients who received at least one dose of the assigned treatment. This trial was registered at ClinicalTrials.gov, NCT05257408, and is ongoing.

Findings Between Jan 5, 2023, and April 8, 2024, 381 patients were randomly assigned to the combination group (n=188) or to the nab-paclitaxel monotherapy group (n=193). Patients receiving relacorilant plus nab-paclitaxel had a statistically significant improvement in progression-free survival assessed by blinded independent central review compared with those receiving nab-paclitaxel monotherapy (hazard ratio 0·70 [95% CI 0·54–0·91]; median 6·54 months [95% CI 5·55–7·43] *vs* 5·52 months [3·94–5·88]; stratified log-rank p=0·0076). At the planned interim analysis, there was a clinically meaningful difference in overall survival with the addition of relacorilant to nab-paclitaxel (0·69 [95% CI 0·52–0·92]; 15·97 months [95% CI 13·47–not reached] *vs* 11·50 months [10·02–13·57]; log-rank p=0·0121). Adverse events were similar across study groups when adjusted for nab-paclitaxel exposure; no new safety signals were observed.

Interpretation The addition of relacorilant to nab-paclitaxel prolonged progression-free survival and interim results also showed an improvement in overall survival. Together, the results position the combination of relacorilant and nab-paclitaxel as a potential new standard treatment for patients with platinum-resistant ovarian cancer.

Funding Corcept Therapeutics.

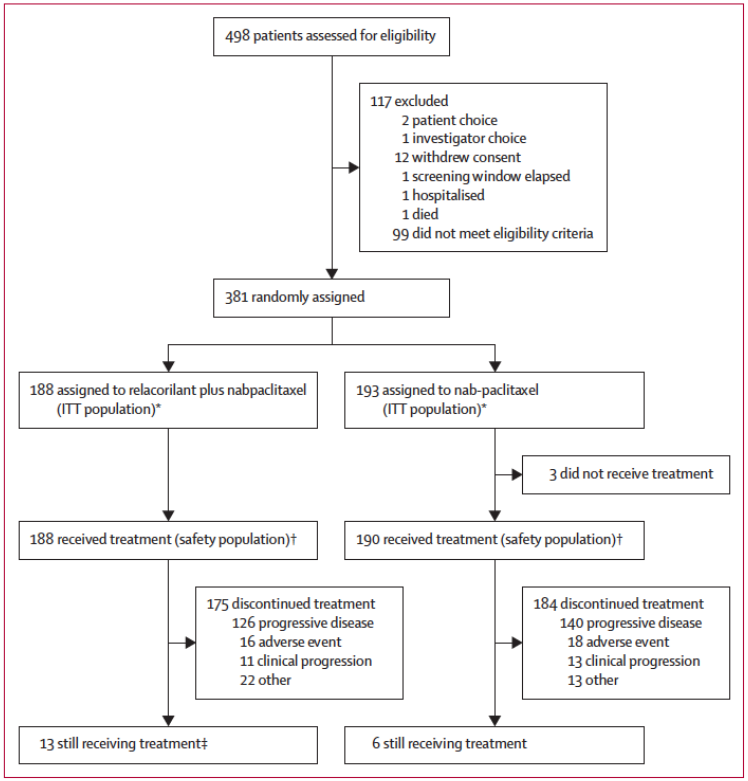


Figure 1: **Trial profile**
Three patients in the nab-paclitaxel monotherapy group withdrew consent and did not receive treatment. ITT=intent-to-treat. *All randomly assigned patients were analysed according to the randomised treatment group. †All randomly assigned patients who received at least one dose of study treatment (ie, relacorilant plus nab-paclitaxel or nab-paclitaxel monotherapy). ‡Refers to patients on nab-paclitaxel at the data cutoff.

	Relacorilant plus nab-paclitaxel (n=188)	Nab-paclitaxel monotherapy (n=193)
Age, years	61·0 (26–85)	62·0 (33–86)
≥65	72 (38%)	80 (41%)
Race		
White	136 (72%)	135 (70%)
Black or African American	3 (2%)	2 (1%)
Asian	22 (12%)	26 (13%)
Other or not reported	27 (14%)	30 (16%)
Ethnicity		
Hispanic or Latino	16 (9%)	17 (9%)
Non-Hispanic or Latino	145 (77%)	146 (76%)
Not reported or unknown	27 (14%)	30 (16%)
Geographical region		
North America	45 (24%)	45 (23%)
Europe	107 (57%)	109 (56%)
South Korea, Australia, and Latin America	36 (19%)	39 (20%)
Eastern Cooperative Oncology Group performance status score		
0	135 (72%)	127 (66%)
1	53 (28%)	62 (32%)
2	0	1 (1%)
Missing	0	3 (2%)
Stage at initial diagnosis*		
1–3	110 (59%)	114 (59%)
4	65 (35%)	66 (34%)
Missing data	13 (7%)	13 (7%)
BRCA mutation		
BRCA1 or *BRCA2* mutation	23 (12%)	24 (12%)
BRCA1 and *BRCA2* wildtype	133 (71%)	128 (66%)
Unknown	32 (17%)	41 (21%)
Previous lines of systemic therapy		
1	15 (8%)	18 (9%)
2	92 (49%)	89 (46%)
3	81 (43%)	86 (45%)
Previous lines of therapy in the platinum-resistant setting		
0	121 (64%)	111 (58%)
1	55 (29%)	68 (35%)
2	12 (6%)	14 (7%)

(Table continues on next page)

	Relacorilant plus nab-paclitaxel (n=188)	Nab-paclitaxel monotherapy (n=193)
(Continued from previous page)		
Previous taxane in the platinum-resistant setting	8 (4%)	7 (4%)
Previous exposure		
Bevacizumab	188 (100%)	193 (100%)
Taxane	187 (99%)	192 (99%)
Pegylated liposomal doxorubicin	121 (64%)	125 (65%)
Poly (ADP-ribose) polymerase inhibitor	114 (61%)	120 (62%)
Mirvetuximab soravtansine	3 (2%)	5 (3%)
Primary platinum-free interval		
1 to ≤3 months	13 (7%)	13 (7%)
>3 to ≤6 months	41 (22%)	45 (23%)
>6 months	134 (71%)	135 (70%)
Most recent taxane-free interval		
≤6 months	22 (12%)	33 (17%)
>6 to ≤12 months	37 (20%)	30 (16%)
>12 months	128 (68%)	129 (67%)
Ascites	8 (4%)	7 (4%)

Data are n (%) or median (range). Region (North America *vs* Europe *vs* South Korea, Australia, and Latin America) and previous lines of therapy (1 *vs* >1) per the Interactive Response Technology System data were stratification factors. Percentages might not add to 100 due to rounding. *BRCA*=Breast Cancer gene. *Based on the International Federation of Gynecology and Obstetrics cancer staging system.[24]

Table 1: **Baseline demographics and clinical characteristics (intent-to-treat population)**

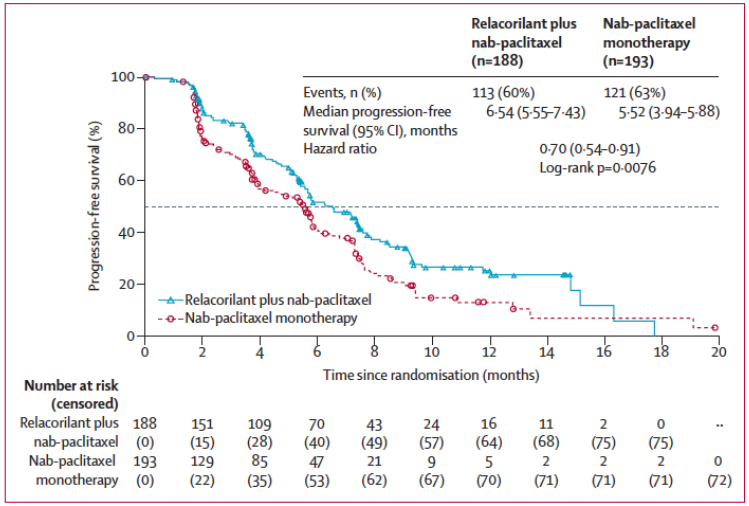


Figure 2: **Efficacy findings comparing relacorilant plus nab-paclitaxel with nab-paclitaxel monotherapy for progression-free survival**

Kaplan–Meier estimates of the dual primary endpoint progression-free survival assessed by blinded independent central review in the relacorilant plus nab-paclitaxel group and the nab-paclitaxel monotherapy group are shown. Analyses were performed in the intent-to-treat population.

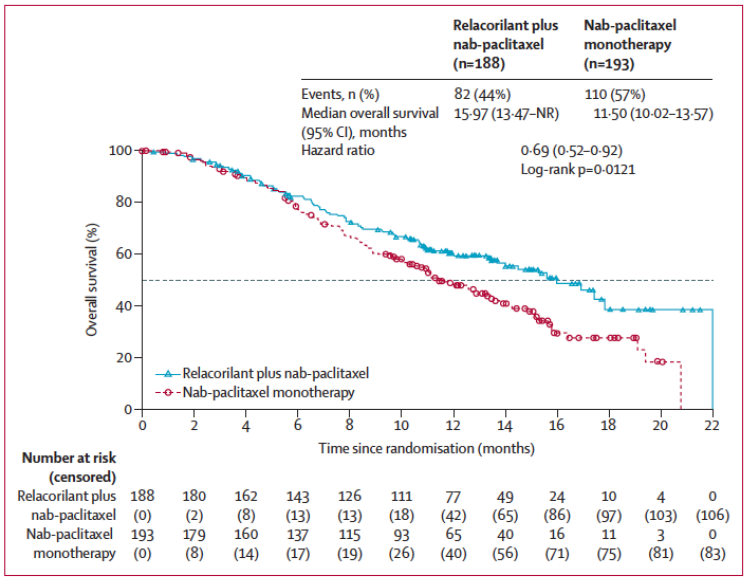


Figure 3: **Efficacy findings comparing relacorilant plus nab-paclitaxel with nab-paclitaxel monotherapy for the interim overall survival analysis**

Kaplan–Meier estimates of the dual primary endpoint of overall survival (at an interim analysis) in the relacorilant plus nab-paclitaxel group and the nab-paclitaxel monotherapy group are shown. Analyses were performed in the intent-to-treat population. 30 (8%) of 381 patients were censored in the first 6 months of the overall survival Kaplan–Meier curve, 13 in the combination group and 17 in the nab-paclitaxel monotherapy group; six patients were lost to follow-up and 24 withdrew consent.NR=not reached.

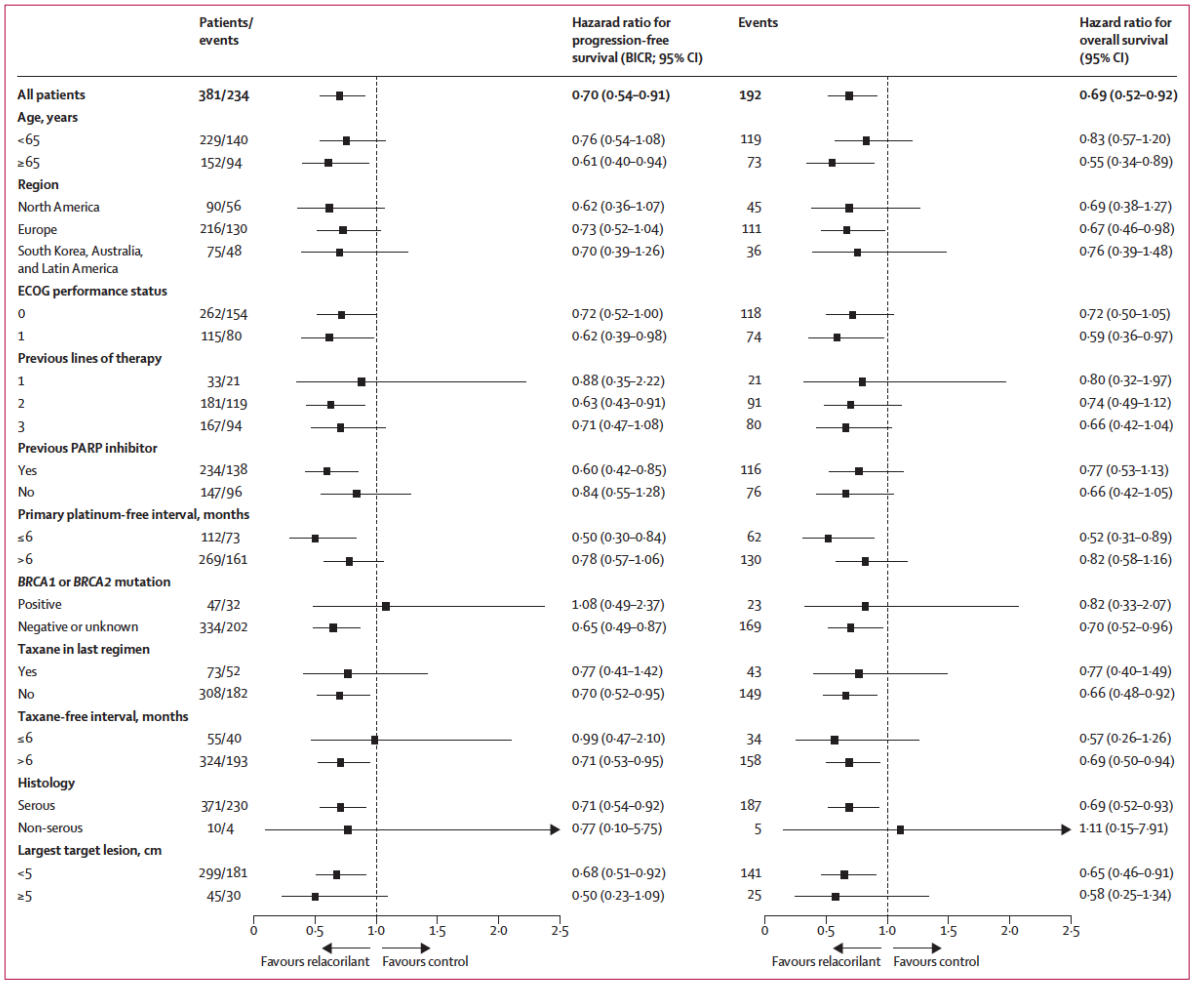


Figure 4: **Efficacy findings comparing relacorilant plus nab-paclitaxel with nab-paclitaxel monotherapy in subgroup analyses of progression-free survival and overall survival**

The results of exploratory subgroup analyses of progression-free survival assessed by blinded independent central review and overall survival in the intent-to-treat population are shown. The hazard ratios reported throughout this figure are based on a Cox proportional-hazards model, stratified according to the randomisation factors that were collected in the interactive response technology system, except when the randomisation factor is the subgroup under analysis; then, only a single stratification variable was used. Under the assumption of proportional hazards, a hazard ratio of less than 1 indicates a reduction in the hazard in favour of the combination group. BICR=blinded independent central review. *BRCA*=breast cancer gene. ECOG=Eastern Cooperative Oncology Group. PARP=poly (ADP-ribose) polymerase.

	Relacorilant plus nab-paclitaxel (n=188)		Nab-paclitaxel monotherapy (n=190)	
	Any grade	Grade ≥3	Any grade	Grade ≥3
Any adverse events	188 (100%)	140 (74%)	189 (99%)	113 (59%)
Treatment-related adverse events*				
Related to relacorilant	146 (78%)	74 (39%)	..	..
Related to nab-paclitaxel	177 (94%)	113 (60%)	172 (91%)	78 (41%)
Related to both relacorilant and nab-paclitaxel	138 (73%)	69 (37%)	..	..
Serious adverse events	66 (35%)	60 (32%)	45 (24%)	39 (21%)
Treatment interruptions due to adverse events				
Nab-paclitaxel (plus relacorilant)†	137 (73%)	..	104 (55%)	..
Dose reductions due to adverse events				
Relacorilant‡	13 (7%)	..	..	..
Nab-paclitaxel	91 (48%)	..	60 (32%)	..
Discontinuations due to adverse events				
Relacorilant	18 (10%)	..	..	..
Nab-paclitaxel (plus relacorilant)†	17 (9%)	..	15 (8%)	..
Adverse events leading to death	4 (2%)	..	0	..
Most frequent adverse events occurring in ≥20% of study participants in either group (by preferred term)§				
Neutropenia¶	120 (64%)	82 (44%)	93 (49%)	48 (25%)
Anaemia||	115 (61%)	34 (18%)	105 (55%)	16 (8%)
Fatigue**	99 (53%)	17 (9%)	85 (45%)	3 (2%)
Nausea	82 (44%)	7 (4%)	66 (35%)	6 (3%)
Diarrhoea	74 (39%)	7 (4%)	52 (27%)	3 (2%)
Alopecia	72 (38%)	1 (1%)	59 (31%)	0
Constipation	61 (32%)	1 (1%)	51 (27%)	0
Abdominal pain	55 (29%)	4 (2%)	54 (28%)	2 (1%)
Vomiting	48 (26%)	5 (3%)	43 (23%)	3 (2%)
Decreased appetite	41 (22%)	3 (2%)	22 (12%)	1 (1%)
Hypomagnesaemia	40 (21%)	3 (2%)	36 (19%)	2 (1%)

Data are n (%). Adverse events were graded according to the National Cancer Institute Common Terminology Criteria for Adverse Events (version 5.0). *The relatedness of adverse events to treatment was determined by the investigator. †Relacorilant was always interrupted or discontinued when nab-paclitaxel was interrupted. ‡Ten patients had one dose reduction and three patients had two dose reductions. §Adverse events were coded using the MedDRA dictionary (version 27.0) and sorted by descending incidence using the relacorilant plus nab-paclitaxel group. ¶Combined term including neutropenia, decreased neutrophil count, and febrile neutropenia. ||Combined term including anaemia, decreased haemoglobin, and decreased red blood cell count. **Combined term including fatigue and asthenia.

***Table 2*: Adverse events that occurred during the treatment period in the safety population**

	Relacorilant plus nab-paclitaxel (n=188)		Nab-paclitaxel monotherapy (n=190)		EAIR difference (95% CI)*
	EAIR (95% CI)†	Total PYE‡	EAIR (95% CI)†	Total PYE‡	
All treatment-emergent adverse events	4063·1 (3503·1 to 4687·3)	4·6	3850·1 (3320·7 to 4439·9)	4·9	213·0 (–585·5 to 1011·5)
Neutropenia§	284·3 (235·7 to 340·0)	42·2	230·5 (186·1 to 282·4)	40·3	53·8 (–15·5 to 123·1)
Anaemia¶	248·5 (205·2 to 298·3)	46·3	243·4 (199·1 to 294·6)	43·1	5·11 (–60·0 to 70·2)
Ascites	10·5 (5·0 to 19·3)	95·6	25·6 (15·7 to 39·6)	78·1	–15·2 (–27·6 to –2·7)
All serious adverse events	82·8 (64·1 to 105·4)	79·7	62·5 (45·6 to 83·6)	72·0	20·3 (–7·0 to 47·6)
Febrile neutropenia	4·1 (1·1 to 10·5)	97·2	1·2 (0·0 to 6·9)	80·9	2·9 (–2·1 to 7·8)
System organ class of infection and infestation (including sepsis)	16·8 (9·6 to 27·2)	95·4	11·5 (5·3 to 21·9)	78·0	5·2 (–6·1 to 16·6)

EAIR=exposure-adjusted incidence rates. PYE=patient-years exposure. *EAIR difference: ([relacorilant plus nab-paclitaxel]– nab-paclitaxel monotherapy). The exact CI for the EAIR difference between the two treatment groups is based on two independent Poisson distributions. †EAIR is defined as event incidence rate per 100 PYE: (total number of patients with an event / total PYE) × 100. The exact 95% CI is based on a Poisson distribution for EAIR. ‡The total PYE to a treatment is the sum of individual patient's PYE within the treatment exposure period. §Combined term including neutropenia, decreased neutrophil count, and febrile neutropenia. ¶Combined term including anaemia, decreased haemoglobin, and decreased red blood cell count.

***Table 3*: EAIR of selected adverse events in the safety population**

Research in context

Evidence before this study

In a search of PubMed for articles published up to April 15, 2025, using the search terms "selective" AND "glucocorticoid receptor" AND ("cancer" or "carcinoma") with no language restrictions, we found that data have been published on selective glucocorticoid receptor antagonism in ovarian cancer for only three clinical trials, two with the selective glucocorticoid receptor antagonist relacorilant and one with the less selective ORIC-101. The first trial (NCT03928314) was a phase 1 dose escalation and expansion study to determine the recommended phase 2 dose of ORIC-101 in combination with nab-paclitaxel in patients with advanced solid cancers. The second trial (NCT02762981) was a phase 1/2 study to determine the recommended phase 2 dose of relacorilant plus nab-paclitaxel in patients with advanced solid cancers. The third trial (NCT03776812) was a randomised, phase 2 study evaluating the combination of relacorilant plus nab-paclitaxel in patients with platinum-resistant ovarian cancer.

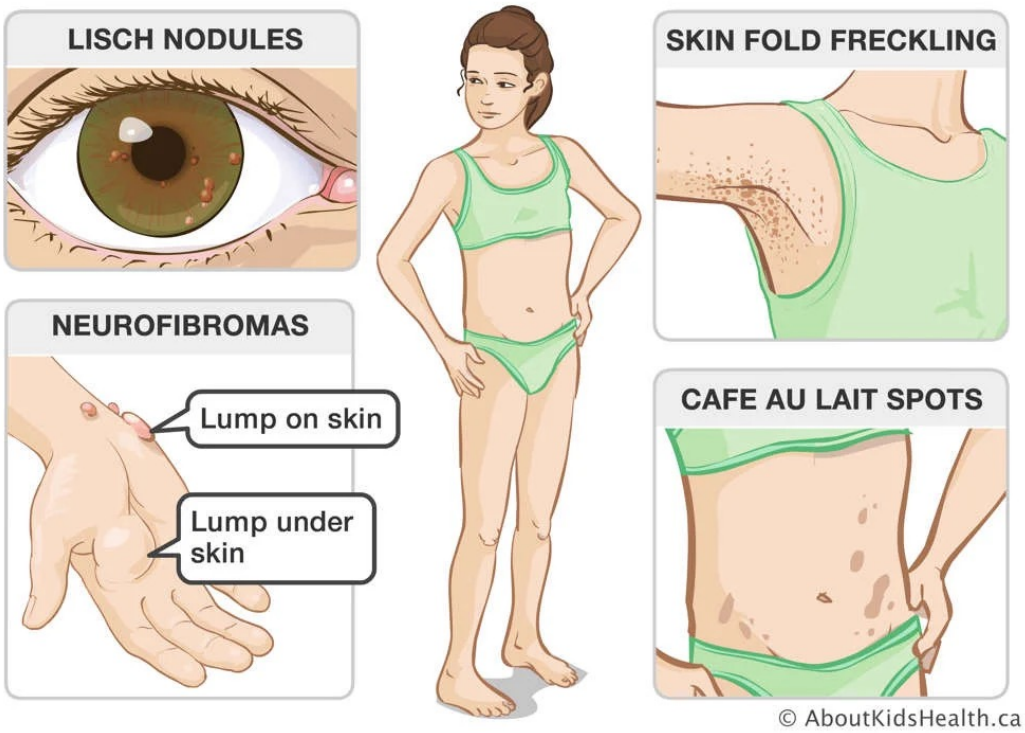
Added value of this study

The positive progression-free survival results with supportive interim overall survival data from ROSELLA (GOG-3073, ENGOT-ov72) confirm the findings from previous phase 1 and 2 studies of relacorilant in patients with solid tumours. A study of ORIC-101 concluded that it did not show meaningful clinical benefit in patients who previously progressed on taxanes when combined with nab-paclitaxel. These differences between ORIC-101 and relacorilant suggest that the properties of relacorilant and its selective glucocorticoid receptor antagonism could be a crucial pharmacological attribute that underpins its clinical efficacy.

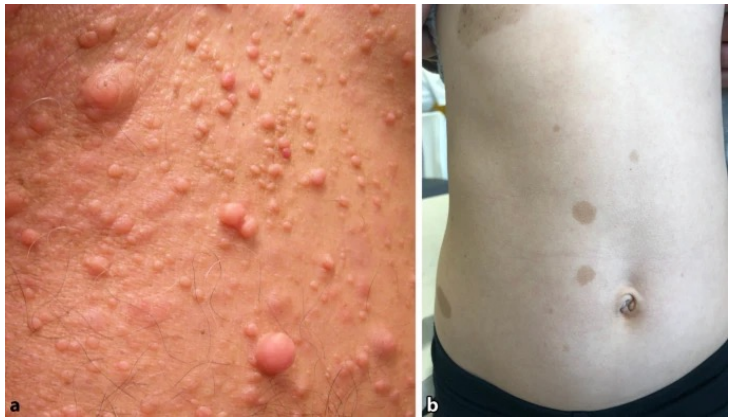
Implications of all the available evidence

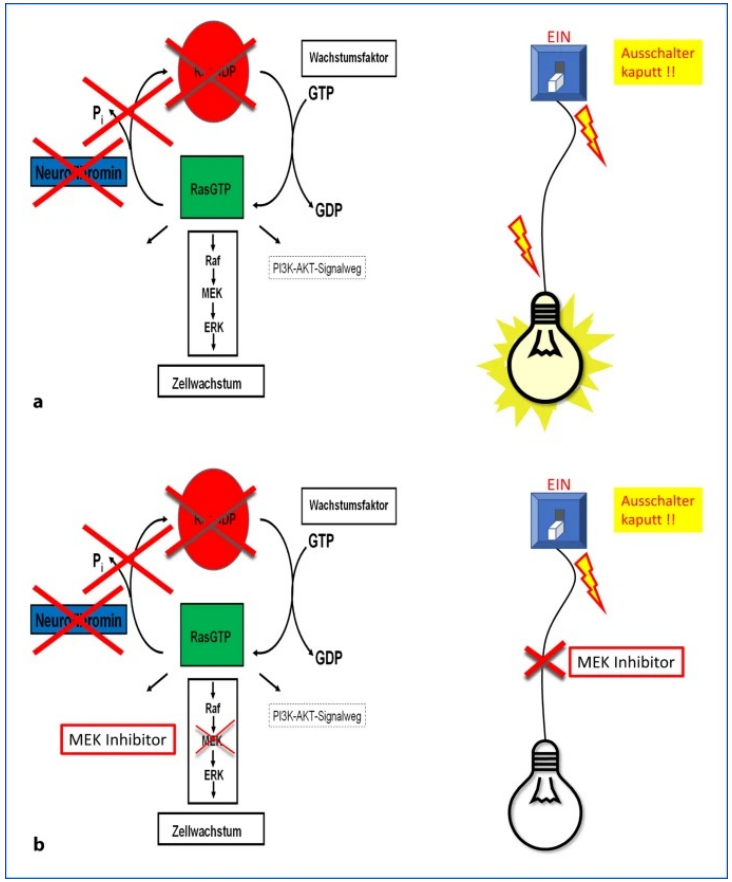
Combined with the evidence from previous studies, our study supports relacorilant plus nab-paclitaxel as a potential new standard of care for patients with platinum-resistant ovarian cancer, without the need for biomarker selection. This study is the first positive clinical trial conducted with registrational intent for a selective glucocorticoid receptor antagonist in patients with cancer. The data are expected to prompt the evaluation of relacorilant in other solid cancer indications and in combination with other classes of anti-cancer agents. The targeted agent bevacizumab also extends progression-free survival in combination with a weekly taxane in this setting. As relacorilant has an orthogonal mechanism of action to bevacizumab, our findings support further research to evaluate the triplet combination of relacorilant, nab-paclitaxel, and bevacizumab in patients with platinum-resistant ovarian cancer. Translational and mechanistic research might inform further rational clinical development and research on future generations of selective glucocorticoid receptor antagonists. The findings from ROSELLA might also prompt prospective clinical studies to evaluate the impact of glucocorticoid use on the efficacy of chemotherapy in ovarian cancer. Additional follow-up time will improve precision in the estimated overall survival benefit and further clarify the clinical benefit of the relacorilant combination tested herein.

Die Neurofibromatose Typ 1 ist die häufigste Form der Neurofibromatose (90 % der Fälle). Der krankheitsverursachende Gendefekt betrifft bei der Neurofibromatose Typ 1 das NF1-Gen auf dem langen Arm von Chromosom 17 (Genlokus 17q11.2). Das Gen kodiert für das Protein Neurofibromin, das im gesunden Zustand als negativer Regulator von Ras fungiert. Meist handelt es sich um Punktmutationen. Durch die mutationsbedingte Funktionsstörung kommt es zur andauernden Aktivierung des Ras. Dies wirkt förderlich auf die Entstehung von Neoplasien und wird als Ursache der Neurofibromatose Typ 1 angesehen.
Die Neumutationsrate für das NF1-Gen ist hoch. Etwa die Hälfte der neu auftretenden Fälle sind auf eine Neumutation zurückzuführen. Die andere Hälfte wird autosomal-dominant vererbt und weist dabei eine vollständige Penetranz auf.

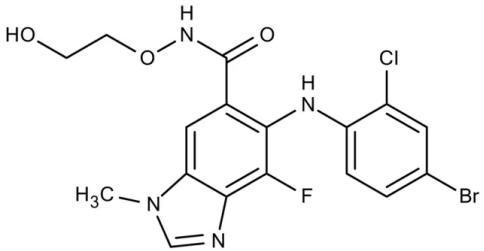


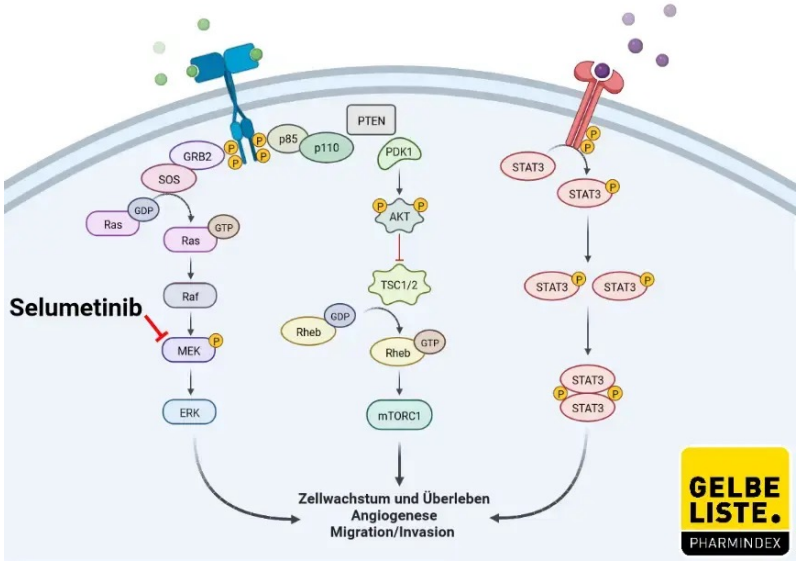
Plexiforme Neurofibrome können bösartig werden und scheinen bei Personen mit NF1 die häufigsten Vorläufer für maligne periphere Nervenhüllentumoren zu sein. Schwannome sind aus Schwann-Zellen abgeleitet, unterziehen sich selten einer malignen Transformation und können überall im Körper in peripheren Nerven auftreten.





Selumetinib ist ein MEK-Inhibitor aus der Klasse der Serin/Threonin-Kinase-Hemmer.
Der Arzneistoff wurde für die Therapie der Neurofibromatose Typ 1 (NF1) entwickelt.
Selumetinib hemmt die MAP-Kinasen MEK1 und MEK2, die ein wichtiger Teil des Ras/Raf/MAPK-Signalwegs sind. Eine Mutation des Protoonkogens BRAF kann zu einer Entgleisung dieses Signalwegs und so zu einer überaktiven nachgeschalteten Signalübertragung durch MAP-Kinasen führen. Sie phosphorylieren die Proteinkinase ERK, wodurch verschiedene Transkriptionsfaktoren aktiviert werden, was die Proliferation von Tumorzellen angeregt.
Durch die selektive Bindung des Wirkstoffs an MEK1 und MEK2 wird diese Kaskade unterbrochen und das unkontrollierte Zellwachstum gehemmt.





Efficacy and safety of selumetinib in adults with neurofibromatosis type 1 and symptomatic, inoperable plexiform neurofibromas (KOMET): a multicentre, international, randomised, placebo-controlled, parallel, double-blind, phase 3 study

Summary

Background Currently, no worldwide approved therapies exist for adults with neurofibromatosis type 1 (NF1) and symptomatic, inoperable plexiform neurofibromas. The KOMET study aimed to evaluate selumetinib (ARRY-142886, AZD6244) efficacy and safety in this population.

Methods This ongoing multicentre, international, randomised, placebo-controlled, phase 3, parallel, double-blind trial randomly assigned adults with NF1-plexiform neurofibroma 1:1 to 28-day cycles of oral selumetinib 25 mg/m^2 twice daily, or placebo with crossover to selumetinib at confirmed radiological progression or the end of cycle 12. The primary endpoint was objective response rate (confirmed partial or complete response) established by use of independent central review per Response Evaluation in Neurofibromatosis and Schwannomatosis (REiNS) criteria by cycle 16 (selumetinib *vs* placebo). This study (KOMET) is registered with ClinicalTrials.gov, NCT04924608 and is ongoing.

Findings Overall, of 184 participants enrolled, 145 adults were randomly assigned to selumetinib (n=71) or placebo (n=74). Selumetinib led to a rapid response (median 3·7 months), with an objective response rate of 20% (n=14/71; 95% CI 11·2 to 30·9) by cycle 16 versus 5% (n=4/74; 1·5 to 13·3) with placebo (p=0·011). Participants with baseline chronic pain intensity scores of at least 3 had a greater reduction in score at cycle 12 with selumetinib versus placebo (least-squares mean [SE] –2·0 [0·30] –2·6 to –1·4, *vs* –1·3 [0·29] –1·8 to –0·7; p=0·070), although this did not reach significance; and a clinically meaningful improvement from baseline. Change from baseline to cycle 12 in PlexiQoL total scores between treatment groups was not significant (least-squares mean difference [SE] –0·1 [0·59]; –1·2 to 1·1). Adverse events were consistent with the known selumetinib safety profile.

Interpretation In the first international, randomised, placebo-controlled trial in adults with NF1-plexiform neurofibromas, selumetinib achieved a significant objective response rate versus placebo. No new safety concerns were identified. The observations of reduction in tumour volume by cycle 16, reduction in chronic and spike pain, reduction in analgesia, and decrease in pain interference over placebo show that selumetinib is effective at treating plexiform neurofibromas in adults with NF1.

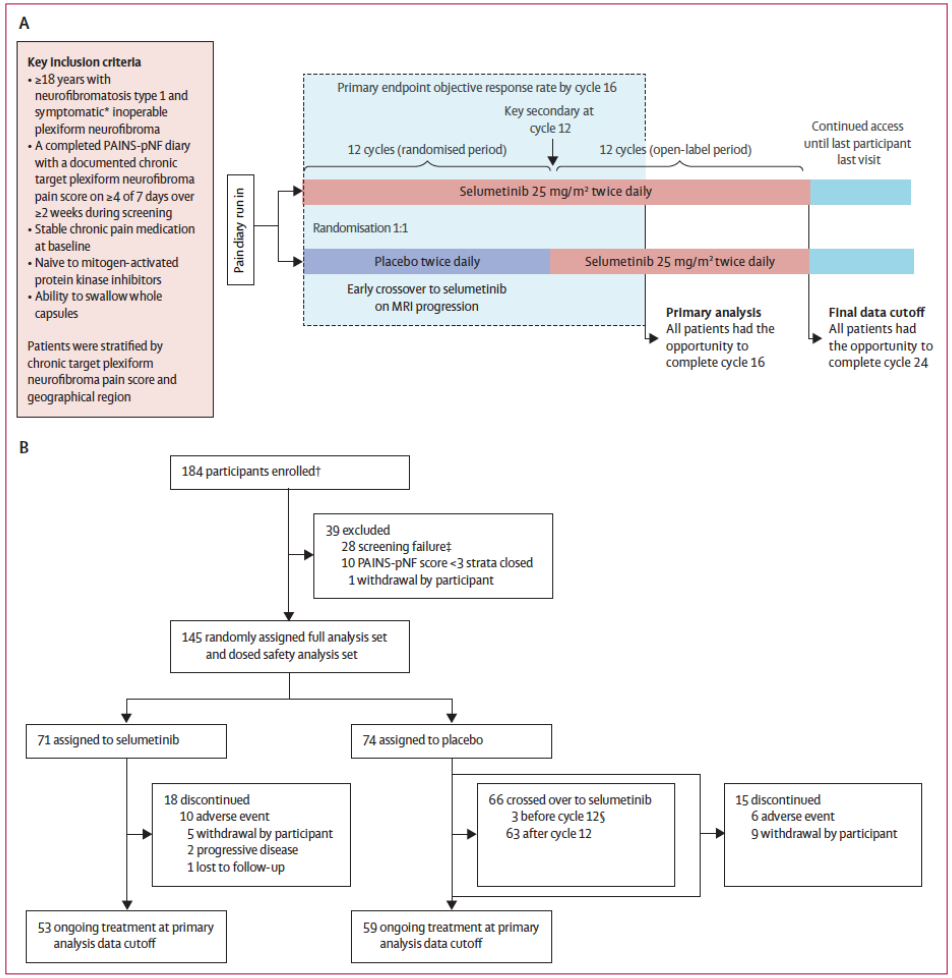


Figure 1: **Study design (A) and study disposition (B)**
(A) The first participant was enrolled in KOMET on Nov 19, 2021. The protocol included an interim analysis data cutoff for the KOMET study when the 100th randomly assigned patient had the opportunity to complete cycle 16. The primary analysis for the KOMET study was done when the last participant had the opportunity to complete their cycle 16 assessment (Aug 5, 2024). (B) The data cutoff was Aug 5, 2024. NF1=neurofibromatosis type 1. PAINS-pNF=Pain Intensity Scale for Plexiform Neurofibromas. *Symptoms could include, but were not limited to, pain, motor morbidity, and disfigurement. †Participants who signed the informed consent form. ‡Non-fulfilment of inclusion or exclusion criteria. §Two due to disease progression and one due to important protocol deviation.

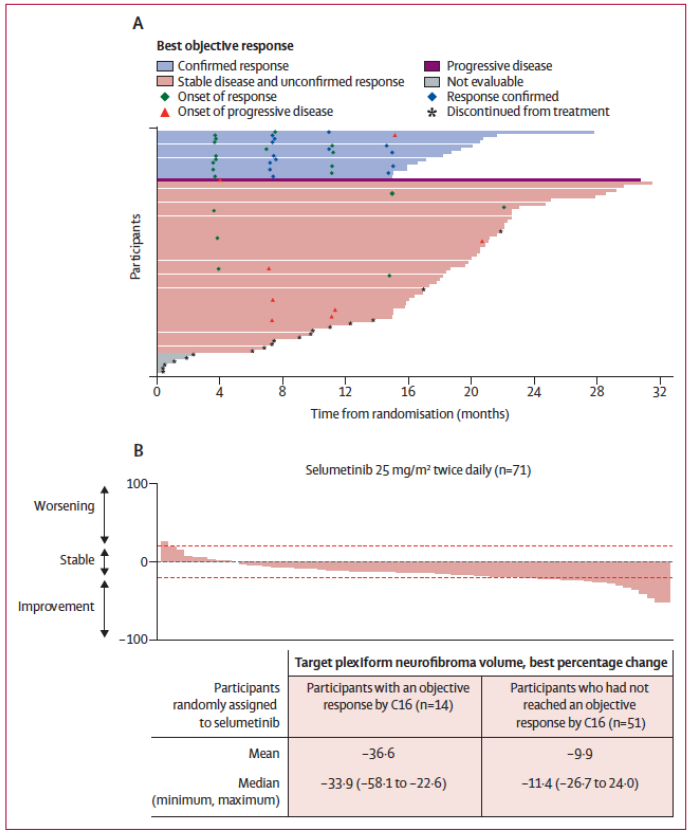
	Selumetinib n=71	Placebo n=74
Age at screening, years		
n	71	74
Mean (SD)	32·6 (11·4)	29·8 (8·7)
Median (IQR)	31·0 (24·0–40·0)	28·0 (24·0–36·0)
Minimum, maximum	18, 60	18, 53
Sex		
Male	33 (46%)	42 (57%)
Female	38 (54%)	32 (43%)
Race		
Asian	22 (31%)	23 (31%)
Black or African American	6 (8%)	3 (4%)
White	38 (54%)	43 (58%)
Other	2 (3%)	3 (4%)
Not reported	3 (4%)	2 (3%)
Region*		
China	11 (15%)	13 (18%)
Japan	7 (10%)	8 (11%)
Europe	31 (44%)	30 (41%)
Rest of the world	22 (31%)	23 (31%)
Time from diagnosis of NF1, years		
n	70†	74
Mean (SD)	23·1 (13·5)	18·6 (12·7)
Median (IQR)	23·0 (14·8–32·1)	18·7 (7·9–27·3)
Minimum, maximum	0·06, 60·9	0·04, 47·0
Time from diagnosis of inoperable plexiform neurofibroma, years		
n	70†	74
Mean (SD)	8·69 (11·4)	8·10 (11·3)
Median (IQR)	2·5 (0·3–15·1)	2·3 (0·2–14·4)
Minimum, maximum	0·04, 45·9	0·03, 38·9
Target plexiform neurofibroma overall location		
Neck-trunk	8 (11%)	11 (15%)
Trunk-extremity	16 (23%)	11 (15%)
Head and neck	7 (10%)	5 (7%)
Head	5 (7%)	7 (10%)
Extremity	13 (18%)	18 (24%)
Body	1 (1%)	2 (3%)
Trunk	21 (30%)	19 (26%)
Other	0	1 (1%)
Target plexiform neurofibroma volume, mL		
Mean (SD)	480·91 (1231·0)	539·53 (927·2)
Median (IQR)	91·95 (25·0–355·2)	221·85 (49·7–529·6)
Minimum, maximum	0‡, 6264·3	9·1, 5621·9
Target plexiform neurofibroma symptoms§		
Any symptoms	71 (100%)	74 (100%)
Pain	62 (87%)	61 (82%)
Motor weakness	14 (20%)	19 (26%)
Decreased range of motion	19 (27%)	19 (26%)
Sensory deficit	8 (11%)	13 (18%)
Plexiform neurofibroma-related disfigurement	23 (32%)	17 (23%)
Other symptoms¶	12 (17%)	19 (26%)

(Table 1 continues on next column)

	Selumetinib n=71	Placebo n=74
(Continued from previous column)		
Baseline PAINS-pNF intensity score		
<3	21 (30%)	21 (28%)
≥3	50 (70%)	53 (72%)
Any non-target plexiform neurofibroma		
No	53 (75%)	44 (59%)
Yes	18 (25%)	30 (41%)
Non-target plexiform neurofibroma overall location		
Neck-trunk	4 (6%)	4 (5%)
Trunk-extremity	2 (3%)	9 (12%)
Head and neck	5 (7%)	2 (3%)
Head	1 (1%)	1 (1%)
Extremity	0	4 (5%)
Trunk	6 (9%)	8 (11%)
Other	0	2 (3%)

Data are n (%) unless stated otherwise. The data cutoff was Aug 5, 2024. Percentages have been rounded up from one decimal place and, therefore, might add up to more than 100%. eCRF=electronic case report form. NF1=neurofibromatosis type 1. PAINS-pNF=Pain Intensity Scale for Plexiform Neurofibromas. *Europe includes France (selumetinib group: n=3; placebo group: n=2), Germany (selumetinib group: n=2; placebo group: n=8), Italy (selumetinib group: n=7; placebo group: n=8), Poland (selumetinib group: n=4; placebo group: n=1), Russia (selumetinib group: n=4; placebo group: n=3), Spain (selumetinib group: n=5; placebo group: n=4), and the U K (selumetinib group: n=6; placebo group: n=4). Rest of the world includes Australia (selumetinib group: n=6; placebo group: n=4), Brazil (selumetinib group: n=7; placebo group: n=13), Canada (selumetinib group: n=6; placebo group: n=3), and the USA (selumetinib group: n=3; placebo group: n=3). †Time from diagnosis of NF1 (years): time from diagnosis of NF1 to start of study intervention was greater than 60 years as it was calculated on the basis of date of birth and age at screening, which was recorded on the eCRF and not calculated. The sample size for time from diagnosis of NF1 was 70 rather than 71 for the selumetinib group because data for one rescreened patient who had provided initial screening information on disease diagnosis were not transferred. The date of diagnosis of NF1 was collected in the eCRF, and the time to diagnosis of NF1 was defined as the difference between the first dose date and the date of diagnosis of NF1. Time from diagnosis of inoperable plexiform neurofibroma (years): Participants could have had more than one NF1 diagnostic criteria. ‡The minimum value of 0 for selumetinib is an error in data from one participant. §A participant could have had multiple symptoms and overall morbidity types. ¶Other symptom categories with less than 10% are not shown in the table.

Table 1: **Baseline demographics and disease characteristics**



	Target plexiform neurofibroma volume, best percentage change	
Participants randomly assigned to selumetinib	Participants with an objective response by C16 (n=14)	Participants who had not reached an objective response by C16 (n=51)
Mean	−36·6	−9·9
Median (minimum, maximum)	−33·9 (−58·1 to −22·6)	−11·4 (−26·7 to 24·0)

Figure 2: **Best response* in participants randomly assigned to selumetinib (swimmer plot), full analysis set (A) and target plexiform neurofibroma volume and best percentage change at the primary analysis data cutoff—waterfall plot, full analysis set (B)**

FAS=full analysis set. NF1=neurofibromatosis type 1. REiNS=Response Evaluation in Neurofibromatosis and Schwannomatosis. (A) *Best objective response is the response a participant had following the start of intervention, but before starting any subsequent NF1-PN therapy and up to and including progression or the last evaluable MRI assessment in the absence of progression. The on-treatment MRI volumetric assessment period was from the first dose until discontinuation or data cut-off (whichever occurs first), excluding data during prolonged study intervention interruption (>28 continuous days of no study intervention). According to REiNS criteria, a sustained response is at least 6 months. (B) Data cutoff was Aug 5, 2024. Waterfall pre-planned visualisation. Table data are from post-hoc analyses. SD of the mean was 11·3 for responders and 10·5 for non-responders. For responders, quartile 1 was−46·5 and quartile 3 was −28·1. For non-responders, quartile 1 was −17·3 and quartile 3 was −11·4. C16=cycle 16, etc.

	Selumetinib		Placebo		Selumetinib *vs* placebo	
	n	Least-squares mean	n	Least-squares mean	Least-squares mean difference	p value
Pain full analysis set*	42	−2·0 (0·30; −2·6 to −1·4)	42	−1·3 (0·29; −1·8 to −0·7)	−0·8 (0·41; −1·6 to −0·1)	0·07
Baseline PAINS-pNF level						
≥2	45	−2·0 (0·28; −2·6 to −1·5)	44	−1·2 (0·28; −1·7 to −0·6)	−0·9 (0·39; −1·6 to −0·1)	0·03 (nominal)
≥1	50	−1·9 (0·26; −2·4 to −1·3)	49	−1·0 (0·26; −1·5 to −0·5)	−0·8 (0·36; −1·5 to −0·1)	0·02 (nominal)
Full analysis set	57	−1·6 (0·22; −2·0 to −1·1)	62	−0·9 (0·21; −1·3 to −0·5)	−0·7 (0·30; −1·3 to −0·1)	0·02 (nominal)

Data are mean (SE; 95% CI). Statistical analysis model: Mixed Model for Repeated Measures with randomised treatment, cycle, baseline score, geographical region, pain strata, treatment group by cycle number, and baseline PAINS-pNF score by cycle number. Unstructured covariance matrix. Scale meaningful score difference ≤−2 points. PAINS-pNF=Pain Intensity Scale for Plexiform Neurofibromas. *Pain FAS (baseline PAINS-pNF ≥3), first key secondary endpoint, confirmatory analysis; baseline PAINS-pNF ≥1, ≥2, post-hoc analyses; Full analysis set (all participants regardless of baseline PAINS-pNF score), preplanned supplementary exploratory analysis.

Table 2: **Change from baseline in PAINS-pNF chronic target plexiform neurofibroma pain intensity score at cycle 12, according to population analysed**

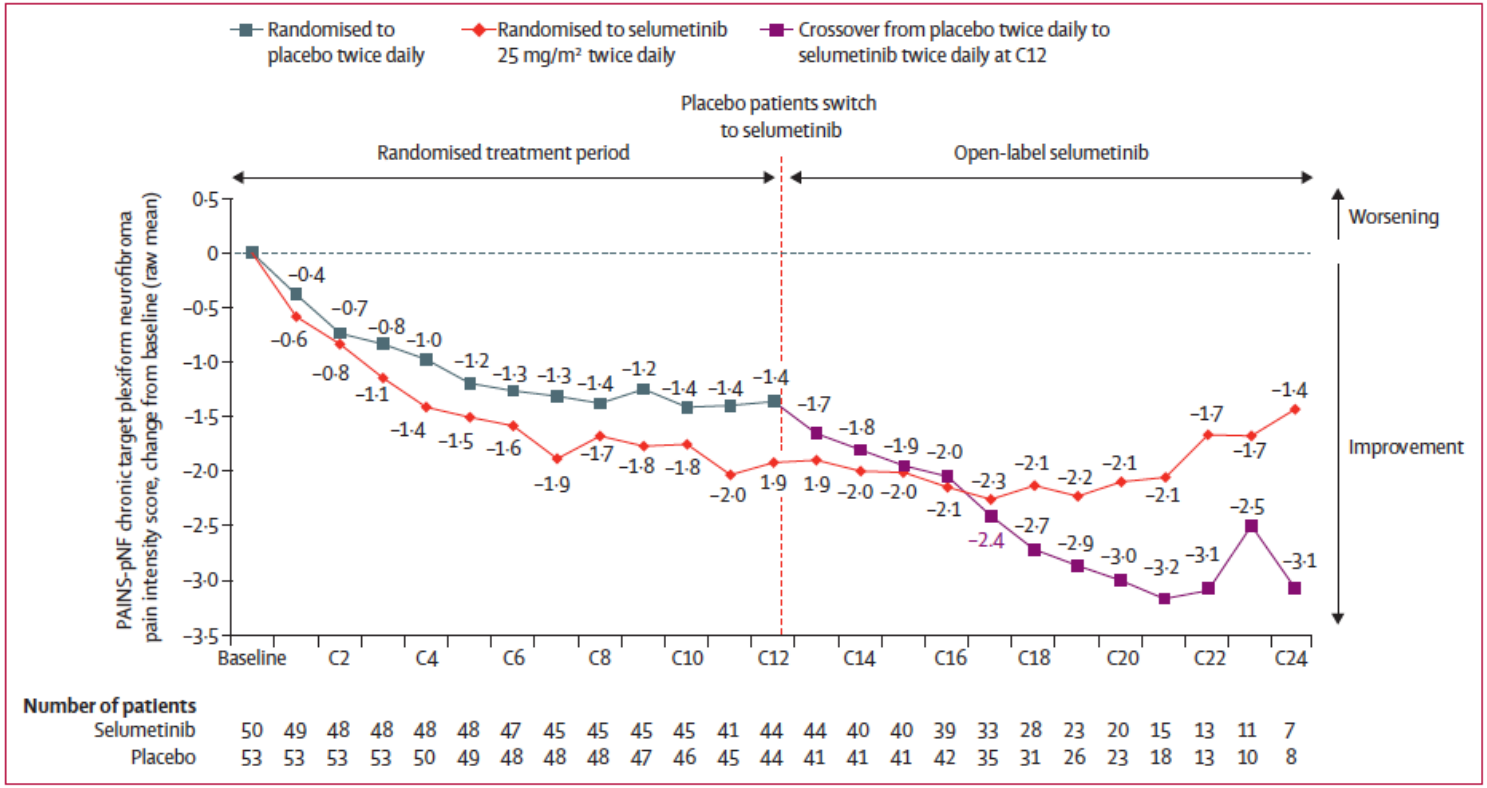


Figure 3: **Change from baseline in PAINS-pNF chronic target plexiform neurofibroma pain intensity score over time, pain full analysis set***

Supplementary analysis. Descriptive analysis. Three placebo participants crossed over to selumetinib before cycle 12. PAINS-pNF=Pain Intensity Scale for Plexiform Neurofibromas. *Pain full analysis set—participants randomly assigned to study intervention with a baseline pain intensity score of at least 3.

	Selumetinib n=71	Placebo n=74
Any adverse events	71 (100%)	68 (92%)
Adverse event, possibly related*	68 (96%)	42 (57%)
Adverse event, CTCAE grade 3 or higher	23 (32%)	13 (18%)
CTCAE grade 3 or higher, possibly related*	14 (20%)	1 (1%)
Outcome of death	0	0
Serious adverse event (including events with outcome of death)	10 (14%)	9 (12%)
Serious adverse event (including events with outcome of death), possibly related*	4 (6%)	1 (1%)
Serious adverse event leading to discontinuation	4 (6%)	4 (5%)
Serious adverse event leading to discontinuation, possibly related*	2 (3%)	0
Adverse event leading to discontinuation	9 (13%)	5 (7%)
Adverse event leading to discontinuation, possibly related*	6 (8%)	1 (1%)
Adverse event leading to dose modification†	27 (38%)	10 (14%)
Adverse event leading to dose interruption	19 (27%)	8 (11%)
Adverse event leading to dose reduction	10 (14%)	3 (4%)
Any AESIs‡	47 (66%)	16 (22%)
Any other significant adverse events§	0	0
Maximum reported CTCAE grade		
1	16 (23%)	22 (30%)
2	32 (45%)	33 (45%)
3	19 (27%)	11 (15%)
4	4 (6%)	2 (3%)
System organ class with a higher percentage of participants with adverse events in the selumetinib group		
Infections and infestations	38 (54%)	33 (45%)
Psychiatric disorders	7 (10%)	2 (3%)
Nervous system disorders	20 (28%)	20 (27%)
Eye disorders	12 (17%)	9 (12%)
Ear and labyrinth disorders	6 (8%)	4 (5%)
Respiratory, thoracic, and mediastinal disorders	12 (17%)	12 (16%)
Gastrointestinal disorders	53 (75%)	32 (43%)
Hepatobiliary disorders	3 (4%)	2 (3%)
Skin and subcutaneous tissue disorders	64 (90%)	26 (35%)
Musculoskeletal and connective tissue disorders	19 (27%)	17 (23%)
Renal and urinary disorders	6 (8%)	5 (7%)
Reproductive system and breast disorders	5 (7%)	3 (4%)
Congenital, familial, and genetic disorders	1 (1%)	0
General disorders and administration-site conditions	36 (51%)	21 (28%)
Investigations	44 (62%)	21 (28%)
Injury, poisoning, and procedural complications	11 (15%)	9 (12%)

(Table 3 continues in next column)

(Continued from previous column)

	Selumetinib n=71	Placebo n=74
Adverse events had by ≥10% of participants in either treatment group by preferred term		
Dermatitis acneiform	42 (59%)	8 (11%)
Diarrhoea	30 (42%)	9 (12%)
Blood creatine phosphokinase increased	32 (45%)	4 (5%)
Nausea	18 (25%)	12 (16%)
Vomiting	18 (25%)	6 (8%)
Fatigue	14 (20%)	10 (14%)
Alopecia	13 (18%)	8 (11%)
Dry skin	13 (18%)	4 (5%)
Aspartate aminotransferase increased	13 (18%)	4 (5%)
COVID-19	11 (15%)	15 (20%)
Oedema peripheral	11 (15%)	1 (1%)
Alanine aminotransferase increased	11 (15%)	5 (7%)
Rash	11 (15%)	3 (4%)
Paronychia	9 (13%)	3 (4%)
Headache	8 (11%)	9 (12%)
Stomatitis	7 (10%)	3 (4%)
Constipation	7 (10%)	1 (1%)
Pruritus	7 (10%)	5 (7%)
Anaemia	5 (7%)	8 (11%)
Pain in extremity	5 (7%)	8 (11%)
Arthralgia	3 (4%)	8 (11%)
Decreased appetite	1 (1%)	8 (11%)

Data are n (%). Randomised period: first dose date until earliest of last dose of cycle 12, crossover, 30 days after discontinuation, day before the start of subsequent therapy, or data cutoff. Percentages have been rounded up from one decimal place and, therefore, might add up to more than 100%. AESI=adverse event of special interest. CTCAE=Common Terminology Criteria for Adverse Events (version 5.0). *As assessed by the investigator. †Action taken either a drug interruption or a dose reduction, or both. ‡Per protocol, AESIs included ocular toxicity, hepatotoxicity, muscular toxicity, and cardiac toxicity events (see appendix p 13, 25). §Significant adverse events, other than serious adverse events and those adverse events leading to discontinuation of study intervention, which are of particular clinical importance are identified and classified as other significant adverse events.

Table 3: **Number of participants with adverse events in the randomised period, safety analysis set**

Research in context

Evidence before this study

We searched PubMed for published articles using the terms "neurofibromatosis type 1" or "NF1" and "plexiform neurofibroma" or "PN", or "NF1-PN", and "adults". Neurofibromatosis type 1 (NF1) is a rare, heterogenous, genetic condition. NF1 has an estimated prevalence of approximately one in 2500 to one in 6000 people. Up to 50% of individuals with NF1 develop plexiform neurofibromas, which can impair quality of life. In addition to plexiform neurofibromas, more than 50% of individuals with NF1 report having substantial pain and discomfort. Selumetinib is a potent, selective, allosteric inhibitor of mitogen-activated protein kinase kinases 1 and 2 that was first approved by the US Food and Drug Administration in April 2020 for children (aged ≥2–17 years) with NF1 and symptomatic, inoperable plexiform neurofibromas, and has since been approved for this patient population by the European Medicines Agency (aged ≥3–17 years old) and the regulatory bodies in multiple other countries (aged ≥2 or 3 years, region dependent), at a dosage of 25 mg/m² twice daily. These approvals were based on the pivotal SPRINT study, in which selumetinib showed an overall response rate of 68% and provided a clinically meaningful reduction in tumour pain intensity. In February, 2025, mirdametinib was approved in the USA for adults and children aged at least 2 years with NF1 and symptomatic plexiform neurofibromas not amenable to complete resection on the basis of the results of a single arm, phase 2b study. However, as of May, 2025, there are no worldwide approvals of medical treatments for adults with NF1 and symptomatic, inoperable plexiform neurofibromas. Further clinical trials of medical treatments in adults are needed given the high burden of disease in this population.

Added value of this study

KOMET is the first and, as of May 2025, the only international, randomised, placebo-controlled trial of an inhibitor of mitogen-activated protein kinase kinases 1 and 2 in adults with NF1 who also have symptomatic, inoperable plexiform neurofibromas. KOMET is an ongoing trial that will assess the effects of selumetinib over a period of at least 24 months of treatment.

Implications of all the available evidence

Data from the primary analysis of KOMET indicate that selumetinib treatment achieved a significant objective response rate versus placebo by cycle 16, a clinically meaningful reduction in chronic target plexiform neurofibroma pain intensity score at cycle 12 compared with baseline in adults with a baseline chronic target plexiform neurofibroma pain intensity score of at least 3, and a decrease in chronic pain medication versus placebo at cycle 12. Selumetinib 25 mg/m² taken orally twice daily had a manageable safety and tolerability profile in adults with NF1-PN; no new safety concerns were identified. The observations of reduction in tumour volume by cycle 16, reduction in chronic and spike pain, reduction in analgesia, and improvement in pain-interfering activities at primary analysis show that selumetinib is effective at treating plexiform neurofibromas in adults with NF1.

The President's Malaria Initiative (PMI) is a U.S. Government initiative to control and eliminate malaria, one of the leading global causes of premature death and disability. The initiative was originally launched by U.S. president George W. Bush in 2005, and has been continued by each successive U.S. president.

PMI was originally created with a mission to "reduce malaria-related mortality by 50 percent across 15 high-burden countries in sub-Saharan Africa". PMI has since expanded to 24 malaria-endemic countries in sub-Saharan Africa and 3 additional countries in the Greater Mekong Subregion of Southeast Asia, where it seeks to further reduce malaria burden and assist countries in achieving malaria elimination. PMI works closely with national malaria programs and global partners including the World Health Organization, Roll Back Malaria, and Global Fund. Global malaria efforts, including those of PMI, have cut malaria mortality by over 60%, saved nearly 7 million lives, and prevented more than 1 billion malaria cases between 2000 and 2015. PMI currently supports malaria prevention and control for over 500 million at-risk people in Africa.



USAID
FROM THE AMERICAN PEOPLE

In order to be consistent with the President's Executive Orders, this website is currently undergoing maintenance as we expeditiously and thoroughly review all of the content.

Estimating the potential malaria morbidity and mortality avertable by the US President's Malaria Initiative in 2025: a geospatial modelling analysis

Summary

Background Since its inception in 2005, the US President's Malaria Initiative (PMI) has played a major role in the reductions in malaria morbidity and mortality observed across Africa. With the status of PMI funding and operations currently uncertain, we aimed to quantify the impact that a fully functioning PMI would have on malaria cases and deaths in Africa during 2025.

Methods We combined detailed spatiotemporal information on planned 2025 PMI and non-PMI malaria commodity procurement and distribution in Africa (focusing on insecticide-treated bednets, artemisinin-based combination therapies, seasonal malaria chemoprevention, and indoor residual spraying of insecticides) with spatiotemporal Bayesian models of intervention coverage and *Plasmodium falciparum* transmission and burden in Africa. By comparing coverage scenarios with and without planned PMI contributions (ie, business-as-usual and no-PMI scenarios), we estimated the number of malaria cases and deaths that PMI investment would avert in 2025. For all interventions, the no-PMI scenario was defined in the absence of any mitigation strategies. Coverage supported by PMI under the business-as-usual scenario was assumed to be lost.

Findings We estimated that business-as-usual PMI contributions to vector control, seasonal malaria chemoprevention, and routine malaria treatment in Africa would avert 13·6 million (95% uncertainty interval [UI] 11·4–16·4 million) malaria cases and 104 000 (69 000–161 000) deaths in 2025. These estimates represent 11·3% (95% UI 9·9–12·9) of the total burden of malaria morbidity and 37·5% (34·2–41·5) of the total burden of malaria mortality in PMI's focus geographies across 27 African countries. These estimates do not account for the additional impact of PMI-supported provision of diagnostics or severe case management commodities, nor preventive treatment for pregnant individuals, which would further lessen these burdens.

Interpretation PMI investment in supporting procurement and distribution of malaria control commodities would directly translate into millions of malaria cases averted and approximately 100 000 lives saved across its focus geographies in Africa throughout 2025.

Funding National Health and Medical Research Council, Australia.

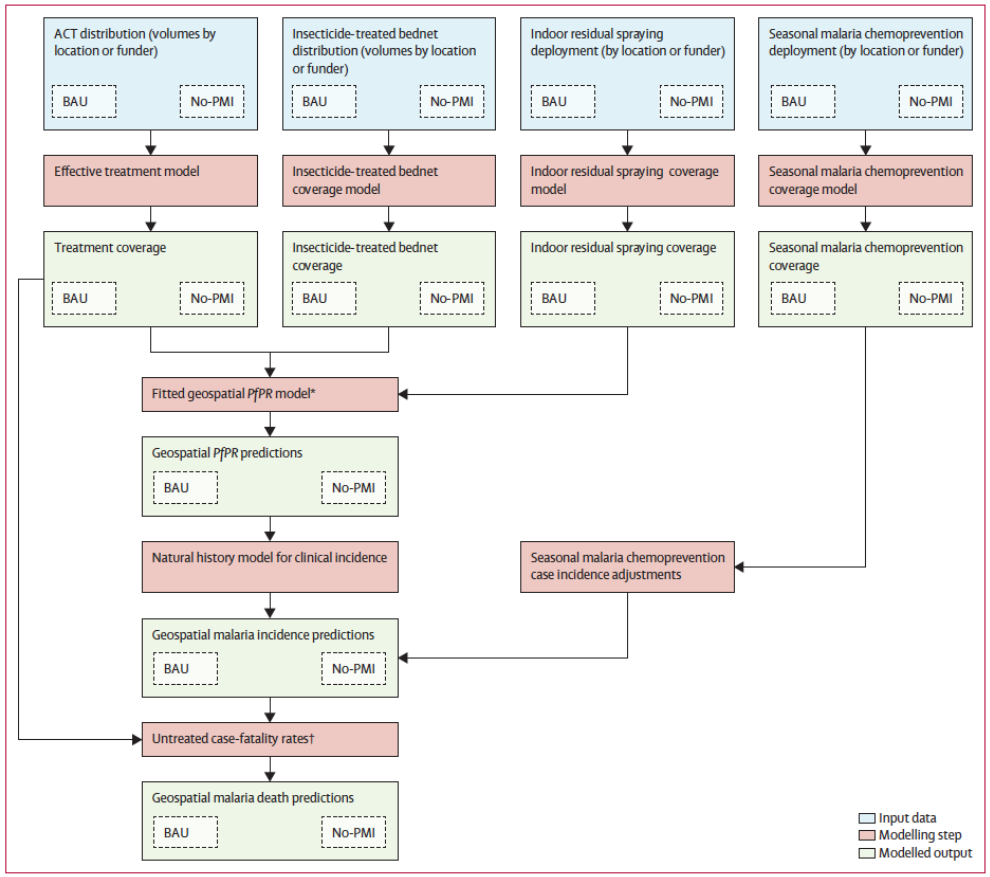


Figure 1: **Schematic summary of the methodological framework**
Blue rectangles represent input datasets, some of which are modelled results from preceding analyses. Red rectangles represent modelling steps. Green rectangles are the results of the analysis. ACT=artemisinin-based combination therapy. BAU=business-as-usual scenario. No-PMI=scenario with PMI-funded interventions removed. *Pf*PR=*Plasmodium falciparum* parasite rate. PMI=US President's Malaria Initiative. *Intervention effect sizes learned from 50 000 co-observed historical *Pf*PR and intervention coverage datapoints. †Consistent with 2024 WHO World Malaria Report estimates.[2]

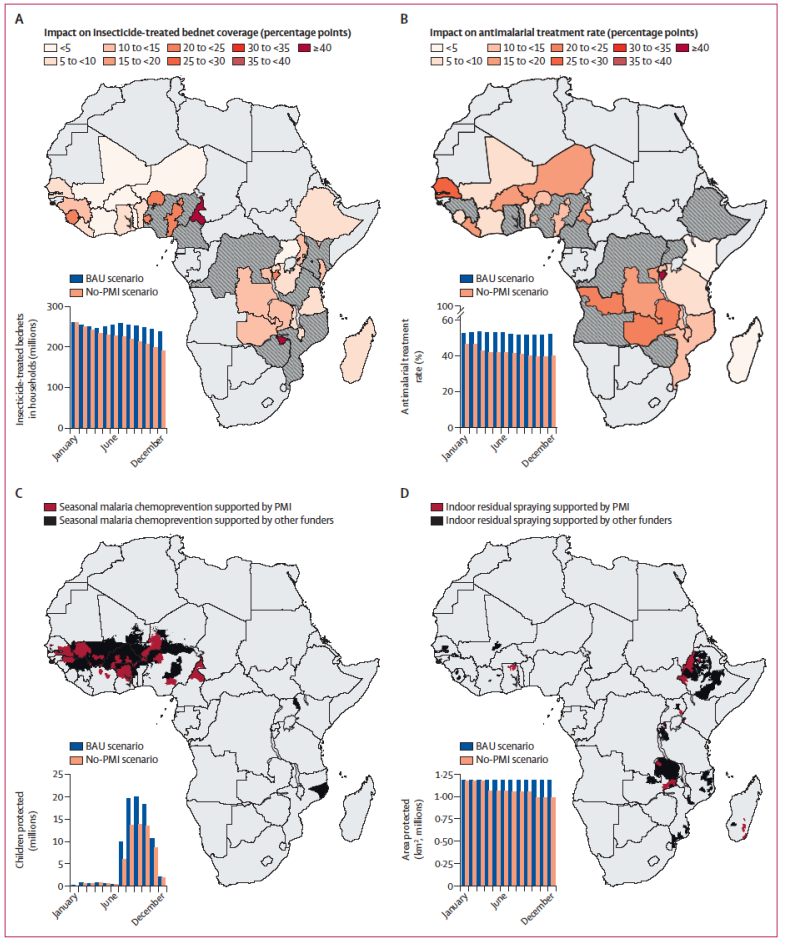


Figure 2: **Projected contributions of PMI to malaria interventions in 2025 under BAU and no-PMI scenarios**
(A) Percentage-point difference in access to insecticide-treated bednets between BAU and no-PMI scenarios, projected in December, 2025. Hashed areas correspond to regions of PMI-focus countries in which PMI does not procure insecticide-treated bednets or support their distribution. The inset shows projected numbers of inseciticide-treated bednets in households for January–December, 2025. (B) Percentage-point difference in the proportion of clinical malaria cases receiving effective treatment between BAU and no-PMI scenarios, projected in December, 2025. Hashed areas correspond to regions of PMI-focus countries in which PMI does not procure artemisinin-based combination therapies. The inset shows projected effective antimalarial treatment rates of clinical malaria cases for January–December, 2025. (C) Projected spatial extent of seasonal malaria chemoprevention in 2025, classified by funding support (PMI *vs* other funders). The inset shows projected numbers of children (younger than 5 years) protected by seasonal malaria chemoprevention for January–December, 2025. (D) Projected spatial extent of indoor residual spraying of insecticides in 2025, classified by funding support (PMI *vs* other funders). The inset shows projected areas (in km²) protected by indoor residual spraying of insecticides for January–December, 2025. BAU=business-as-usual scenario. No-PMI=scenario with PMI-funded interventions removed. PMI=US President's Malaria Initiative.

	Malaria cases averted	Malaria deaths averted
Angola	165 000 (117 000–221 000)	1800 (1000–3200)
Benin	251 000 (217 000–287 000)	1200 (840–1800)
Burkina Faso	888 000 (754 000–1 040 000)	7200 (4800–11 000)
Burundi	1 040 000 (766 000–1 360 000)	11 000 (7100–18 000)
Cote d'Ivoire	459 000 (344 000–599 000)	2600 (1800–3900)
Cameroon (PMI focus region)	1 510 000 (1 350 000–1 650 000)	4400 (3300–5900)
Democratic Republic of the Congo (PMI focus provinces)	1 260 000 (983 000–1 610 000)	11 000 (6200–20 000)
Ethiopia	190 000 (150 000–233 000)	400 (120–930)
Ghana	248 000 (219 000–273 000)	590 (500–700)
Guinea	200 000 (173 000–225 000)	450 (340–600)
Kenya	148 000 (120 000–177 000)	1100 (950–1400)
Liberia	120 000 (88 700–158 000)	1200 (740–1900)
Madagascar	36 000 (26 400–47 900)	220 (69–470)
Mali	515 000 (430 000–618 000)	2800 (2000–3900)
Mozambique	419 000 (276 000–594 000)	4900 (2700–9300)
Malawi	312 000 (221 000–428 000)	2500 (1800–3600)
Niger	770 000 (563 000–1 060 000)	7900 (5200–12 000)
Nigeria (PMI focus states)	2 850 000 (2 490 000–3 280 000)	20 000 (14 000–30 000)
Rwanda	98 100 (71 500–127 000)	690 (510–920)
Senegal	946 000 (676 000–1 250 000)	7700 (2700–17 000)
Sierra Leone	171 000 (140 000–201 000)	1200 (700–1900)
Togo	5350 (4140–6460)	9 (6–13)
Tanzania	582 000 (417 000–767 000)	9300 (7400–12 000)
Uganda	107 000 (91 100–125 000)	140 (100–230)
Zambia	298 000 (218 000–402 000)	3300 (2500–4600)
Zimbabwe	6940 (4820–9310)	20 (6–47)
Africa (PMI focus areas)	13 600 000 (11 400 000–16 400 000)	104 000 (69 000–161 000)

Data are n (95% UI). Africa-wide estimates are rounded to the nearest 100 000 cases or 1000 deaths. The total Africa estimates correspond to the sums across all PMI focus geographies. PMI=US President's Malaria Initiative.

Table: **Estimated mean numbers of malaria cases and deaths averted in Africa in 2025 by PMI investment**

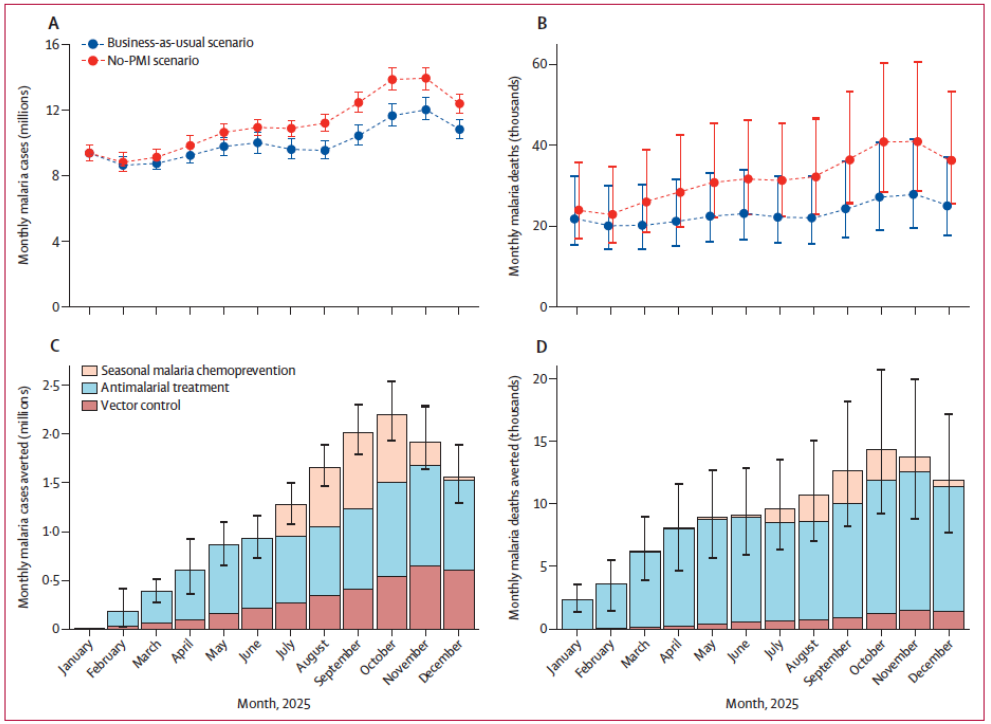


Figure 3: **Estimates of malaria burden averted by PMI investment in Africa in 2025**
Bars indicate 95% UIs. (A) Number of *Plasmodium falciparum* clinical cases (in millions) by month. (B) Number of *P falciparum* deaths by month. Plotted monthly estimates are offset in the no-PMI scenario for presentation and ease of interpretation. (C) Number of *P falciparum* clinical cases (in millions) averted by PMI-funded interventions by month, disaggregated by intervention class. (D) Number of *P falciparum* deaths averted by PMI-funded interventions by month, disaggregated by intervention class. Vector control consists of both coverage with insecticide-treated bednets and indoor residual spraying of insecticides. No-PMI=scenario with PMI-funded interventions removed. PMI=US President's Malaria Initiative. UI=uncertainty interval.

Research in context

Evidence before this study

We searched PubMed on Feb 25, 2025 with the search term "President's Malaria Initiative" AND (impact OR evaluation) AND (burden OR malaria cases OR malaria deaths) and no publication date cutoffs or language restrictions. 102 articles were returned, of which four directly addressed the question of impacts attributable to the US President's Malaria Initiative (PMI) on malaria burden across all PMI focus geographies. One article focused solely on case management and did not provide quantitative results. A study focusing on mortality found a strong association between PMI investment and declines in all-cause infant mortality. Another study used a generalised estimating equation approach to assess PMI's impact, concluding a strong association between PMI spending and reductions in malaria burden, and a 2017 study estimated PMI's historic contribution to reductions in malaria morbidity and mortality (with future projections to 2020) with a mechanistic malaria model.

Added value of this study

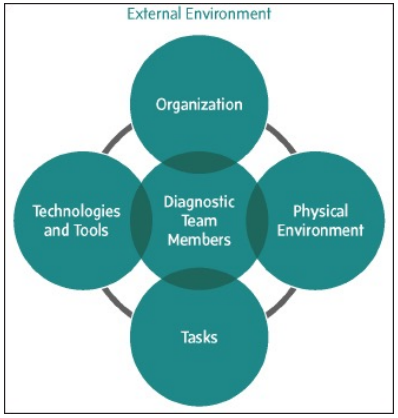
In this study, we synthesised the most up-to-date information of all-funder volumes of key malaria control interventions (ie, insecticide-treated bednets, indoor residual spraying of insecticides, artemisinin-based combination therapy, and seasonal malaria chemoprevention) with PMI data on planned volumes and spatial targeting of funding in 2025 to derive near-real-time projections of malaria control intervention coverage in Africa under two scenarios: a business-as-usual scenario in which PMI commodities are procured and distributed as previously planned versus a no-PMI scenario in which PMI funding and technical assistance is absent. These scenario-based estimates of coverage were propagated through an empirical geospatial malaria model, coupled to mechanistic models of clinical incidence, to estimate the number of malaria infections, clinical cases, and deaths PMI activities could expect to avert in Africa in 2025. With the most up-to-date information on key malaria control intervention volumes combined with geospatial models of malaria transmission and burden, this study yields timely estimates of the life-saving impact of PMI activities, reflecting the context of present-day malaria epidemiology and control efforts from other funders. The use of geospatial methods has allowed estimates at granular geographical levels, providing a valuable resource for stakeholders and decision makers seeking to target constrained resources.

Implications of all the available evidence

Building on previous evidence of PMI's historical impact, our findings quantify the importance of PMI-funded malaria control for the continued suppression of malaria transmission and mortality across its focus areas, and especially in high-burden settings.

What is diagnostics?

- adjective
  - 1. of, relating to, or used in diagnosis.
  - 2. serving to identify or characterize; being a precise indication.
- a device or substance used for the analysis or detection of diseases or other medical conditions.
- A medical professional in the field of **diagnostic medicine** has the assignment to accurately classify symptoms, detect a patient's disease and to find the best available treatment option for the given illness.



What happens after the patient encounter?

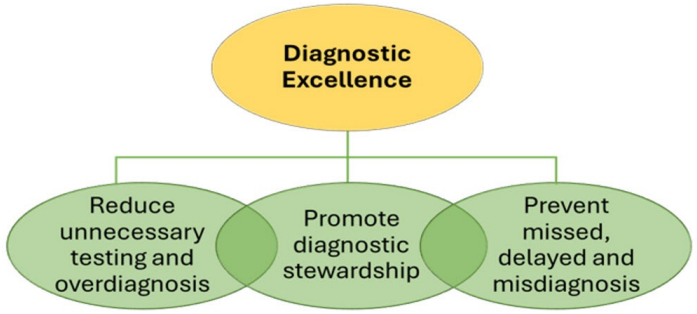
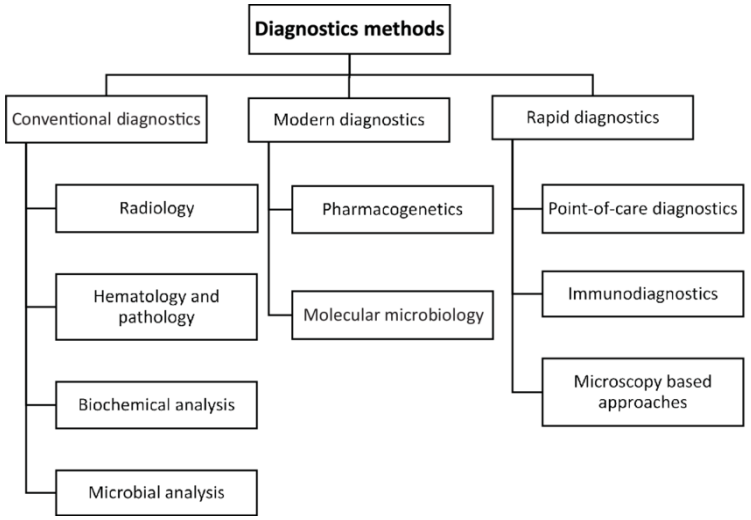


Figure 1: Diagram showing the aspects of diagnosis that are part of diagnostic excellence to be addressed by these Core Elements.

Imaging, laboratory, documentation, decisions



Moving the dial on diagnostics: an update from the *Lancet* Commission on diagnostics

The *Lancet* Commission on diagnostics made recommendations for ten topics: national strategy (including national essential diagnostics lists), access in primary care, workforce, regulatory framework, national financing, affordability, appropriate use of technology, needs in conflict or fragile situations, advocacy, and an international alliance with oversight capabilities. Since 2021, progress in these areas has benefitted greatly from the adoption of a World Health Assembly resolution on diagnostics and the work of a broad coalition, as assessed by literature surveys by subject matter experts, quantitative findings (where feasible), and an anonymous survey of knowledgeable and engaged individuals. Greater progress was observed where there was political will and the production of diagnostics coincided with industrial policy goals, also in areas where changing the legal and health policy frameworks was involved. Progress was slower on recommendations with substantial resource implications (eg, labour force, affordability, and diagnostics for conflict situations). It is expected that the Global Diagnostics Coalition will consolidate and accelerate progress.

Introduction

The *Lancet* Commission[1] on diagnostics reported in October, 2021 and had five key messages, arguably the most important of which was our estimate that 47% of the world's population has little to no access to even the most basic diagnostics. In low-income countries, this figure rises to 81%. The Commission made ten recommendations to reverse this huge gap, five at the national level and five for the international community.

As the Commission report was being finalised, the COVID-19 pandemic swept the world and, among the many lessons learned, it served to highlight the fundamental importance of accurate timely diagnosis both to health care and in response to public health threats. The importance of diagnostics applies to all conditions, whether communicable (eg, COVID-19) or non-communicable (eg, diabetes). Given the learnings from the COVID-19 pandemic, the statistic that 47% of the global population has little to no access to diagnostic tests has major implications.

What has happened since the Commission report was published? In the relatively brief period since publication, which, if any, of the recommendations have been implemented? Has there been any progress on these recommendations? Are there any other developments—whether in disease conditions, technology, socioeconomics, and so on—that are relevant? For example, a major response to the COVID-19 pandemic has been the establishment of numerous international organisations charged, along with existing organisations, with preparing for the next pandemic. Have these organisations helped improve access to diagnostics more generally?

	Commission recommendation	Measures of progress	Progress observed
1	National diagnostics strategy, based on an integrated and tiered network, including an evidence-based EDL, with a prioritised subset for universal health coverage	Establishment of a diagnostics strategy; number of countries with a national EDL	Increase from one to eight now published, 13 more in development; 55 countries have some other similar types of lists
2	Primary health centre diagnostic availability and accessibility	Proportion of population with access to basic diagnostics at health centres	Very few new surveys have occurred, but funding constraints did not permit analysis of these
3	Health workforce expansion and upskilling for contemporary diagnostic skills	Expanded workforce capacity; existence of contemporary curricula for education and training; increased use of digital diagnostics and artificial intelligence	Examples provided of two regional networks and frameworks and five new national curricula
4	Governance and regulatory frameworks to support and oversee diagnostic quality and safety	Monitor regulations nationally and internationally using selected key tests	Process metrics: numbers of countries achieving 1 of top 2 levels of a global benchmarking tool (regarding the maturity of regulatory system for medical products); 17 of the 22 affiliate members of the International Medical Device Regulators Forum's regional harmonisation initiative are LMICs
5	National financing strategy to provide sufficient, long-term financing to plan and implement diagnostics, including infrastructure	Use of new financing sources; specific line item for diagnostics within universal health coverage budgets	Two case studies provided (India and Brazil), brief reference to Association of Southeast Asian Nations
6	Improve the affordability of diagnostics	Creation of forum; compare domestic prices of selected key diagnostics internationally	Requires funding and WHO oversight
7	Foster development and appropriate use of technology to benefit everyone	LMIC share of global market for production of diagnostics; Global Digital Health Index (now called Global Digital Health Monitor)	Global Digital Health Monitor ranks Latin American countries at 3–4, African countries mostly 2–3, south and southeast Asia 2–4, and high-income countries mainly at 5 of 5
8	Address the diagnostics needs of populations living in fragile and conflict situations	Increase the portfolio of clinical trials, studies, projects, and programmes dedicated to fragile and conflict populations by 10% annually for next decade; work needs to start now given the urgency	No progress given aid budget cuts; however, WHO is developing an EDL for emergencies, which will influence future UN emergency health kits
9	Advocate at all levels to ensure that diagnostics receive appropriate recognition and funding	Number of countries with a national integrated, tiered network and EDL; measure degree of integration using the Human Service Integration Scale; number of countries where diagnostics are integrated into universal health coverage benefits packages; bibliometric measures (eg, mentions of diagnostics in the media); numbers of pathology, laboratory medicine, and radiology professionals in the international policy arena	First key message from the Commission remains widely cited on the internet as of June, 2024 and is found on sites of various international organisations and health news websites in at least eight countries
10	International Diagnostics Alliance to support and monitor the effort in transforming diagnostics	No measure specified	Global Diagnostics Coalition set to launch in May, 2025

EDL=essential diagnostics list. LMIC=low-income and middle-income country.

Table 1: **List of original measures proposed to evaluate progress on recommendations of the diagnostics Commission[1] and progress summary**

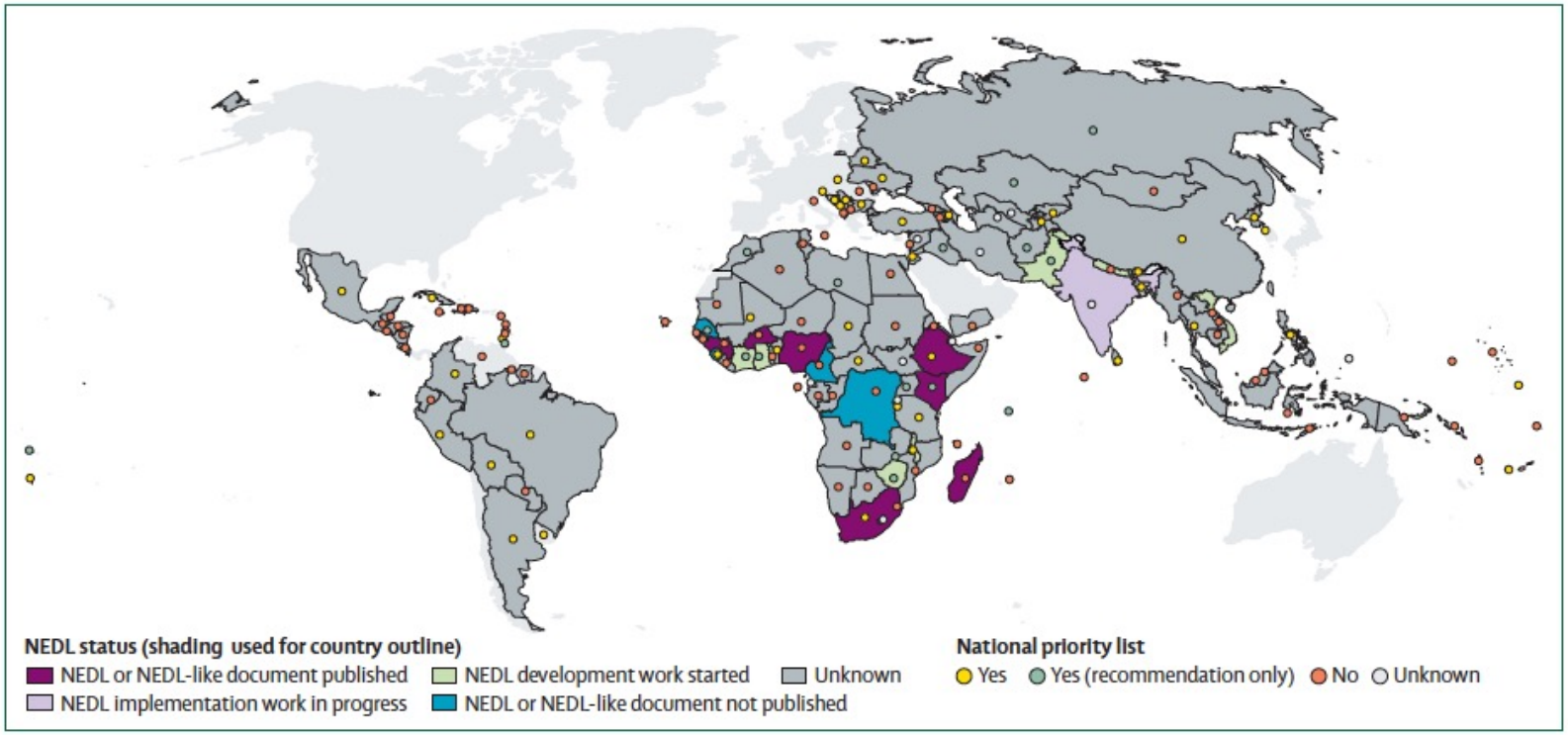


Figure: **Diagnostics lists in low-income and middle-income countries**
NEDL list information was gathered by MK from WHO regional offices, country Ministries of Health, from the study by Koster and colleagues,[4] and from information on national priority lists from the WHO Global Atlas of Medical Devices.[3] NEDL=national lists of essential in-vitro diagnostics.

Panel 1: Transforming access to diagnostics in Africa

Africa continues to have disproportionately high rates of infectious diseases and frequent outbreaks of emerging and re-emerging infections. In 2023 alone, there were 180 declared public health emergencies across the continent, 90% of which were infectious diseases and 70% of zoonotic origin.[14] Access to quality assured in-vitro tests, especially those that can be deployed in remote sites, is crucial for responding to outbreaks quickly and effectively.

Access to diagnostics has been a major issue for COVID-19 response and is a bottleneck to mount an effective prevention and response strategy for mpox. The quest for diagnostics access has been elevated to the next level when the World Health Assembly in its 76th edition adopted a historic resolution on diagnostics. Following the adoption of the resolution, the Future of Diagnostics in Africa initiative was launched by a broad coalition of partners, which, via a very consultative process, has identified strategic areas of intervention. Working groups have highlighted a set of systems-strengthening interventions based on expected impact and sustainability, following discussion at an African Society for Laboratory Medicine Special Convention on Diagnostics in Abidjan in October, 2024.[15]

There have been considerable improvements in the laboratory system capacity in Africa as a legacy from COVID-19 pandemic. Molecular detection and genome sequencing capacity has been expanded to more than 42 Africa Union member states and this helped to immediately track the spread of mpox clades. More than 964 sequences of *MPXV* from 17 member states had been shared as of October, 2024 (unpublished Africa Centres for Disease Control and Prevention data).

One recent Africa Centres for Disease Control and Prevention initiative has been to identify a priority list of diseases, focusing on those that cause frequent disease outbreaks and not necessarily reflecting the burden of diseases.[16] The African Continental Laboratory Technical Working Group developed and disseminated guidance on how to build testing capacity for diseases at risk of developing into epidemics.[17]

The challenge with the introduction of new diagnostic technologies into public health programmes is the paucity in the clinical and analytical performance of test kits. Moreover, existing regulatory frameworks in Africa require companies to submit their products for evaluation in every country individually, despite the availability of performance data from evaluations in other countries. To address this challenge, a manual has been developed with a proposal to create a biobanking network representing all regions of Africa.[18] The biobanks have been supported to expand their cold chain storage capacity, 24 h temperature monitoring, information systems to manage biobanks, and liquid nitrogen plants. The biobanks will play a crucial role in the multicentre evaluation of diagnostics in a coordinated manner, with evaluation programmes independently led by the Africa Diagnostics Advisory Committee. The results from these evaluation studies have facilitated the regulatory approval of a locally developed PCR test kit for mpox that is used already in outbreaks in three African countries. These technical and regulatory changes are transforming access to diagnostics in Africa.

Panel 2: The needs and technology-based opportunities for low-resource areas: the promise of connected diagnostics

- Diagnostic support: artificial intelligence (AI) algorithms assist in diagnosing diseases, especially in resource-constrained settings
- Virtual health provision: telemedicine and telediagnostics powered by AI enables remote consultations, bridging geographical gaps
- Training and task shifting: AI tools help address workforce knowledge and skills gaps, providing support and added confidence in decision making
- Personalised medicine: tailored treatment plans are based on individual patient characteristics
- Patient participatory health: patients can self-manage their health
- Addressing health inequities: open and accessible health data from different geographies help stakeholders gain a better understanding and design tailored algorithmic applications for diagnosis and treatment
- Research: train global clinical models on data from multiple locations, making the data more robust and generalisable
- Epidemic surveillance: integrated technology assists with identifying, testing, and monitoring during disease outbreaks

Panel 3: My experience leading the resolution on diagnostics: from the perspective of Bawelile Philomena Simelane[1]

My country had just assumed the role of regional coordinator for health matters within the African Group [when I met with colleagues from the *Lancet* Commission and the Foundation for Innovative New Diagnostics]. They spoke passionately about diagnostics and the lack of diagnostics led to dire consequences to the lives of women and girls, under privileged persons in society.

I was inspired and told them that I would bring the suggestion [of a resolution on diagnostics] to the members of the African Group. Someone [from the African Group] suggested why Eswatini could not lead this resolution and then others could co-sponsor the resolution? I sprang into action and boldly asked the Principal Secretary of the Ministry of Health if I could do a resolution for the country. He said, "I see the passion in your eyes and I know that you can do it": he also informed me that this [resolution] would be Eswatini's maiden resolution. I then approached colleagues in the Governing Bodies Secretariat and began asking questions about how I can bring the resolution to the World Health Assembly.

When I engaged with WHO AFRO [African Region] and member states, I heard stories of how the lack of diagnostics leads to deaths, even misdiagnosis also leads to deaths. I was intrigued to do more. With the assistance of WHO, we discussed the scope of the paper and registered on the website our informal consultations [there were no less than seven informal consultations, with the final one occurring literally the evening before the start of the executive board meeting in January, 2023]. I was amazed by the interest and countries that never participate in informal consultations were in attendance.

We soon realised that each region seemed to have its own description of diagnostic tools and as such [we had] to hold extensive meetings of experts to formulate definitions endorsed by WHO [the process of negotiation of the text was arduous, due to proposals by various member states to include language on some contentious broader issues]. After much deliberation, delegations felt that it was best for us to have a green text and avoid bracketing paragraphs [green text is text to which no member state has an objection; bracketed paragraphs indicate lack of consensus]. The resolution was adopted at the executive board session in 2023. In May, [2023] it was endorsed by the [World Health] Assembly.

Bawelile Philomena Simelane[1] (Philo) served in the Permanent Mission of the Kingdom of Eswatini in Geneva from 2017 to 2023, with the responsibility for human rights and health issues. She was the regional coordinator of health matters of the African group in Geneva from May, 2022 until February, 2023. In this capacity, she led the member state discussions and negotiations for the World Health Assembly Resolution on Strengthening Diagnostics Capacity (WHO, 2023). This panel is an edited and abridged summary of a longer statement she wrote about her experience in the process, before her untimely death in March, 2024. The diagnostics community is indebted to Philo for her role in bringing forward the resolution.

	Recommendations from the Commission	Progress score (IQR)
1	National diagnostics strategy, based on an integrated and tiered network, including an evidence-based EDL, with a prioritised subset for universal health coverage	3·5 (2–4)
2	Primary health centre diagnostic availability and accessibility	2 (1–2)
3	Health workforce expansion and upskilling for contemporary diagnostic skills	2·5 (1–3)
4	Governance and regulatory frameworks to support and oversee diagnostic quality and safety	3 (2–4)
5	National financing strategy to provide sufficient, long-term financing to plan and implement diagnostics, including infrastructure	2 (1–2)
6	Improve the affordability of diagnostics	2 (1–2)
7	Foster development and appropriate use of technology to benefit everyone	3 (2–4)
8	Address the diagnostics needs of populations living in fragile and conflict situations	2 (2–3)
9	Advocate at all levels to ensure that diagnostics receive appropriate recognition and funding	2 (2–3)
10	International Diagnostics Alliance to support and monitor the effort in transforming diagnostics	2 (1–2·5)

A score (maximum of 5) was categorised as: 1=no or very limited progress, 2=limited progress, 3=moderate progress, 4=good progress, and 5=very good progress. Scores reported are the median with IQR. Respondents could also not respond and had the option to provide qualitative comments to each of the ten questions (appendix pp 2–4).

Table 2: **Summary of progress on the ten Commission recommendations from a survey of 28 knowledgeable informants**

When writing the *Lancet* Commission, we were frequently told that, unlike pharmaceuticals, there was no global forum where diagnostic stakeholders could get together. The emergence of a potential Global Diagnostics Coalition will be crucial in consolidating progress and moving forward, building on the WHO Director-General's reporting in May, 2025 on progress since the diagnostics resolution from 2023. There is encouraging momentum around the proposed Global Diagnostics Coalition, which would take the form of a WHO-managed network with broad stakeholder inclusion. While its mission and composition are still under discussion, the coalition is intended to serve as a collaborative platform and convening body to provide strategic direction and coordinate efforts to strengthen diagnostics capacity.



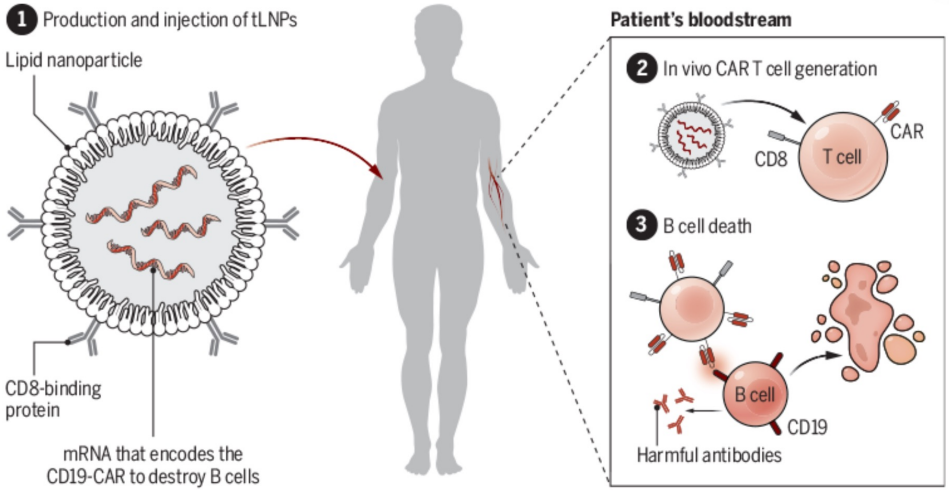
Engineering immunotherapy from within

Harnessing a patient's own immune cells to combat diseases while leaving healthy cells unharmed, called adoptive immunotherapy, is considered a powerful treatment option. Indeed, a type of immunotherapy in which T cells are engineered to express a protein—a chimeric antigen receptor (CAR)—that redirects them to disease-causing cells within the body has been explored for more than two decades. However, because CAR T cells are generated outside the body, these therapies require a substantial infrastructure and thus are expensive. Hunter *et al*. report the engineering of CAR T cells inside the body (in animal models) using nanoparticles that effectively deplete targeted B cells. The achievement has implications for treating B cell malignancies and autoimmune diseases, advancing the quest to generate immune effectors in vivo, and moving immunotherapy with CAR T cells to wider clinical use.

To remove the need for ex vivo CAR T cell production and chemotherapy, Hunter *et al*. developed a method to generate CAR T cells in vivo using targeted lipid nanoparticles (tLNPs) that can carry a desired mRNA cargo (see the figure). The approach minimizes the risk of damaging DNA in T cells because mRNA does not integrate into the genome as would a DNA cargo. One challenge of in vivo mRNA (or DNA) delivery with lipid nanoparticles is their unspecific uptake by the reticuloendothelial system of the liver, which removes foreign substances from the blood. To overcome this hurdle, the authors formulated an ionizable lipid (L829) and incorporated it into lipid nanoparticles that target CD5, which is expressed on T cells. The CD5-L829-tLNPs were injected into animal models—mouse, rat, and cynomolgus monkey—to evaluate their distribution. Compared with a standard nontargeting ionizable lipid nanoparticle, CD5-L829-tLNP exhibited favorable biodistribution in that their uptake by the liver was limited.

In vivo generation of CAR T cells

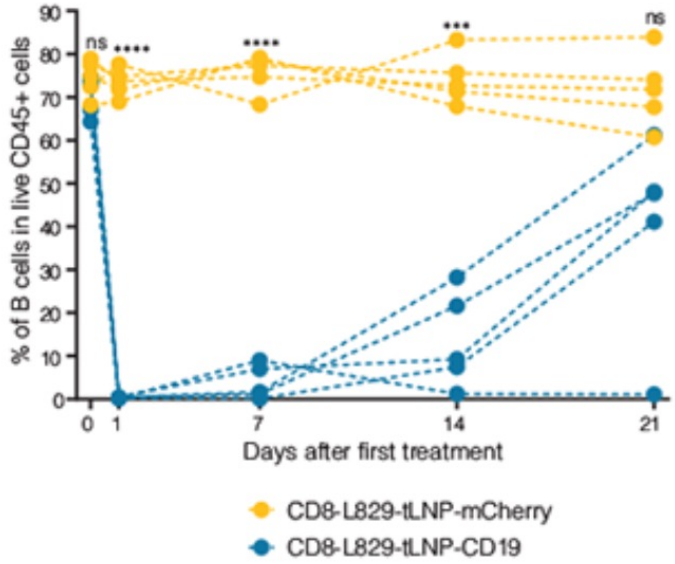
The depicted in vivo approach to engineer chimeric antigen receptor (CAR) T cells in humans is based on preclinical studies in rodents and nonhuman primates. In this scenario, (**1**) targeted lipid nanoparticles (tLNPs) are engineered to carry mRNA that encodes a CAR that recognizes a B cell–specific protein (CD19). These nanoparticles are also designed to bear a protein that binds to CD8 at the surface of specific T cells. After production, the tLNPs are stored and infused as a ready-to-administer drug product based on the patient's condition. (**2**) The tLNPs are injected into a patient and reprogram CD8-expressing T cells into CD19-CAR T cells. (**3**) The CAR T cells recognize and kill harmful, antibody-producing B cells that express CD19.



In vivo CAR T cell generation to treat cancer and autoimmune disease

Chimeric antigen receptor (CAR) T cell therapies have transformed treatment of B cell malignancies. However, their broader application is limited by complex manufacturing processes and the necessity for lymphodepleting chemotherapy, restricting patient accessibility. We present an in vivo engineering strategy using targeted lipid nanoparticles (tLnPs) for messenger RnA delivery to specific T cell subsets. These tLnPs reprogrammed CD8⁺ T cells in both healthy donor and autoimmune patient samples, and in vivo dosing resulted in tumor control in humanized mice and B cell depletion in cynomolgus monkeys. In cynomolgus monkeys, the reconstituted B cells after depletion were predominantly naïve, suggesting an immune system reset. By eliminating the requirements for complex ex vivo manufacturing, this tLnP platform holds the potential to make CAR T cell therapies more accessible and applicable across additional clinical indications.

F

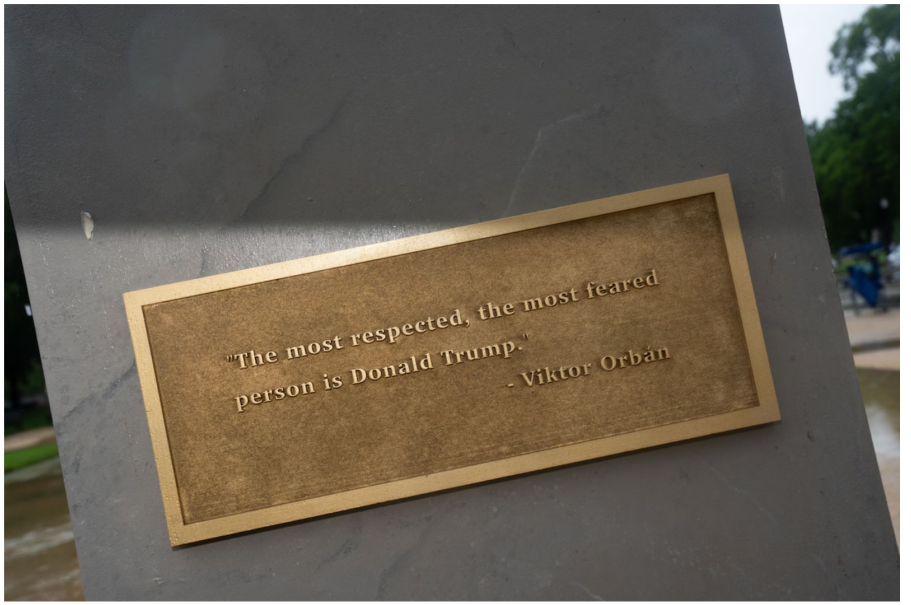


(**F**) Percent of circulating B cells of human CD45⁺ cells in NCG-CD34⁺ humanized mice after three doses every 3 days of indicated tLNP. Statistical analysis by one-way (C) or two-way [(D) and (F)] ANOVA with post hoc multiple comparisons. (****P* ≤ 0.001, *****P* ≤ 0.0001; ns = not significant, *P* > 0.05).

Eight-foot-tall ‘Dictator Approved’ sculpture appears on National Mall



An anti-Trump statue has popped up on the National Mall in Washington. (Maxine Wallace/The Washington Post)



Plaques on the sculpture’s base include quotes from Russian President Vladimir Putin, Hungarian Prime Minister Viktor Orban, former Brazilian president Jair Bolsonaro and North Korea’s Kim Jong Un. (Maxine Wallace/The Washington Post)

Diktator genehmigt